NTNU
Norwegian University of
Science and Technology

Cost Efficient Industrial Heat Recovery through Heat Pumps

Morten Akre Aarnes

Master of Science in Mechanical Engineering
Submission date: June 2016
Supervisor: Trygve Magne Eikevik, EPT
Co-supervisor: Ignat Tolstorebrov, EPT

Norwegian University of Science and Technology
Department of Energy and Process Engineering

NTNU

Norwegian University
of Science and Technology

Department of Energy
and Process Engineering

EPT-M-2016-02

MASTER THESIS

for

Student Morten Akre Aarnes

Spring 2016

Cost Efficient Industrial Heat Recovery through Heat Pumps

Kosteffektiv varmegjenvinning fra industrielle prosesser ved bruk av varmepumper

Background and objective

The project objectives focus on development of industrial waste heat recovery solutions that aim at:

- recovering large quantities of waste heat, upgrading it to higher temperatures and reusing as thermal energy in internal industrial processes,
- high system durability expressed as at least 20 years life span
- reducing primary energy consumption,
- decarburization and resource efficiency of the energy supply

The first two statements define whether the proposed technological solutions and practices will be widely accepted by the end users or not, and are essential conditions, if we aim at their wide market penetration and large scale impact. The last two statements have a straightforward direct impact on optimum exploitation of the energy resources, as well as on environmental protection.

Recently, the heat pumps technology appears considerable application in household sector. Demonstrating the superior performance of the technology is essential in order to facilitate its large penetration in the industrial sector and demonstrate that can apply in pilot plants at industrial sites by improving this technology in terms of:

- heat supply at temperature range (+90 to +140°C or more)
- energy efficiency, e.g. heat recovery from 60°C waste heat (COP/SCOP 5.0 – 6.1)
- cost effectiveness

The following tasks are to be consider:

1. Literature review of the main topic of the scope of work
2. Further developing of the simulation model, including pressure drop in the pipes and components and the suggestions from the project work
3. Implement an economical model including component costs, with evaluation of investment and operational costs
4. Compare the operational costs for a traditional solution and the heat pump solution
5. Make draft scientific paper of the main results from the work
6. Make suggestion for the further work

-- " --

Within 14 days of receiving the written text on the master thesis, the candidate shall submit a research plan for his project to the department.

When the thesis is evaluated, emphasis is put on processing of the results, and that they are presented in tabular and/or graphic form in a clear manner, and that they are analyzed carefully.

The thesis should be formulated as a research report with summary both in English and Norwegian, conclusion, literature references, table of contents etc. During the preparation of the text, the candidate should make an effort to produce a well-structured and easily readable report. In order to ease the evaluation of the thesis, it is important that the cross-references are correct. In the making of the report, strong emphasis should be placed on both a thorough discussion of the results and an orderly presentation.

The candidate is requested to initiate and keep close contact with his/her academic supervisor(s) throughout the working period. The candidate must follow the rules and regulations of NTNU as well as passive directions given by the Department of Energy and Process Engineering.

Risk assessment of the candidate's work shall be carried out according to the department's procedures. The risk assessment must be documented and included as part of the final report. Events related to the candidate's work adversely affecting the health, safety or security, must be documented and included as part of the final report. If the documentation on risk assessment represents a large number of pages, the full version is to be submitted electronically to the supervisor and an excerpt is included in the report.

Pursuant to "Regulations concerning the supplementary provisions to the technology study program/Master of Science" at NTNU §20, the Department reserves the permission to utilize all the results and data for teaching and research purposes as well as in future publications.

The final report is to be submitted digitally in DAIM. An executive summary of the thesis including title, student's name, supervisor's name, year, department name, and NTNU's logo and name, shall be submitted to the department as a separate pdf file. The final report in Word and PDF format, scientific paper and all other material and documents should be given to the academic supervisor in digital format on a DVD/CD-rom or a memory stick at the time of delivery of the Master Thesis.

☐ Work to be done in lab (Water power lab, Fluids engineering lab, Thermal engineering lab)
☐ Field work

Department of Energy and Process Engineering, January 18th 2016

Prof. Olav Bolland
Department Head

Prof Trygve M. Eikevik
Academic Supervisor
e-mail: Trygve.m.eikevik@ntnu.no

Research Advisor:
PhD Ignat Tolstorebrov

e-mails
Ignat.tolstorebrov@ntnu.no

Preface

This master thesis is written at the Norwegian University of Science and Technology between January and June 2016. This thesis investigates industrial heat pumps capable of heat recovery using environmentally friendly refrigerants.

I would like to thank my supervisor, Professor Trygve M. Eikevik for his guidance during the work. I would also like to thank my co-supervisor, Ignat Tolstorebrov for being available during the work and answering my questions.

A special thank also goes to Moderne Kjøling AS, SGP Varmeteknikk AS and Johnson Controls Norway AS for helping me finding suitable components and answering my questions.

Morten Akre Aarnes

Abstract

Industrial waste heat often contains large amounts of useable energy that cannot be utilized in its current form, and has to be used together with a waste heating technology to become useful. With increasing energy prices and carbon taxes, efficient use of energy is increasingly important to be able to reduce the net energy consumption and the emissions of greenhouse gases.

This thesis aims at finding suitable, environmentally friendly and high efficiency heat pump solutions for waste heat recovery. This is done for a case where heat is extracted from the flue gas of a natural gas boiler, and used by a heat pump to produce hot water for washing purposes. It is important to have a reliable, efficient and long lasting heat pump, that can provide the desired heat and temperature to show their potential and to further increase their market share.

A review of recent literature was conducted, giving an overview of recent developments in the field. A single-stage vapor compression cycle was chosen to solve the case, and suitable components were found. Simulation models were developed to investigate the performance of the heat pump using R600, R600a and R1234ze(Z) at different operating conditions. The results of the simulations were then used to do economic evaluations of the heat pump in regards to investment and annual costs. The costs of choosing a heat pump over a natural gas boiler were also investigated.

The results from the simulations shows the importance of reducing the losses in the heat pump cycle, especially in the evaporator. By increasing the evaporation temperature, thus the area of the heat exchanger, resulted in a significantly lower pressure drop. This reduced the work input in addition to reduce the required compressor volume and condenser size. R1234ze(Z) achieved the highest COP equal to 3,8 and the lowest annual cost of 325 000 NOK/year resulting in a pay-off time of 3,3 years when compared to a natural gas boiler. R600 achieved higher performance than R600a. The operational costs were the biggest contributor to the annual costs, optimizing the operating conditions for the compressor are therefore of significant importance. This is especially important when the difference in electricity and natural gas prices are large, to be able to be a competitive heating solution.

Heat pumps have the potential to reduce the energy consumption in industrial heating processes and at the same time being a profitable investment, even in markets where the electricity prices are a lot higher than fossil alternatives. However, the importance of optimizing the cycle is increasingly important when the electricity prices are high. A heat pump might cost less to operate yearly than a natural gas boiler, but if the savings are minimal the additional cost

might make it in an unprofitable investment. It is therefore important to do economic evaluations when considering to invest in a heat pump solution.

Further work should investigate further improvements to the heat pump cycle. Such as using flooded evaporators, optimizing the suction gas heat exchanger and finding the optimal operating conditions. The required safety measures for the selected refrigerants should also be looked into and how they affect the investment costs.

Sammendrag

Industriell spillvarme inneholder ofte store mengder energi som ikke kan bli nyttiggjort i sin nåværende form, og må bli brukt sammen med varmegjenvinningsteknologi for å kunne bli utnyttet. Med økende energipriser og utslippsavgifter, er effektiv bruk av energi stadig viktigere for å kunne redusere netto energibruk og utslipp av klimagasser.

Denne masteroppgaven tar sikte på å finne egnede, miljøvennlige og effektive varmepumpeløsninger for varmegjenvinning. Dette er blitt gjort for et case hvor varme hentes fra avgassene fra en naturgasskjel og brukes av en varmepumpe til å produsere varmtvann for vasking. For å kunne øke markedsandelen til varmepumper, er det viktig å ha et pålitelig og effektivt system med lang levetid som kan oppnå den ønskede varmeavgivelsen og temperaturen.

En gjennomgang av nyere litteratur har blitt gjennomført, noe som gir en oversikt over den siste utviklingen innen fagfeltet. En ett-trinns dampkompresjonsvarmepumpe ble valgt til å løse caset, og egnede komponenter ble funnet. Simuleringsmodeller ble utviklet for å undersøke ytelsen til varmepumpen ved bruk av R600, R600a og R1234ze(Z) ved ulike driftsforhold. Resultatene fra simuleringene ble så brukt til å gjøre økonomiske vurderinger av varmepumpen, med tanke på investeringskostnader og årlige kostnader. Kostnadene ved å velge en varmepumpe over en naturgasskjel ble også undersøkt.

Resultatene fra simuleringene viser viktigheten av å redusere tapene i varmepumpesyklusen, spesielt i fordamperen. Ved å øke fordampningstemperaturen, og dermed øke størrelsen av varmeveksleren, resulterte i et vesentlig lavere trykkfall. Dette reduserte kompressorarbeidet i tillegg til å redusere det nødvendige slagvolumet og kondensatorstørrelsen. R1234ze(Z) oppnådd høyeste COP med en verdi på 3,8 og den lavest årlige kostnaden tilsvarende 325 000 NOK/år som resulterer i en inntjeningstid på 3,3 år sammenlignet med en naturgasskjel. R600 oppnådd høyere ytelse enn R600a. Driftskostnadene var den største bidragsyteren til de årlige kostnadene, og det er derfor viktig å optimalisere driftsforholdet for kompressoren. Dette er spesielt viktig, når forskjellen i elektrisitets- og naturgassprisene er så store, for å være et konkurransedyktig alternativ.

Varmepumper har potensialet til å redusere energiforbruket i industrioppvarmingsprosesser og samtidig være en lønnsom investering, selv i markeder hvor kraftprisen er vesentlig høyere enn fossile energikilder. Viktigheten av å optimalisere syklusen er imidlertid betydelig høyere når kraftprisen er høy. En varmepumpe kan ha lavere årskostnad enn en naturgasskjel, men hvis besparelsene er minimal vil tilleggsinvesteringen gjøre investeringen ulønnsom. Det er derfor viktig å gjøre økonomiske vurderinger når man vurderer å investere i en varmepumpeløsning.

Videre arbeid bør undersøke ytterligere forbedringer i varmepumpesyklusen. For eksempel ved å bruke resirkulasjonsfordamper, optimalisere sugegassvarmeveksleren og ved å finne optimale driftsparametere. Nødvendige sikkerhetstiltak for de utvalgte kjølemediene bør undersøkes nærmere og hvordan disse påvirker investeringskostnadene.

Contents

List of Figures

Appendix:

List of Tables

Nomenclature

Latin Letters

a	Annuity Factor	-
AC	Annual Costs	NOK/year
b	Height of Corrugation	m
B	Annual Earnings/Savings	NOK
Bo	Boiling Number	-
Bd	Bond Number	-
c	Heat Capacity	*J/kgK*
CC	Capital Cost	*NOK/year*
D	Diameter	*m*
d_h	Hydraulic Diameter	*m*
e	Energy Price	*NOK/kWh*
f	Friction Factor Coefficient	-
g	Gravitational Constant	m/s^2
G	Mass Flux	kg/m^2s
h	Heat Transfer Coefficient	W/m^2K
I_0	Additional Investment	*NOK*
k	Thermal Conductivity	*W/mK*
KE	Kinetic Energy	*J*
L	Length	*m*
$\dot{m}$	Mass Flow Rate	*kg/s*
MC	Maintenance Cost	*NOK/year*
n	Deprecation Time	*Years*
N_{ch}	Number of Channels	-
Nu	Nusselt Number	-
OC	Operational Cost	*NOK/year*
P	Pressure	*Pa*
p	Corrugation Pitch	*m*
PO	Pay-Off Time	*Years*
Pr	Prandtl Number	-
PR	Pressure Ratio	-
PV	Present Value	*NOK*
Q	Heat Duty	*W*
q''	Heat Flux	W/m^2
r	Real Interest Rate	*%*
Re	Reynolds Number	-
T	Temperature	*K*
th	Thickness	*M*
U	Overall Heat Transfer Coefficient	W/m^2K
u	Velocity	*m/s*
V	Volume	m^3
w	Width	*n*
W	Work	*W*
We	Weber Number	-
x	Vapor Quality	-
y	Length	*m*

Greek Letters

β	Chevron Angle	^{o}
Δ	Difference	-
γ	Latent Heat of Vaporization	*J/kg*
η	Efficiency	-
μ	Viscosity	*kg/ms*
ρ	Density	kg/m^3
σ	Surface Tension	*N/m*
λ	Volumetric Efficiency	-
Φ	Enlargement Factor	-

Subscripts

acc	Acceleration
C	Cold
comp	Compressor
cond	Condenser
crit	Critical
cross	Cross Sectional
eq	Equivalent
evap	Evaporator
fric	Frictional
g	Vapor
G	Gravitational
gas	Gas Boiler
H	Hot
HP	Heat Pump
is	Isentropic
l	Liquid
lo	Liquid Only
m	Mean/Homogenous
max	Maximum
p	Port
plate	Heat Exchanger Plate
ref	Refrigerant
sc	Subcool
sh	Superheat
tot	Total
tp	Two-Phase
w	Water
wall	Plate Wall

Abbreviations

BPHE	Brazed Plate Heat Exchanger
CAHP	Compression Absorption Heat Pump
CBD	Conventional Batch Distillation
CFC	Chlorofluorocarbon
COP	Coefficient Of Performance
EES	Engineering Equation Solver
GWP	Global Warming Potential
HC	Hydrocarbons
HFC	Hydrofluorocarbons
HFO	Hydrofluoroolefin
HVAC	Heating, Ventilating, and Air Conditioning
LMTD	Logarithmic Mean Temperature Difference
MVR	Mechanical Vapor Recompression
ODP	Ozone Depletion Potential
ORC	Organic Rankine Cycle
PHE	Plate Heat Exchanger
SGHE	Suction Gas Heat Exchanger
TVR	Thermal Vapor Recompression
VHC	Volumetric Heating Capacity
VRBD	Vapor Recompressed Batch Distillation
VRC	Vapor Recompression

1 Introduction

Industrial waste heat often contains large amounts of useable energy that cannot be utilized in its current form, and has to be used together with a waste heating technology to become useful. Temperature is one of the most important factors when determining if the waste heat is useable directly, or if it can be considered as an energy source. High temperature waste heat can often be used directly through a heat exchanger, while low temperature waste heat has to be upgraded (Brückner et al., 2015). Heat pumps are excellent at utilizing the energy contained in waste heat, either by upgrading it to a usable temperature level or using it as heat source.

The heat pump technology has matured over the past two decades and heat pumps are found increasingly in households and buildings, showing their capability and high performance. Their use is not so widespread in the industry, due to the higher investment cost and that they are seen as difficult and not very reliable (IEA-HPC, 2014b).

With increasing energy prices and carbon taxes, conservation and efficient use of energy will become increasingly important in industrial operations (Chua et al., 2010). High temperature heat pumps are capable of replacing combustion systems and electric heaters in several applications, reducing fuel and energy consumption and in turn reducing emissions of greenhouse gasses (Fukuda et al., 2014).

However, many of the refrigerants used in high temperature applications have had a large negative impact on the environment. The increased focus on the environmental effects of the refrigerants, together with stricter regulation is forcing a shift towards a generation of refrigerants defined by a focus on global warming (Calm, 2008). Some of the potential candidates for industrial heat pumps applications are the natural refrigerants; ammonia, carbon dioxide, hydrocarbons, water and a new generation of synthetic refrigerants called hydrofluoroolefins (HFOs).

When deciding for an industrial heat pumps, it is important to choose the optimal heat pump cycle for the given scenario. To further increase the efficiency, it is important to find the optimal operating conditions, and to reduce the losses in the system, especially for the compressors and heat exchangers. The main goal with improving the heat pump performance is to optimize the energy usage, making heat pumps more profitable, and as a result reduce the carbon footprint from many energy intensive industries (Chua et al., 2010).

1.1 Objective

The objective of this master thesis is to investigate the potential of heat recovery from an industrial process using heat pumps. A suitable heat pump solution is found on the basis of the given case, where it is desired to utilize waste heat from a natural gas boiler in Lamborghinis production facility and use it to produce hot water for washing purposes. There is a wish to make the heat pump compact, for easier integration into an industrial plant and to use environmentally friendly refrigerants to meet upcoming regulations. The heat pump solutions will be evaluated based on both technical and economic feasibility.

Simulation models are developed to investigate the technical feasibility of heat pumps using different refrigerants and to find suitable components on the market. The results are then used to economic evaluations of the heat pump solutions and to investigate the economic feasibility of choosing a heat pump over a competing heating solution.

1.2 Structure of the Thesis

Chapter 2 presents a short overview of different high temperature heat pump cycles and some modifications to increase the efficiency for some of the cycles.

Chapter 3 presents a literature review of recent work and developments in the field of industrial heat pumps. It also includes some of the recent developments done to refrigerants for industrial heat pumps.

Chapter 4 gives a short overview of plate heat exchangers and suitable compressors.

Chapter 5 presents the criteria for suitable refrigerants for high temperature heat pumps, in addition to giving a brief description of the different refrigerants.

Chapter 6 presents the case and the selection of suitable components.

Chapter 7 gives a description of the simulation models.

Chapter 8 gives a description of the economic model.

Chapter 9 presents the results from the simulations with an evaluating discussion.

Chapter 10 gives the conclusion.

Chapter 11 gives suggestions for further work.

2 Principle of Industrial Heat Pumps

2.1 Closed Vapor Compression Cycle

A basic closed vapor compression cycle consists of four components: an evaporator, a compressor, a condenser and an expansion valve. A working fluid/refrigerant is circulating inside the closed cycle. In the evaporator, the refrigerant absorbs heat from the heat source, equal to the latent heat of vaporization (Ekroth and Granryd, 2009). The compressor compresses the refrigerant, increasing the pressure and temperature. The refrigerant enters the condenser where it rejects heat to the heat sink through condensation. The refrigerant returns to original state in the evaporator by going through an expansion device, reducing the pressure and temperature. See Figure 2.1 for a principle schematic of a cycle.

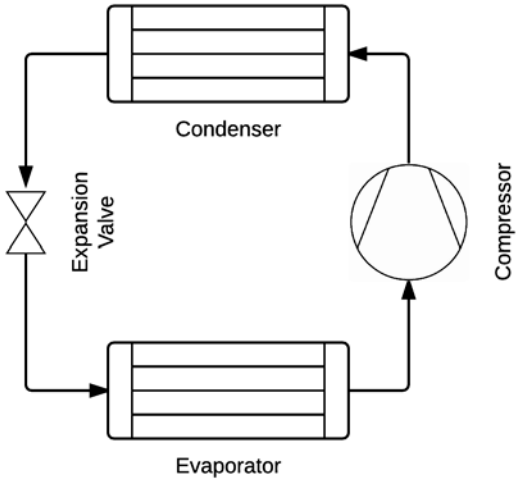

Figure 2.1 Closed vapor compression cycle

2.1.1 Multistage Vapor Compression Cycle

Having large temperature lifts and high-pressure ratios in heat pump systems imply lower compression efficiencies, high discharge gas temperature out of the compressor, which may cause degeneration of the lubricant, and high expansion losses. The main argument for having a multistage system is to reduce the compressor losses and reduce the expansion losses (Stene, 1997). You can classify multistage vapor compression systems as either compound or cascade systems. A compound system has two or more compression stages connected in series. See Figure 2.2 and Figure 2.3 for two system solutions for a two-stage system.

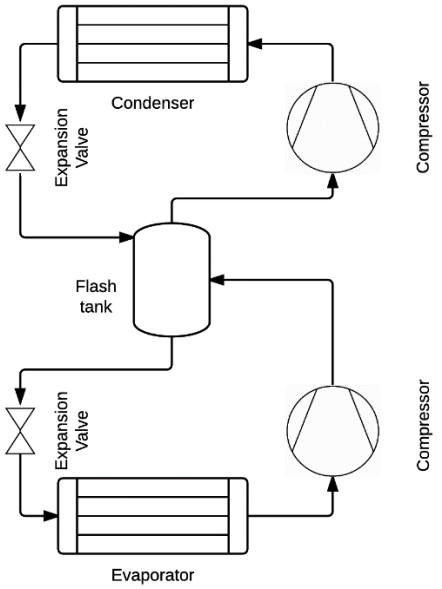

Figure 2.2 Two-stage system with full intercooling

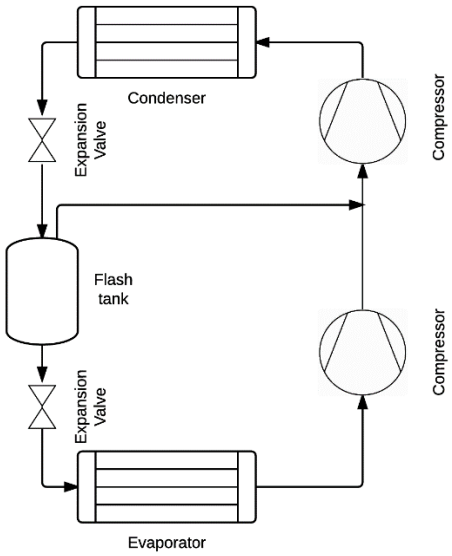

Figure 2.3 Two-stage system with partial intercooling

The interstage pressure is the pressure between the discharge pressure of the high-stage compressor and the suction pressure of low-stage compressor. The interstage pressure that gives the highest coefficient of performance for a two-stage system, gives close to equal compression ratios between the two compression stages (Chua et al., 2010).

A cascade system consists of two or more separate single-stage systems connected by a cascade condenser. The condenser in the lower system works as an evaporator in the higher system (Chua et al., 2010). See Figure 2.4 for a cascade system solution.

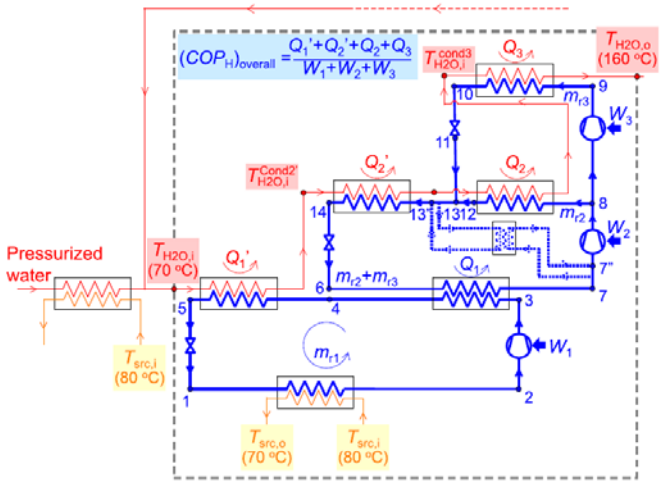

Figure 2.4 Cascade system with R1234ze(Z) and R365mfc (Kondou and Koyama, 2015).

A cascade cycle makes it possible to use different refrigerants in the different stages, making it possible to have individual control of each stage in the cycle. The ability to choose a refrigerant to a specific part of the cycle makes it possible to lower the operating pressure, and get good system efficiency within the given boundaries. It is also possible to choose different piping dimensions between the different stages and suitable lubricants for the compressors (Ekroth and Granryd, 2009). A cascade cycle has an irreversible loss due to heat transfer in cascade condenser. The heat transfer loss is dependent on the operating conditions and can reduce the coefficient of performance significantly (Kondou and Koyama, 2015).

The multistage systems come at a higher investment cost compared to single stage cycles, but the increased efficiency of the cycle will reduce the operating cost. To check if the additional investment in a more complex system is justifiable, an economic analysis has to be performed.

2.1.2 Transcritical Cycles

The refrigerant in a transcritical heat pump cycle operates in both supercritical and subcritical states. In the supercritical state, the refrigerant is a compressed gas and the temperature is independent of the pressure. Due to this independency, heat rejection occurs at constant pressure with a reduction in temperature. In a transcritical cycle, the condenser is therefore exchanged for a gas cooler. Using CO_2 in a transcritical cycle, has shown to be very efficient at heating water with a large temperature difference (Nekså et al., 1998). For a CO_2 transcritical cycle an optimal gas cooler pressure exists and it depends on the operating conditions. Finding the optimum gas cooler pressure will increase the performance of the system. This can also be observed for other refrigerants in transcritical cycles (Sarkar et al., 2007).

2.1.3 Subcooler

Having a high temperature difference over the expansion valve will have a high impact on the expansion losses in the system which in turn affects the COP (Stene, 1997). The same applies for heat pump systems operating close to the critical point (Sarkar et al., 2007). A subcooler will utilize parts of the internal energy in the refrigerant in the subcooler, instead of losing it as expansion losses in the expansion valve (Kondou and Koyama, 2015). This will reduce the expansion losses in the system and will increase the heat output from the system without increasing the work of the compressor (Stene, 1997). See Figure 2.5 for a schematic of a heat pump cycle using a subcooler and a desuperheater. The subcooler can be used to preheat the heat carrier before it enters condenser. The typical increase in COP for the system are approximately 1% per degree K of subcooling, but this is dependent on the properties of the refrigerant (Soroka, 2015).

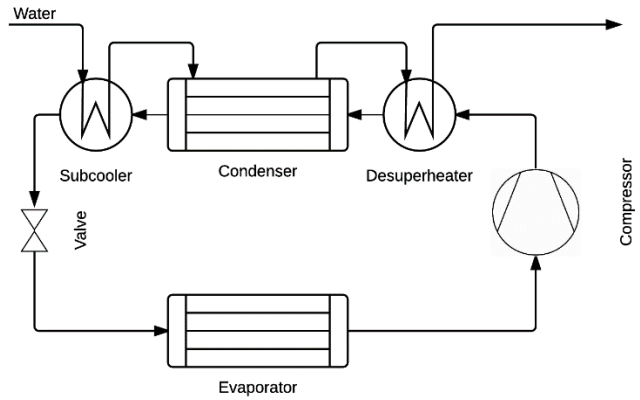

Figure 2.5 Heat pump cycle with desuperheater and subcooler

2.1.4 Desuperheater

The maximum achievable temperature for the heat carrier in the condenser is the condensation temperature. By adding a desuperheater to the cycle, it is possible to extract more heat from the system at a higher temperature by cooling the exhaust gas exiting the compressor down to condensation temperature. The heat carrier can achieve a higher outbound temperature from the system, without increasing the condensation temperature. By adding a desuperheater, the system will have a reduced exposure time to high temperatures. This can reduce the degeneration of the lubricant used in the system, which reduces the possibility for compressor failure and increases the lifetime of the system (Stene, 1997).

2.1.5 Internal Heat Exchanger

In an internal heat exchanger (suction gas heat exchanger, SGHE), heat exchange occurs between the condensed refrigerant exiting the condenser and the gas entering the compressor (suction gas). The condensed refrigerant is subcooled, while the suction gas is superheated. The subcooling reduces the expansion losses in the system. Due to the superheating of the suction gas, the exhaust gas temperature is increased which increases the superheating losses for the system (Stene, 1997). Using an SGHE can increases the systems COP, if it is using refrigerants with high expansion losses, like propane (R290). Ammonia on the other hand should not use a SGHE, due to high exhaust gas temperatures. An internal heat exchanger reduces the chance for compressor failure because it ensures superheated gas to the compressor, avoiding wet compression (compression of droplets) (Kondou and Koyama, 2015).

2.2 Vapor Recompression Cycle

There are two types of vapor recompression heat pump systems (VRC). The two types are mechanical vapor recompression (MVR) and thermal vapor recompression (TVR).

2.2.1 Mechanical Vapor Recompression

In many cases, low-pressure steam is rejected to the atmosphere as waste heat in energy intensive industrial processes such as distillation and evaporation. MVR makes it possible to recover this high quality waste heat efficiently by increasing the pressure and temperature of the vapor (IEA-HPC, 2014a). Steam is the most common type of vapor compressed by MVR systems but it is also possible to compress other types of waste gases (Soroka, 2015). The most common configuration of MVR systems is a semi-open type, where the vapor is compressed directly before it rejects heat in a condenser to the heat sink. See Figure 2.6 below.

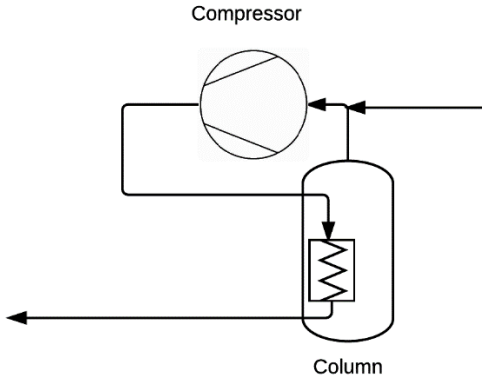

Figure 2.6 Simple schematic of a MVR system.

MVR systems can have a very high COP but it dependent on the temperature lift. Figure 2.7 shows the COP versus temperature lift for a typical MVR system with a screw compressor.

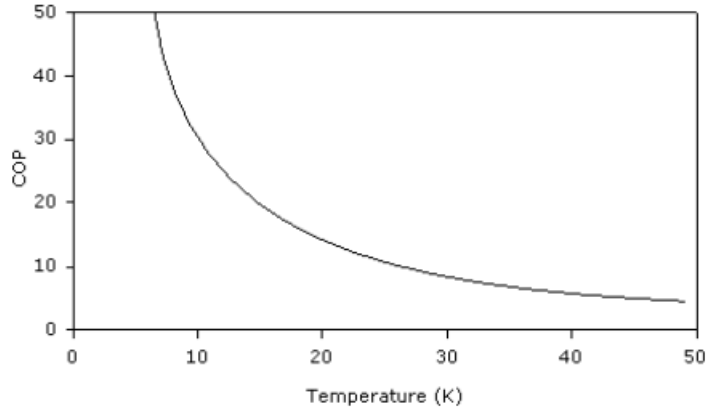

Figure 2.7 COP versus temperature lift for a MVR system (Soroka, 2015).

2.2.2 Thermal Vapor Recompression

In a TVR system, heat pumping is achieved with an ejector and high-pressure vapor. The principle of the system is shown in Figure 2.8 below. A TVR system is driven by steam generated by a heating process and not by mechanical energy. TVR systems may therefore be a good solution if the price of fuel is a lot lower than electricity price.

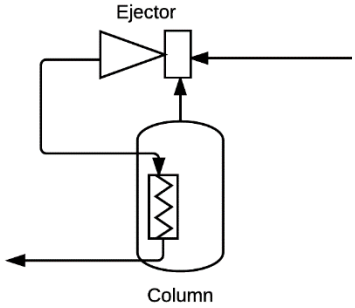

Figure 2.8 Simple sketch of a TVR system.

The COP versus temperature lift for a TVR is shown below in Figure 2.9. The COP for a TVR system is defined as the relation between the heat of condensation of the vapor leaving the TVR and heat input with the motive vapor (Soroka, 2015).

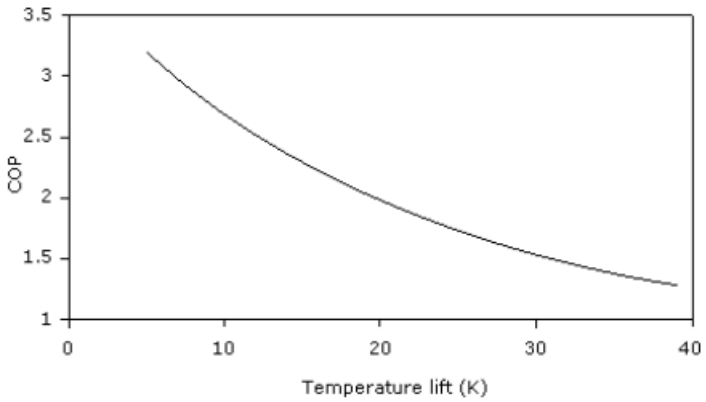

Figure 2.9 COP versus temperature lift for a TVR system (Soroka, 2015)

2.3 Absorption Heat Pump

Absorption heat pump systems distinguish themselves from the traditional heat pump systems by being driven by heat, and not mechanical work. The absorption systems are classified as either type I or type II. Type I is referred to as absorption heat pump and is a heat increasing process. While type II is referred to as a heat transformer and is a temperature increasing process (Stene, 1993). The difference between the two systems is the pressure level, and its influence on the temperature levels, in the four main heat exchangers (evaporator, absorber, desorber/generator and condenser) (IEA-HPC, 2014a). An absorption heat pump system is similar to a vapor compression system; it has a condenser, an expansion system and an evaporator. However, an absorption circuit replaces the compressor. The absorption circuit consists of an absorber, a pump, a desorber/generator and an expansion device. See Figure 2.10 for a schematic of an absorption heat pump system. The most common mixture used in industrial applications is a lithium bromide solution in water ($LiBr/H_2O$) and an ammonia/water solution (NH_3/H_2O) (Brückner et al., 2015). Absorption heat pumps are most suitable for countries where electricity is generated in thermal power plants and electricity prices are high (Stene, 1993).

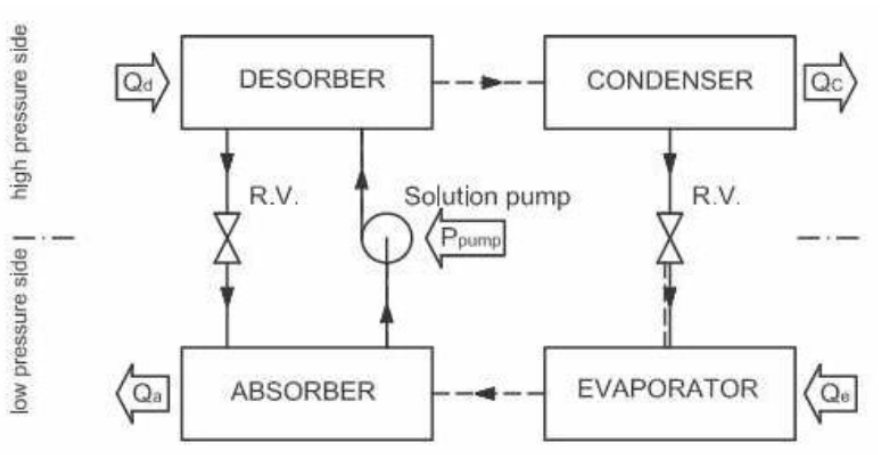

Figure 2.10 Schematic of an absorption heat pump (IEA-HPC, 2014a)

2.4 Compression-Absorption Heat Pumps

A compression-absorption heat pump (CAHP), often called a hybrid heat pump, is based on the mechanical vapor compression cycle. The simplest compression-absorption heat pump cycle is the Osenbrück cycle. In the Osenbrück cycle heat transfer are performed by an absorption and a desorption processes (Jensen et al., 2015a). A hybrid heat pump system uses a zeotropic working fluid, which is a mixture of two or more components that will evaporate or condense at a gliding temperature. A common zeotropic mixture used in hybrid systems are ammonia and water (Stene, 1993). A hybrid compression-absorption system is shown in Figure 2.11 below.

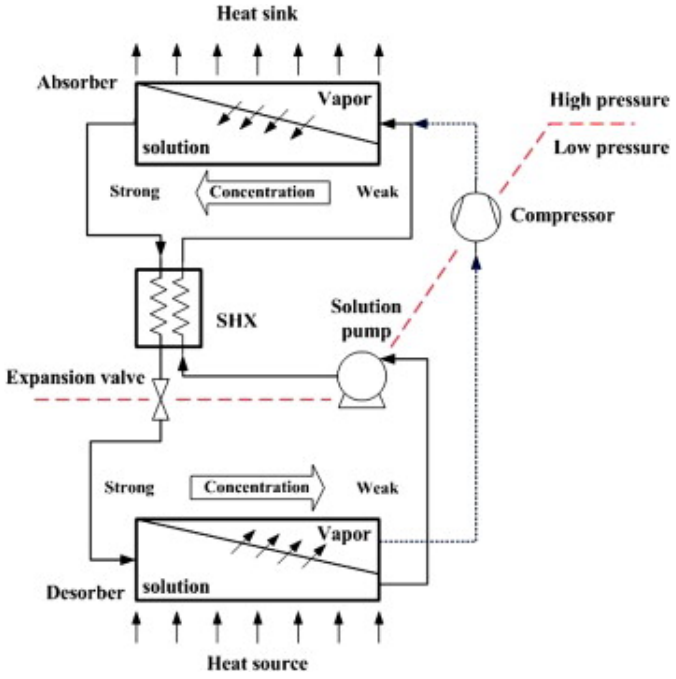

Figure 2.11 Schematic diagram of a hybrid heat pump (Kim et al., 2013).

Advantages of hybrid system is the temperature glides of the absorption and desorption processes, and a reduction of the vapor pressure, compared to the vapor pressure of a pure working fluid (Jensen et al., 2015b). The advantage of the gliding temperature benefits the system both in system efficiency and in an economic manner. It is economically viable if the temperature between the heat sink and heat source is greater than 10K, when compared to a regular vapor compression cycle. This makes the hybrid heat pump suitable for processes that require large sink-source temperature glides (Jensen et al., 2015a). The reduction in vapor pressure makes it possible to achieve higher supply temperatures at similar working pressures.

3 Examples on Heat Pumps in Industrial Applications

3.1 Vapor compression

Vapor compression heat pumps operate in a wide variety of applications ranging from refrigeration systems to high temperature heat pump systems, like district heating systems and process water heating systems. These heat pump systems are applicable with a wide variety of refrigerants including natural and synthetic refrigerants.

Ommen et al. (2015) compares the technical and economic working domains for a single stage vapor compression heat pumps using different natural refrigerants. Performance was calculated with constant efficiencies and the heat pump did not have any cycle improvements. The refrigerants that was compared are R717, R600a, R290, R744 and R134a for comparison. Best available technology was found by comparing net present value and payback period for the different solutions. The low pressure and high pressure R717 systems was found to be the best choice of available technology at low and medium sink temperatures and was found to be limited by high discharge gas temperatures rather than economic constraints. Based on economic criteria R600a heat pump was the most suitable system at high sink temperatures (>85 ºC), but the economic feasibility was reduced with increasing temperature lifts. For large temperature lifts a transcritical R744 solution may be the best solution (Ommen et al., 2015).

Aarhus University Hospital in Denmark installed two heat pumps in 2010 with a heating capacity of 450 kW and cooling capacity of 325 kW using R600a as refrigerant. The system's primary function is to deliver cold water. The system is also capable of delivering hot water at 80 ºC to match the district heating system. The R600a was chosen due to its low pressure levels, high performance and the ability to use semi-hermetic compressors, which were readily available on the market. An ammonia system was considered, but at that time, it was not possible to produce 80 ºC (Pachai and Harraghy, 2013).

Using water as a refrigerant with vapor compression cycles for high temperature applications has been limited by technical and feasibility difficulties. Having suitable compression technology has been the largest obstacle to overcome. Suitable compressor should satisfy requirements like; a high compression ratio corresponding to a temperature lift of 40K, high volumetric flow capacity and high isentropic efficiency (Chamoun et al., 2012). If the most expensive compression machinery was excluded, not one of the industrial compressors that were tested in 2009 could meet these requirements (Chamoun et al., 2012).

A new twin screw compressor was therefore developed in the PACO project by modifying an air compressor to meet the requirements using water vapor (Chamoun et al., 2014). The goal of the PACO project is to develop high temperature (<140 ºC) heat pump system (700kW heating capacity), using water as refrigerant for industrial applications. The compressor developed should also be useful for MVR systems, used in concentration and drying applications (IEA-HPC, 2014a).

Chamoun et al. (2014) developed a heat pump circuit for an experimental study with condensing temperatures in the range of 130 – 140 ºC. The heat pump circuit is connected to two separate water loops to simulate an industrial process and the use of waste heat. This system is based on an experimental simulation of a heat recovery heat pump system for food industry done by Assaf et al. (2010). The prototype heat pump that was developed can be seen in Figure 3.1. A new dynamical model was also developed to take into account the non-condensable gases and the purging mechanism related to start up procedure. The numerical simulation gave similar results to the experimental results that were gathered. An evaluation of performance shows good performance, but the performance is heavily dependent on the waste heat temperature and process temperature. A short timeframe for return of investment is expected if a furnace is replaced with this kind of heat pump (Chamoun et al., 2014). The experimental tests have shown the technical feasibility of the system however, the expected performance is not reached, due to mechanical problems with the screw compressor they had developed. It has now been replaced by a centrifugal compressor and is currently in a test phase (IEA-HPC, 2014a).

Figure 3.1 Prototype heat pump with water as refrigerant (Chamoun et al., 2014).

Madsboell et al. (2015) has developed a centrifugal water vapor compressor for industrial heat pumps in the 100-500kW range for temperature up to 110 ºC. The compressor is based on a

high speed gear from automotive turbochargers making it compatible with standard electrical motors. The temperature lift of the compressor is between 20-25K; higher temperatures lifts can be achieved by serial coupling the compressors. The configuration in Figure 3.2 is capable of delivering a temperature lift of approximately 75K. Making it suitable for a drying application that requires a large temperature lift. Their main objective of their studies is to develop a cost effective heat pump for process industries in the capacity range up to 2000 kW.

Figure 3.2 Compressor set up in parallel combined with serial coupling to achieve a higher temperature lift. (Madsboell et al., 2015)

High discharge gas temperature often makes the installation of a desuperheater a feasible solution. Christensen et al. (2015) showed that dimensioning the desuperheater based on the LMTD method for an ammonia system will give an underestimation of the required heat transfer area, causing an increase in the condensation pressure. This is due to a deviation in UA-value of approximately 10% between the LMTD method and a discretized calculation at normal temperature conditions, due to large variations in C_p-value at high pressures and temperatures. Using LMTD method with R600a will cause a slightly over dimensioning of the needed heat transfer area for relatively low condensation pressures.

There have also been some developments on industrial heat pumps using hydrofluorocarbons (HFCs) as refrigerants, however with stricter legislation and regulations development have shifted towards alternative refrigerants with low(er) global warming potential (GWP) (IEA-HPC, 2014a).

Bobelin et al. (2012) developed an industrial heat pump capable of reaching 140 ºC with temperature lifts up to 80K, using a HFC-mixture. The system consisted of scroll compressors, brazed plate heat exchangers for evaporator, condenser and subcooler and an electronic expansion valve. 1000 hours of testing have been conducted showing a reliable heat pump capable of delivering heat at 125 ºC with good performance. The highest acceptable temperature at the inlet of the expansion valve is 120 ºC, which at the highest condensation temperatures limits the operation due to the large subcooling requirement. The system's performance is also affected by low compressor efficiency at high pressure ratios (IEA-HPC, 2014a).

The HFO R1234ze(Z), has been estimated by Brown et al. (2009) to have similar thermodynamic properties and performance as the chlorofluorocarbon (CFC) R114. R114 was one of the most commonly used refrigerant for high temperature heat pumps before the Montreal Protocol (Longo et al., 2014). The estimation was based on prediction methods that showed reasonable estimates when it was tested with R1234yf. R1234yf was the only HFO with a more extensive data basis, than the bare minimum in open literature at the time. With no ozone depletion potential (ODP) and the low GWP of R1234ze(Z), Brown et al. (2009) concluded that the refrigerant deserved further considerations as to be a possible replacement for R114 in industrial heat pumps.

Fukuda et al. (2014) did a study where they compared thermodynamically, experimentally and numerically the HFOs R1234ze(E) and R1234ze(Z) in a high temperature single-stage vapor compression cycle. The experimental apparatus consisted of a tube-in-tube condenser and evaporator, a compressor developed for R410A, an oil separator and a solenoid expansion valve. A schematic of the setup can be seen in Figure 3.3. An assessment of the irreversible losses for the four main components in addition to the pressure drop effects based on a simple simulation was also conducted. It showed a reduction in the sum of irreversible losses and a drastic reduction in losses related to pressure drop at increasing temperatures. The results confirm the potential of R1234ze(Z) as a refrigerant for high temperature industrial heat pumps, but also shows that is not optimal for air conditioning and refrigeration systems (Fukuda et al., 2014).

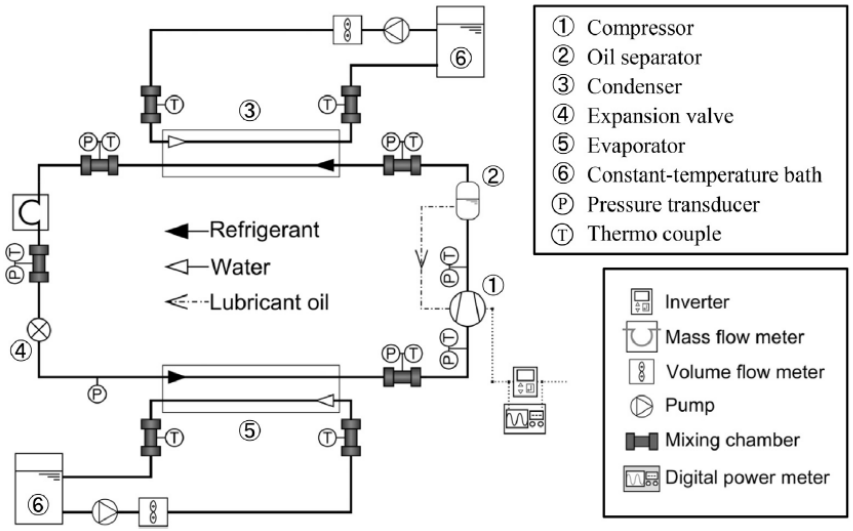

Figure 3.3 Schematic of the experimental apparatus (Fukuda et al., 2014).

Taking the research a step further, Kondou and Koyama (2015) did a thermodynamic assessment of several different heat pump cycles suitable for industrial heat recovery with the refrigerants R717, R365mfc, R1234ze(E), and R1234ze(Z). Calculations were based on a waste heat source of 80 ˚C producing pressurized water at 160 ˚C. The heat recovery systems were optimized with several stages of heat extraction to reduce the throttling losses and exergy losses in the condensers, which are connected in series. The cycles in the assessment is a triple tandem cycle, two stage extraction cycle, three stage extraction cycle and cascade cycle. Their cascade cycle can be seen in Figure 2.4. The systems show promising result, even at reduced heat source temperatures. However, the effects of pressure drop are not taken into account when doing the calculations and several of the cycles operates above their critical temperature.

Another HFO that is a potential candidate for high temperature heat pump applications is DuPonts HFO1336mzz-Z previously known as DR-2. Kontomaris (2012) considered the refrigerant as a low GWP alternative to R245fa. It has a high critical temperature and thermodynamic properties making it suitable for high temperature heat pump cycles and it is also reported to be suitable for Organic Rankine Cycles (ORC). The literature on HFO1336mzz-Z is mainly from DuPont and Kontomaris and the discussion of this refrigerant for high temperature applications is controversial (Fukuda et al., 2014).

Kontomaris (2016) reports that HFO1336mzz-Z is currently under laboratory and field-testing by leading equipment manufacturers in advance of commercialization in 2017.

3.1.1 Transcritical Systems

Nekså et al. (1998) showed the transcritical CO_2 cycle's excellent performance at heating tap water. Heat is rejected at constant pressure and gliding temperatures which gives an excellent temperature fit in the gas cooler, suitable for high temperature lifts. Sarkar et al. (2004) derived a correlation for optimum cycle parameters for a combined heating and cooling system based on gas cooler outlet temperature and evaporator temperature. Showing the importance of an optimum gas cooler pressure, and that the system's COP is increased with a reduction in water inlet temperature in the gas cooler. Transcritical CO_2 cycles operate with greater pressure differences than other refrigerants, leading to greater expansions losses. Throttling losses can be compensated for by using ejectors, expanders or multistage expansion (Austin and Sumathy, 2011). The theoretical COP of a CO_2 cycle is relatively low compared to other refrigerants, but the actual COP of the cycle can be regarded as high, due to high compressor efficiency and

excellent thermodynamic properties of CO_2 (Sarkar et al., 2007). In 2001, the transcritical CO_2 water heater was commercialized in Japan, under the name EcoCute, as an air to water heater capable of providing hot water at 90 ºC. Over 2 million units have been sold by 2009 (Ma et al., 2013). Transcritical CO_2 cycles are also used in refrigeration systems, district heating systems, production of industrial process water and drying applications (IEA-HPC, 2014a). CO_2 systems are capable of delivering both hot and cold water simultaneously. A slaughterhouse in Zürich has installed a CO_2 system using waste heat from an existing ammonia refrigeration system. The system has a total heating capacity of 800 kW at 90/30 ºC and a refrigeration capacity of 564 kW at 20/14 ºC (IEA-HPC, 2014b). A schematic can be seen in Figure 3.4.

The low critical temperature (31.1ºC) of CO_2 limits the ability to use transcritical CO_2 cycles for waste heat recovery. If the temperature of the heat source is close to the critical point the system will be inefficient (Kim et al., 2004).

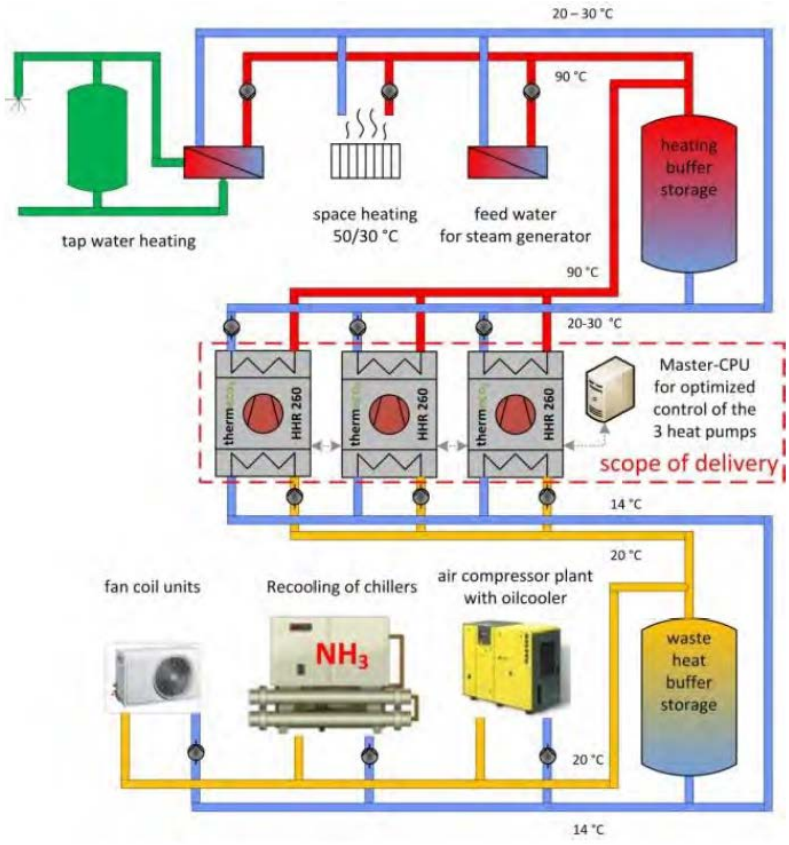

Figure 3.4 Schematic of the CO2 heat pump in the slaughterhouse in Zürich (IEA-HPC, 2014a).

3.2 Compression-Absorption Heat Pumps

Hybrid heat pumps have gotten a renewed interest due to the problems finding suitable compression heat pumps capable of high temperature lifts and temperatures, and the possibility to use low grade waste heat for cooling (Nordtvedt, 2005). Nordtvedt (2005) experimental and theoretical study showed the ability of the hybrid system to deliver both hot and cold water with good performance using waste heat at 50 ºC. The experimental results showed that the capacity could be controlled by adjusting the composition in the solution circuit. An optimum circulation ratio and concentration of ammonia/water exists for given temperature and heating capacity. This has to be considered carefully when designing the system (Nordtvedt, 2005, Kim et al., 2013).

Jensen et al. (2015b) studied the technical and economic working domains of a hybrid heat pump in comparison with vapor compression heat pumps. They showed that the hybrid heat pump can deliver heat at temperatures up to 150 ºC, and with temperature lifts up to 60 K with components that is commercially available. Using a hybrid heat pump was shown to be economical beneficial over a vapor compression heat pumps when the heat supply temperature was above 80 ºC and economically equal to ammonia vapor compression heat pumps for condensation temperatures where they could operate.

Jensen et al. (2015a) studies the development of high temperature hybrid system using ammonia-water. The maximum heat supply temperature is constrained by three dominating factors; the high pressure, the compressor discharge temperature and the vapor ammonia mass fraction. All of these constraints have to be taken into account when increasing the supply temperature. Increasing compressions efficiency by using two-stage compression and oil cooling is suggested to further increase the supply temperature.

Bergland et al. (2015) developed simulation models to optimize a two-stage CAHP at high temperatures. With a maximum compressor discharge temperature of 250 ºC, it was able to reach a maximum supply temperature of 171,8 ºC with an absorber pressure of 47,5 bar and a COP of 2,08. A finned flat tube heat exchangers were found to be most preferable.

In Figure 3.5 there is a schematic of a hybrid heat pump with 650 kW heating capacity installed in 2007 at a slaughterhouse, using waste heat at about 50 ºC. Average efficiency is showed to be 4.5 over three years (Nordtvedt et al., 2013).

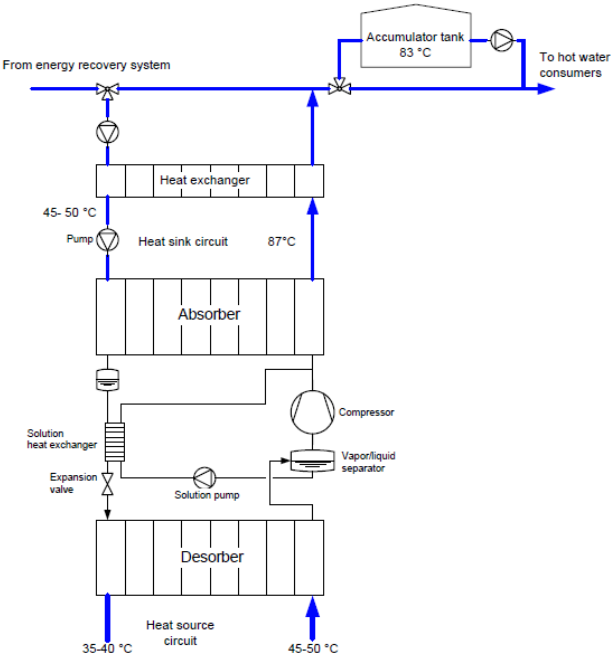

Figure 3.5 Hybrid heat pump installed at Nortura Rudshøgda (Nordtvedt et al., 2013).

3.3 Absorption Heat Pumps

The absorption systems are capable of providing cooling and heating. Absorption chillers can be integrated in plants where there is a demand for cooling and there is waste heat available. The most efficient working fluid for absorption system is a water/lithium bromide mixture (Oluleye et al., 2016). However, they cannot operate below 0 ºC, so for lower temperatures an ammonia/water mixture is used. Absorption chillers can also be used in district cooling systems. The COP of the system is dependent on the temperature of the heat source, higher temperatures gives higher COP (Broberg Viklund and Johansson, 2014).

Qu and Abdelaziz (2015) simulated the use of an absorption heat pump integrated into a coal power plant. The results suggested that the size of the cooling towers and the water usage could be reduced by 17%, reducing the construction and the operational costs. In addition to the reducing the cooling demand of the towers, the absorption heat pump would also produce hot water. Schweighofer Fibre GmbH in Austria has installed a single-stage absorption heat pump in their biomass power plant. A schematic of the installation can be seen in Figure 3.6. It subcools the flue gas in the evaporator, making it possible to use its condensation heat. Steam from the biomass plant is used to drive the generator in the system. The delivered heat from the system is used in a district heating network (IEA-HPC, 2014b).

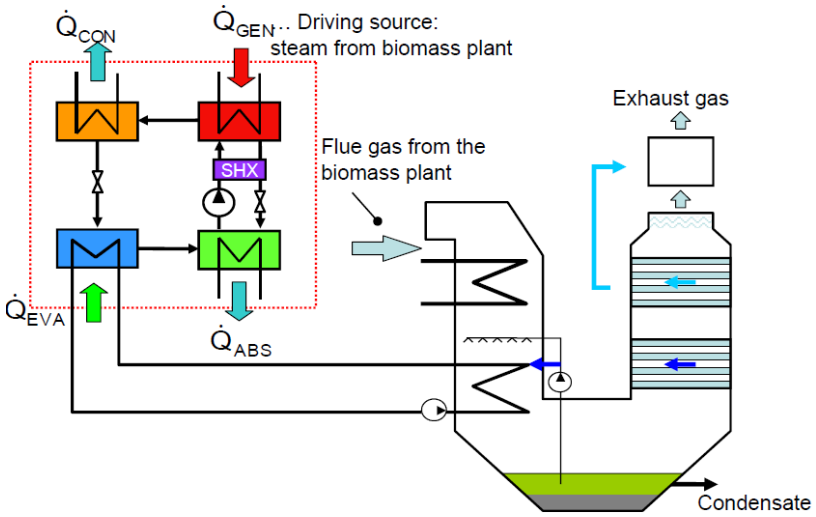

Figure 3.6 Schematic of the absorption heat pump system in the biomass plant (IEA-HPC, 2014b).

3.4 Recompression Systems

Water is an excellent heat carrier and is often used as a heat source and/or heat sink in heat pump installations due to thermodynamic properties and its availability. When using it as a working fluid, water is often used in absorption and hybrid heat pump systems as part of a fluid mixture as mentioned earlier, however water in the form of steam is a widely used working fluid in VRC heat pump systems. MVR and TVR systems are used in a variety of industries such as the chemical industry, food processing industry, industrial washing, industrial drying and etcetera. Typical applications are distillation, drying and heat recovery. Figure 3.7 shows a typical integration of a vapor recompression system for distillation.

Distillation of chemicals is a very energy consuming process, it accounts for nearly 3% of the world's energy consumption (Kazemi et al., 2016). There been a numerous studies focusing in reducing the energy consumption of continuous distillation columns. Few studies have been conducted on increasing the efficiency of batch distillation by using vapor recompression systems (Uday Bhaskar Babu and Jana, 2014). Jana and Maiti (2013) studied the effect of vapor recompressed batch distillation (VRBD) and compared it to conventional batch distillation (CBD). Two cases were studied, an acetone/water mixture and a multicomponent system. The VRBD gave an energy saving of close to 70% for both of the cases. Given a larger investment cost, VRBD is still economical beneficial when compared to CBD, but it comes at an expense of a more complex operation.

Operational experience from IEA HPP ANNEX 35 has shown that standardized MVR systems used in the different industries are reliable, can have a high reduction in primary energy usage which in turn reduces costs and gives a short payback time, especially if the systems are installed in new built plants (IEA-HPC, 2014b).

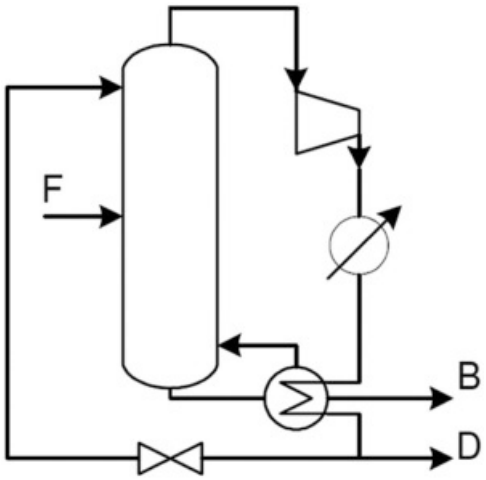

Figure 3.7 Typical vapor recompression distillation process flow sheet (Kazemi et al., 2016).

4 Components

4.1 Plate Heat Exchangers

Plate heat exchangers (PHEs) are a wildly used industrial applications, such as heating, refrigeration, air-conditioning (HVAC), chemical processing, etc. They have a high heat transfer efficiency and a large heat transfer surface area per volume, giving a reduced refrigerant charge compared to other type of heat exchangers. A smaller refrigerant charge gives a reduced environmental impact and lowers the inventory cost (Eldeeb et al., 2016). The 4 most commonly used PHEs are: gasketed plate heat exchangers, brazed plate heat exchangers (BPHEs), welded and semi-welded heat exchangers and shell and plate heat exchangers (Amalfi et al., 2016a). The PHEs are highly flexible; it is possible to specify the amount of plates to get the wanted performance (Shah and Sekulić, 2007). On the gasketed plate heat exchanger it is possible to add or remove plates if there is need for a higher or lower heat output. The plates used in the different heat exchangers are often made of stainless steel. BPHEs consists of several plates brazed together, most commonly by copper or nickel, which allows them to operate under high pressure and temperature conditions. They are highly compact and have a reduced chance of leakage in addition to offering high heat duties. Making them suitable for process water heating and heat recovery (Eldeeb et al., 2016). A schematic with relevant parameters for a plate used in PHEs can be seen in Figure 4.1.

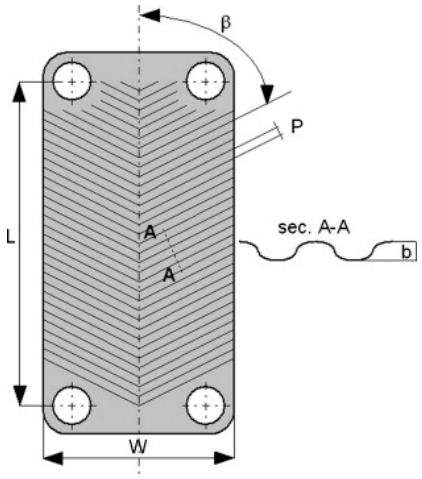

Figure 4.1 Schematic view of a plate (Longo, 2010)

An important parameter when doing calculations on PHEs is the hydraulic diameter d_h, it is defined as (Martin, 1996):

$$d_h = \frac{2b}{\Phi} \qquad (4.1)$$

Where b is the corrugation amplitude and Φ is and enlargement factor given as:

$$\Phi(X) \approx \frac{1}{6}\left(\left(1+\sqrt{(1+X^2)}+4\sqrt{1+\frac{X^2}{2}}\right)\right) \quad (4.2)$$

Where X is dimensionless corrugation parameter given as:

$$X = \frac{b\pi}{\mathrm{p}} \quad (4.3)$$

Where p is the pitch or wavelength of the plate as seen in the figure.

4.2 Compressors

The compressor types that is most used in industrial size applications are reciprocating compressors, screw compressors and turbo compressor. The compressors handle different displacement ranges where the reciprocating compressor handles the smallest compressor volumes while turbo compressors can handle the largest, with the screw compressor in the intermediate range (Eikevik et al., 2016). To find a suitable compressor the required compressor volume in $\frac{m^3}{h}$ is calculated in (4.4):

$$\dot{V}_s = \frac{\dot{m}}{\rho_g \lambda} * 3600 \qquad (4.4)$$

λ is the volumetric efficiency, $\dot{m}$ is the mass flow rate of the refrigerant and ρ_g is the gas density at inlet of the compressor.

Compressor for high temperature refrigerants is not readily available on the market from the different compressor manufacturers, with the exception of ammonia. The use of oil-lubricated compressor for high temperature is limited by high discharge temperatures and the thermal stability of the oil. It is a heavy topic of research and some high temperature compressors are nearing commercialization. Dürr is working on a closed cycle compression heat pump using a reciprocating compressor with R245fa, the lubricating oil is stable up to 130 ºC, marking the maximum operating limit. Higher temperatures led to cooking of the oil, damaging the system (IEA-HPC, 2014a). Operating conditions can be seen in Figure 4.2.

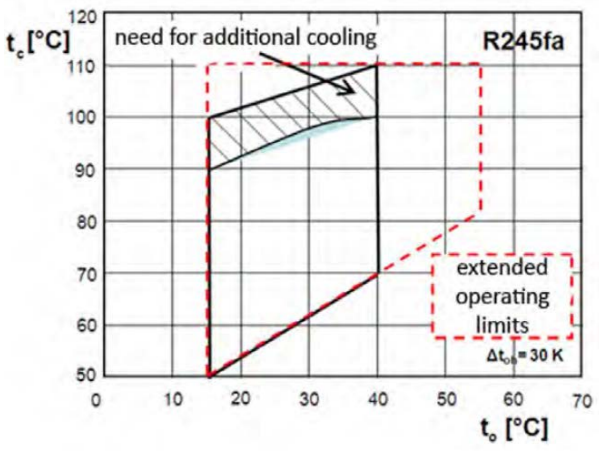

Figure 4.2 Operating limits for reciprocating compressor (IEA-HPC, 2014a)

5 Refrigerants

Finding the “ideal” refrigerant has proven to be a challenge. Some of the criteria for an ideal refrigerant are (Palm, 2014):

- No negative impact on the environment (GWP, ODP)
- Non-toxic and non-flammable
- Stable
- Suitable thermodynamic and physical properties
- Compatible with materials and lubricants
- Low cost

All refrigerants have one or more negative attributes, whether it is toxicity, flammability, very high operating pressure, poor thermodynamic properties or chemical instability (McLinden et al., 2014). When choosing an applicable refrigerant for a given application, all the attributes has to be weighed up against each other, thus finding the optimum refrigerant within the given constraints. A study of refrigerant for high temperature compression heat pumps has shown that a suitable refrigerant would satisfy the following criteria (Bertinat, 1986):

1. A high critical temperature (T_c), to achieve a larger latent heat of evaporation and condensation, resulting in an increased COP.
2. A relatively low normal boiling point (T_{BP}), for a small specific volume of the vapor at the compressor inlet. However, not so low that it gives an excessive discharge temperature.
3. Fairly high critical pressure (P_{crit}), for a small minimum superheat.

Due to the increased importance of minimizing the global environmental effects of the refrigerants, potential refrigerants to be considered are the natural refrigerants and the more recent HFOs. The most promising refrigerants for high temperature vapor compression heat pumps are:

- Ammonia
- Water
- Hydrocarbons (Butane and Pentane)
- R1234ze(Z)
- HFO1336mzz-Z
- Carbon dioxide

A brief description of the different refrigerants is given below.

R717: Ammonia

Ammonia is both toxic and flammable, but it has excellent thermodynamic properties for high temperature heat pumps. It has a high critical temperature (T_{crit} = 132.25 ºC), a high latent heat and no global environmental impact. The pressure levels for ammonia are relatively high, but the pressure ratio is low, giving better compressor efficiency. Ammonia vapor density is low, but due to the high latent heat, the volumetric heating capacity (VHC) is very high and the required compressor volume is moderate. Ammonia systems may be limited by the discharge gas temperature becoming too high (Ommen et al., 2015). Ammonia is also corrosive to copper, and can for this reason not be used with components using copper. Due to the toxicity ammonia heat pumps require additional safety equipment.

R718: Water

Water is neither flammable nor toxic and has excellent thermodynamic properties for high temperature heat pumps. It has a high critical temperature (T_{crit} = 373.95 ºC), very high latent heat, is easily available and has no global environmental impact. The boiling point of water at atmospheric pressure is close to 100 ºC which will cause many cycles to operate partly below atmospheric pressure. This can lead to air infiltration (Chamoun et al., 2014). Even though the pressure levels are low at both the inlet and outlet of the compressor, it is not uncommon to encounter very large pressure ratios. The density of water vapor is very low, giving a small VHC and requiring an extremely large compressor volume. The low vapor density in addition to the high normal boiling point causes excessive discharge gas temperatures. To achieve a tolerable discharge temperature, compression has to be done in several stages with interstage cooling between them (Pearson, 2012). The large required compressor volume in addition to the need of several compressors will increase the cost of the system.

Hydrocarbons

The use of hydrocarbons (HCs) is mostly limited due to safety requirements in regards to flammability. Handling large HC charges require special safety measurements, which in most cases results in a higher cost of the system compared to a system using another refrigerant. Hydrocarbons have a low global environmental impact (low GWP). There have been a gradually acceptance of using HCs as a refrigerant in Europe and some countries in South East Asia. R600a is well established as a refrigerant in domestic refrigerators in northern Europe and propane is used in some commercial installations replacing R22 (Granryd, 2001).

The hydrocarbons of interest for high temperature applications are Butane and Pentane. Both n-butane (R600) and isobutane (R600a) have similar performance to each other at low temperature conditions while the cycle performance of R600 is better in high temperature conditions. The discharge temperature for R600 is also shown to be lower at similar conditions (Pan et al., 2011). R600 has a high critical temperature (T_{crit}=151.98 ºC) and moderate operating pressures. R600a on the other hand has a critical temperature of (T_{crit}=134,66 ºC) and moderate operating pressure, but slightly higher than R600. R601 has a higher critical temperature (T_{crit}=196.55 ºC) and even lower operating pressures. Both refrigerants have low discharge gas temperature, and need some superheating at high temperatures to avoid liquid compression.

R1234ze(Z)

R1234ze(Z) is a newer synthetic refrigerant in the HFO family. It has a high critical temperature (T_{crit}=150.1 ºC), moderate operating pressures and a low environmental effect (low GWP). It is regarded a promising refrigerant with similar potential capabilities as the CFC, R114 (Longo et al., 2014). It is expected to be mildly flammable (Kondou and Koyama, 2015). An experimental study comparing properties of R1234ze(Z) in a commercial brazed plate heat exchanger (BPHE) against commonly used HFCs and HCs showed a much higher heat transfer coefficient and a frictional pressure drop similar to R600a (Longo et al., 2014). See chapter 3.1 for recent developments.

HFO1336mzz-Z

A new HFO from DuPont, it is previously known as DR-2. It is not yet commercially available. It has a high critical temperature (T_{crit}=171.3 ºC), it is expected to be non-toxic and non-flammable and a low environmental effect (low GWP). See chapter 3.1 for recent developments.

R744: Carbon dioxide

CO_2 has a relatively low critical temperature (T_{crit}=31.1 ºC), which makes CO_2 heat pump cycle operate above the critical point, in a supercritical phase. Heat is rejected at constant pressure and gliding temperatures and not through condensation. Transcritical CO_2 cycles operate at very high pressure (Pearson, 2012). The pressure levels for CO_2 are very high, but the pressure ratio is low, giving high compressor efficiency. CO_2 also have a very high vapor density giving a small required compressor volume and very compact compressors. CO_2 is environmentally friendly and is neither toxic nor flammable. The gliding temperature and the excellent thermodynamic properties of CO_2 make it excellent at heating water when the temperature lift

is large. As stated in 3.1.1 the use of CO_2 for industrial heat pumps using waste heat is limited by high temperatures of the heat source.

Table 5.1 lists currently used and potential candidates for high temperature heat pumps using waste heat as its heat source. R114 is listed as a reference for comparison.

Table 5.1: Fundamental characteristics of candidate refrigerants for high temperature heat pumps

Name	**R114**	**R717**	**R718**	**R600**	**R600a**	**R601**	**R1234ze(Z)**	**HFO1336mzz-Z**
Formula	$C_2Cl_2F_4$	NH_3	H_20	C_4H_{10}	C_4H_{10}	C_5H_{12}	$CHF=CHCF_3(Z)$	$CF3CH=CHCF_3(Z)$
Molar mass (kg/kmol)	170,92	17,03	18,02	58,12	58,12	72,15	114,00[a]	164,06[b]
ODP	0,8[e]	0	0	0	0	0	0[a]	0[b]
GWP_{100}	9800[c]	0	0	20[d]	20[d]	20[d]	<1[a]	2[b]
Safety	A1[c]	B2	A1	A3	A3	A3	A2L[a]	A1[b]
NBP (°C)	3,59	-33,33	99,97	-0,49	-11,75	36,06	9,80[a]	33,40[b]
P_c (bar)	32,57	113,33	220,64	37,96	36,29	33,70	35,30[a]	29,00[b]
T_{crit} (°C)	145,68	132,25	373,95	151,98	134,66	196,55	150,10[a]	171,30[b]

Data from REFPROP 9.0 (Lemmon et al.) with the expectations of:
[a] (Kondou and Koyama, 2015)
[b] (Kontomaris, 2014)
[c] (Longo et al., 2014)
[d] (Pan et al., 2011)
[e] (Devotta and Rao Pendyala, 1994)

Pressure Loss in Pipes

The pressure drop for a selection of the refrigerants is given in Table 5.2. The values are calculated using EES inbuilt function Pipeflow (Klein, 2015) for an ideal heat pump with an evaporator capacity of 150 kW. The refrigerant has an evaporation temperature of 40 ºC with no superheat and a condensation temperature of 80 ºC. The pressure drop in Table 5.2 is calculated at the exit of the evaporator. The pipe has diameter of 0,05 m, length of 5 m and a roughness of 0,15 mm equal to commercial galvanized steel pipes (Nellis and Klein, 2009).

Table 5.2 Pressure loss in pipes for equal evaporator capacity

Name	**R114**	**R717**	**R600**	**R600a**	**R601**	**R1234ze(Z)**
$\Delta P\ [Pa]$	51860	838,2	14651	13914	35791	26480
$\dot{m}_{ref}\ [\frac{kg}{s}]$	1,896	0,168	0,6252	0,7331	0,5855	1,03

In Table 5.3 the pressure loss is calculated using the same mass flow rate.

Table 5.3 Pressure loss in pipes with equal mass flowrate

Name	R114	R717	R600	R600a	R601	R1234ze(Z)
$\Delta P\ [Pa]$	14448	29388	37440	25870	104305	24957
$\dot{m}_{ref}\ [\frac{kg}{s}]$	1,00	1,00	1,00	1,00	1,00	1,00

Film Condensation on a Vertical Plate

The heat transfer coefficients are calculated for the different refrigerants using EES inbuilt function Cond_Vertical_Plate (Klein, 2015). With a plate length of 1 m, width of 0,5 m, wall temperature of 80 ºC and a saturation temperature of the fluid of 85 ºC. This function calculates the heat transfer coefficient on the basis of a general correlation based on the Reynolds number. The validity of these values are uncertain, but they can be used to give a perspective on how the heat transfer coefficient of the different fluids compare to each other. Longo et al. (2014) measurements in brazed plate heat exchangers suggests that R1234ze(Z) should have higher heat transfer coefficients than R600a. Cavallini et al. (2006) suggests that R600 has higher heat transfer coefficients is larger than R600a in horizontal tubes. Table 5.4 suggest similar results.

Table 5.4 Heat transfer coefficient

Name	R114	R717	R600	R600a	R601	R1234ze(Z)
h $\left[\frac{W}{m^2K}\right]$	633,8	4557	1140	976,6	1236	1031

6 Case

The Lamborghini automobile manufacturing plant in Sant' Agata Bolognese is vertical integrated, including the production of carbon fiber used in the car manufacturing. The carbon fiber autoclaves are heated by natural gas fired oil boilers. The flue gas that is produced, has a temperature of 200ºC, where 30% of the energy corresponds to sensible heat that can be recovered by an economizer. The remaining energy is latent heat contained in the water vapor generated by the natural gas burning which is released at condensation at approximately 60 ºC. The factory has a need for 90 ºC hot water for washing purposes.

A heat pump solution should be able to recover heat from the carbon fiber production process and use it to cover the hot water demand. An economic and technical evaluation is conducted to investigate; if investing in heat pump solution is favorable over an investment in a natural gas boiler.

A schematic of the plant with an integrated heat pump circuit can be seen in Figure 6.1.

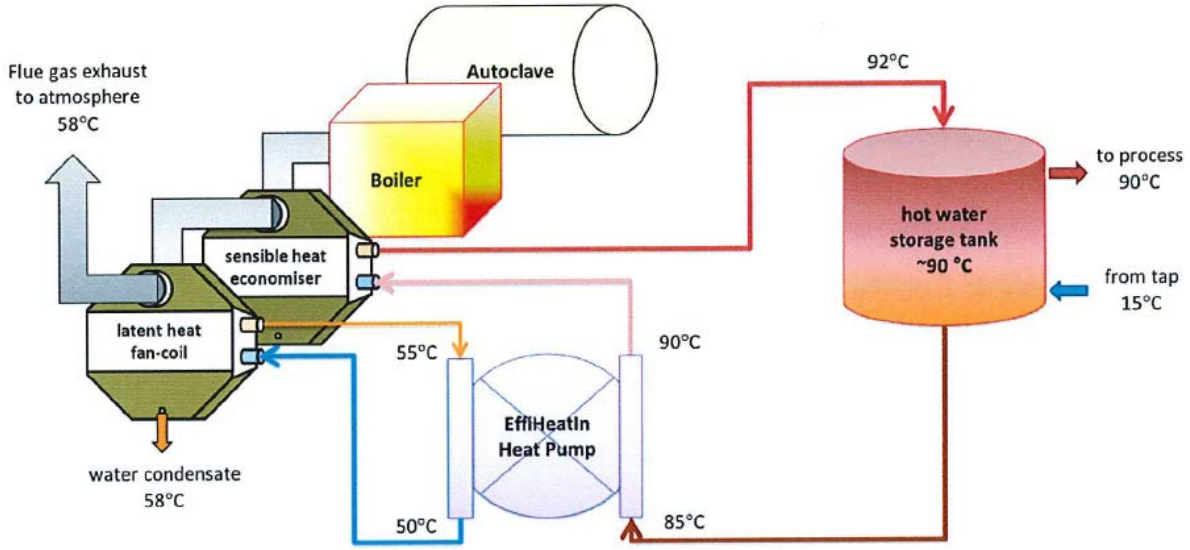

Figure 6.1 Schematic of the plant

6.1 Operating Conditions

The operating time of the heat pump is assumed to be 4400 hours a year, which corresponds to approximately 12 hours a day. The amount of water needed to be heated in the condenser is set to 10 kg/s and the mass flow rate in the evaporator is set to be 7 kg/s. The required heat duty is approximately 210 kW, which equals to a yearly energy consumption of 924 000 kWh.

The base evaporation and condensation temperature is set to 40 ºC and 100 ºC respectively. The evaporation temperature is varied between 40 ºC and 44 ºC while the condensation temperature is kept constant and the evaporation temperature is kept constant when the condensation temperature is varied between 100 ºC and 92 ºC.

6.2 Choosing Suitable Components

A single-stage vapor compression heat pump using R600, R600a and R1234ze(Z) was chosen for the model. This was chosen over a two-stage heat pump due to a low pressure ratio (would be around 2 for the selected refrigerants), only a small increase in energy saving based on simplified calculations, the low discharge superheat for R600 and R600a which could result in liquid compression without sufficient superheating and the fact that is desireable to have a compact system.

Out of the suitable low GWP refrigerants R600a, R600 and R1234ze(Z) was chosen for the simulations mainly due to the lack of suitable heat transfer coeffeicent correlations for the other refrigerants. They are also the refrigerants expected to have the highest performance and be the most suitable for the given boundaries based on the literature that was reviewed.

The components were chosen on the basis of R600 and R600a for high temperature applications and they are assumed to be working with R1234ze(Z) due to the similarities in pressure drop and heat transfer.

The different heat exchangers were chosen by using SWEP's calculation software with inputs given by the simulation model (SWEP, 2016). This resulted in the same evaporator and condenser but different amount of plates in SGHE for R600 and R600a. R1234ze(Z) do not need a SGHE, and it's therefor removed from the calculations.

The compressors series were chosen based on the supplier's calculation tools for R600 and R600a (Johnson Controls Norway, 2016). Their capacity was assumed to be equal to their capacity at 1500 rpm. This assumption is however not correct, since the chosen compressor series had to run at 1000 RPM with R600a, resulting in a larger compressor for R600a than for R600. Which would result in a higher compressor cost for R600a than for R600. The prices for the two smallest compressors was extrapolated basis on the prices given for two larger compressors.

The expansion valve was selected by using Danfoss' selection software for R600a and R600 (Danfoss, 2016). The controller and sensors was then selected on the basis of the expansion valve.

The size of liquid receiver was calculated by using the liquid holdup provided by SWEPs calculation software for the 3 heat exchangers in addition to calculate the volume of the liquid return lines between condenser and evaporator in addition to adding a decent safety margin to allow for the whole charge to be in the receiver in case of maintenance on the system. A receiver size of 40 L was chosen.

The tables below show components chosen for the heat pump model. For R600 and R600a the components are chosen based on the information in this sub chapter. The suppliers did not have components designed and approved for R1234ze(Z) and the components chosen in this thesis is assumed to be compatible.

Table 6.1 Components for the R600 heat pump

Components	
Evaporator	SWEP V200T
Condenser	SWEP B200T
Compressor	Sabroe SMC series
Suction gas heat exchanger	2x SWEP B12x20
Liquid receiver	Carly RLVCY-400
Electronic Expansion valve	Danfoss ETS100
Controller	Danfoss EKC 316A
Sensor	2x Danfoss EKS221

Table 6.2 Components for the R600a heat pump

Components	
Evaporator	SWEP V200T
Condenser	SWEP B200T
Compressor	Sabroe SMC series
Suction gas heat exchanger	SWEP B12x104
Liquid receiver	Carly RLVCY-400
Electronic Expansion valve	Danfoss ETS100
Controller	Danfoss EKC 316A
Sensor	2x Danfoss EKS221

Table 6.3 Components for the R1234ze(Z) heat pump

Components	
Evaporator	SWEP V200T
Condenser	SWEP B200T
Compressor	Sabroe SMC series
Liquid receiver	Carly RLVCY-400
Electronic Expansion valve	Danfoss ETS100
Controller	Danfoss EKC 316A
Sensor	2x Danfoss EKS221

7 Simulation Models

A simulation model have been developed to assess the suitability and performance of a heat pump using different refrigerants for the given case. The model is developed in Engineering Equation Solver (EES) (Klein, 2015). The EES code for the model is given in Appendix B.

The heat pump consists of an evaporator, a condenser, a compressor, a suction gas heat exchanger, a liquid receiver and an expansion valve. A principle schematic of the cycle can be seen in Figure 7.1. The following assumptions and simplifications have been done:

- There is a constant mass flow rate of water on the hot side in a closed loop.
- Water is circulating in a closed loop between the flue gas and the evaporator with a constant mass flow rate.
- The suction gas heat exchanger has a 100% heat transfer efficiency and a constant pressure drop.
- When calculating the temperature and pressure drop in the pipes enthalpy is assumed to be constant.
- Heat loss from the compressor is 10% of the work input.
- Isentropic efficiency and volumetric efficiency is following an equation based on the pressure ratio see chapter 7.6.
- Isenthalpic expansion
- Heat transfer correlations for R600a and R1234yf/ze(E) is used to give an approximation of the performance of R600 and R1234ze(Z).

The correlations are originally designed for R600a and R1234yf/ze(E) and not for the chosen refrigerants, but they should give an approximation of their performance, see 7.2 and 7.3 for more information.

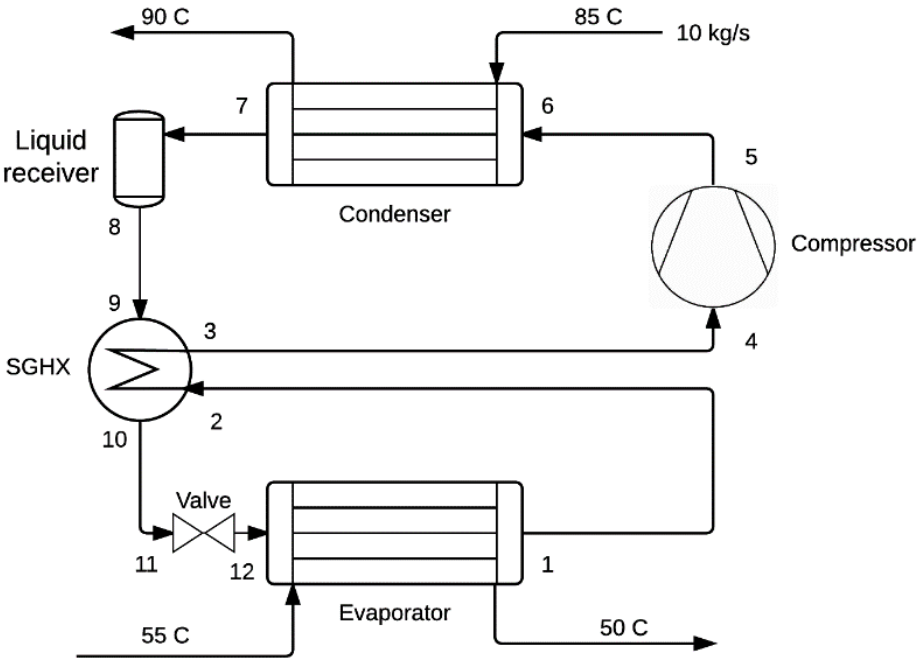

Figure 7.1 Schematic of the heat pump model

7.1 Heat Exchangers

The heat exchangers are modeled with a numerical procedure to find the heat exchanger area and heat transfer needed to meet the required heat duties. The heat exchanger is divided into small control volumes and an energy balance is conducted. The step size for the calculations is chosen to be $3\,m$ and there are 300 integration step equaling to a control volume length of $0{,}01\,m$. The state equations are derived from Nellis and Klein (2009) for a parallel flow plate heat exchanger. The state equation used to calculate the change in water temperature per length in the evaporator can be seen in (7.1) and the condenser in (7.2):

$$\frac{dT_H}{dx} = -\frac{2\,N_{ch}(T_H - T_C)}{\dot{m}_h c_H \left(\frac{1}{h_H w} + \frac{th_m}{k_m w} + \frac{1}{h_C w}\right)} \qquad (7.1)$$

$$\frac{dT_C}{dx} = \frac{2\,N_{ch}(T_H - T_C)}{\dot{m}_C c_C \left(\frac{1}{h_H w} + \frac{th_m}{k_m w} + \frac{1}{h_C w}\right)} \qquad (7.2)$$

Where N_{ch} is the number of channels in the heat exchanger, T_h and T_c is the temperature for the hot and cold fluid, $\dot{m}$ is the mass flow rate hot or cold fluid, c is the heat capacity of the fluid, h is the heat transfer coefficient for the hot and cold fluids, w is the width of the heat exchanger, th_m is the thickness of the plate and k_m is the metal conductivity at the local average temperature.

The change in temperature is used to calculate the enthalpy change, which in turn gives the heat transferred to or from the refrigerant. The next control volume is calculated on the basis of values of the previous control volume, this procedure will go on until the desired outlet conditions are met. The temperature change in the refrigerant is given by the saturation pressure. The saturation pressure is affected by a pressure drop in the heat exchanger leading to a temperature fall.

To be able to calculate the state equations, the heat transfer coefficients for the refrigerant and water has to be found. Several heat transfer coefficients and frictional pressure drop correlations are available for plate heat exchangers in the literature. These correlations are found from experimental setups and are valid within a certain range of operating conditions, defined by i.e. Reynolds number, mass flux, temperatures among others. The correlations that are available is made for temperatures and refrigerants used in typical refrigeration and heat pump applications and not for high temperature heat pumps and for “newer” refrigerants. The correlations used in the model will therefore not give accurate representation of real heat exchangers but a useful

approximation, due to the similarities of the refrigerants. More information about the separate heat exchangers and the correlations can be found in chapter 7.2 and 7.3.

Summaries of correlations for plate heat exchangers is available in (García-Cascales et al., 2007), (Eldeeb et al., 2016) and (Amalfi et al., 2016a).

7.2 Evaporator

Heat is transferred from the warmer water to the refrigerant in the evaporator, cooling the water while increasing the enthalpy and thus the vapor quality of refrigerant. The refrigerant will go through a transition from a two-phase flow at the inlet to a single-phase flow at the outlet of the evaporator. The two-phase heat transfer coefficient is modeled with Amalfi et al. (2016b) correlation for flow boiling in plate heat exchangers. This correlation is valid for a vapor quality between $0 < x < 0{,}90$. The correlation is based on dimensional analysis developed from 1903 heat transfer data points for a wide range of operating conditions, geometries and fluids. The Nusselt is given by:

$$Nu_{tp} = \begin{cases} 982\ \beta^{*1{,}101}\ We_m^{0{,}315} Bo^{0{,}320} \rho^{*-0{,}224} & , Bd < 4 \\ 18{,}495\ \beta^{*0{,}248} Re_v^{0{,}135} Re_{lo}^{0{,}351} Bd^{0{,}235} Bo^{0{,}198} \rho^{*-0{,}223} & , Bd \geq 4 \end{cases} \quad (7.3)$$

Bond number less than 4 represents microscale geometries and macroscale for Bond number greater than or equal to 4. The Bond number is defined as:

$$Bd = \frac{(\rho_l - \rho_v) g d_h^2}{\sigma} \quad (7.4)$$

Where d_h is the hydraulic diameter, ρ_l is the liquid density, ρ_v is the vapor density and g is the gravitational constant. The density ratio ρ^* is defined as:

$$\rho^* = \frac{\rho_l}{\rho_v} \quad (7.5)$$

β^* takes the chevron angle into account and is defined as:

$$\beta^* = \frac{\beta}{\beta_{max}} \quad (7.6)$$

Where $\beta_{max} = 70°$. The homogeneous Weber number We_m is defined as:

$$We_m = \frac{G^2 d_h}{\rho_m \sigma} \quad (7.7)$$

Where σ is the surface tension, G is the mass flux and ρ_m is the homogenous density:

$$\rho_m = \frac{1}{\frac{x_m}{\rho_v} + \frac{1 - x_m}{\rho_l}} \quad (7.8)$$

$$G = \frac{\dot{m}}{A_{cross} N_{ch}} \quad (7.9)$$

x_m is the mean vapor fraction and A_{cross} is the cross dimensional area. The boiling number Bo is defined as:

$$Bo = \frac{q''}{G\gamma} \quad (7.10)$$

q'' is the heat flux and γ is the latent heat of vaporization. The Reynolds number for vapor, Re_v is defined as:

$$Re_v = \frac{Gxd_h}{\mu_v} \quad (7.11)$$

Where x is the vapor fraction and μ_v is the dynamic viscosity for vapor phase. The Reynolds number for a liquid flow, Re_{lo} is defined as:

$$Re_{lo} = \frac{Gd_h}{\mu_l} \quad (7.12)$$

Where μ_l is the dynamic viscosity for the liquid phase. The Nusselt number is used to calculate the heat transfer for the two-phase flow:

$$h_{tp} = \frac{Nu_{tp}\, k_l}{d_h} \quad (7.13)$$

Where k_l is the conductivity for the liquid phase.

When the vapor quality is between $0{,}90 < x < 1$ the heat transfer coefficient will decrease linearly down to $600\frac{W}{m^2K}$ (Eikevik, 2016). When $x = 1$ the heat transfer coefficient for the refrigerant is found using the Martin correlation for single-phase flow in a plate heat exchanger (García-Cascales et al., 2007). The Nusselt number is given by:

$$Nu = 0{,}122Pr^{\frac{1}{3}}\left(\frac{\mu}{\mu_{wall}}\right)^{\frac{1}{6}}(fRe^2\sin(2\beta))^{0{,}374} \quad (7.14)$$

Where μ is the viscosity for the fluid, μ_{wall} is the viscosity at the wall and the friction factor f is given by:

$$\frac{1}{\sqrt{f}} = \frac{\cos\beta}{\left(0{,}18\tan\beta + 0{,}36\sin\beta + \frac{f_o}{\cos\beta}\right)^{1/2}} + \frac{1-\cos\beta}{\sqrt{3{,}8\,f_1}} \quad (7.15)$$

and f_0 and f_1 is defined by the Reynolds number:

$$f_o = \begin{cases} \frac{64}{Re} & , \quad Re < 2000 \\ (1{,}8\log_{10}Re - 1{,}5)^{-2} & , \quad Re \geq 2000 \end{cases} \quad (7.16)$$

$$f_1 = \begin{cases} \frac{597}{Re} + 3{,}85 & , \quad Re < 2000 \\ \frac{39}{Re^{0{,}289}} & , \quad Re \geq 2000 \end{cases} \quad (7.17)$$

The Nusselt number is used to calculate the heat transfer coefficient:

$$h = \frac{Nu\,k}{d_h} \quad (7.18)$$

The heat transfer coefficient for the water in the evaporator is found using the Martin correlation for single-phase flow in a plate heat exchanger.

7.2.1 Frictional Pressure Drop

The frictional pressure drop in the evaporator caused by the refrigerant is predicted using two-phase friction factor coefficient for plate heat exchangers from Amalfi et al. (2016b). The friction factor is based on 1513 pressure drop data points and can be predicted as follows:

$$f_{tp} = C * 15{,}698\, We_m^{-0{,}475} Bd^{0{,}255} \rho^{*-0{,}571} \quad (7.19)$$

Where the C parameter takes the effect of the corrugation angle into consideration:

$$C = 2{,}125\, \beta^{*9{,}993} + 0{,}955 \quad (7.20)$$

When the refrigerant is being superheated the friction factor is calculated using (7.15). The friction factor is used to calculate the frictional pressure drop at each step(Δy) in the evaporator:

$$\Delta P_{fric} = \frac{2\, f\, G^2 \Delta y}{d_h * \rho_m} \quad (7.21)$$

The inputs for the evaporator is given in Table 7.1. The length and width is based on the chosen brazed plate heat exchanger. The height and pitch of the corrugation and chevron angle is taken from (Longo et al., 2015a). The thickness of the plates is chosen based on typical values for BPHE (Wang et al., 2007). The plate thickness needs to be able to withstand the pressure level in the heat exchanger. Maximum number of plates are 250 equal to 125 channels.

Table 7.1 Evaporator inputs

Inputs	**Value**	
Length L	0,450	[m]
Width W	0,243	[m]
Number of channels N_{ch}	Variable	[-]
Maximum number of channels $N_{ch;max}$	125	[-]
Corrugation pitch p	0,008	[m]
Height of the corrugation b	0,002	[m]
Hydraulic diameter d_h	0,0035	[m]
Chevron angle β	45	[deg]
Thickness of plate Th_m	0,0005	[m]
Superheat T_{sh}	5	[K]

7.3 Condenser

In the condenser heat is transferred from the refrigerant to the water, heating the water while decreasing the enthalpy and thus the vapor quality of refrigerant. The refrigerant will go through a transition from a superheated single-phase flow at the inlet to a subcooled single-phase flow at the outlet of the condenser by going through a two-phase region with condensation. The superheated and subcooled region are calculated using the Martin correlation for single-phase flow. The two-phase heat transfer coefficient is modeled with Longo et al. (2015b) correlation for condensation in plate heat exchangers. The correlation is based on and compared against an experimental data set covering a range of operating conditions, geometries and fluids. The heat transfer coefficient is giving by:

$$h_{sat} = 1{,}875\ \Phi \left(\frac{k_l}{d_h}\right) Re_{eq}^{0{,}445} Pr_l^{1/3} \qquad (7.22)$$

Where Φ is an enlargement factor, Pr_l is the liquid Prandtl number and Re_{eq} is the equivalent Reynolds number given by:

$$Re_{eq} = \frac{G_{eq} d_h}{\mu_l} \qquad (7.23)$$

Where the equivalent mass flux is:

$$G_{eq} = G\left[(1 - x_m) + x_m \left(\frac{\rho_l}{\rho_g}\right)^{1/2}\right] \qquad (7.24)$$

The heat transfer coefficient for the water in the condenser is found using the Martin correlation for single-phase flow in a plate heat exchanger.

7.3.1 Frictional Pressure Drop

The frictional pressure drop in the condenser is predicted using a linear equation based on the kinetic energy per unit volume from Longo (2010). The equation is based on experimental data with hydrocarbons in BPHE:

$$\Delta P_{fric} = 1{,}90 \frac{KE}{V} \qquad (7.25)$$

The frictional pressure loss is given in kPa where:

$$\frac{KE}{V} = \frac{G^2}{2\,\rho_m} \qquad (7.26)$$

The frictional pressure drop in the condenser will not be calculated per control volume like it is done in the evaporator, so the temperature during condensation will be constant.

The inputs for the condenser is given in Table 7.2. The length and width is based on the chosen brazed plate heat exchanger. The height and pitch of the corrugation, enlargement factor and chevron angle are from (Longo, 2010). The thickness of the plates is chosen based on typical values for BPHE (Wang et al., 2007). The plate thickness needs to be able to withstand the pressure level in the heat exchanger. Maximum number of plates are 250 equal to 125 channels.

Table 7.2 Condenser inputs

Inputs	**Value**	
Length L	0,450	[m]
Width W	0,243	[m]
Number of channels N_{ch}	Variable	[-]
Maximum number of channels $N_{ch;max}$	125	[-]
Corrugation pitch p	0,008	[m]
Height of the corrugation b	0,002	[m]
Hydraulic diameter d_h	0,0035	[m]
Chevron angle β	45	[deg]
Enlargement factor Φ	1,20	[-]
Thickness of plate th_m	0,0005	[m]
Wanted Subcooling T_{sc}	1	[K]

7.4 Suction Gas Heat Exchanger

The suction gas heat exchangers are simplified in the model. The wanted superheat for the gas is chosen and the enthalpy needed is transferred from subcooling of the liquid with 100% efficiency. On the gas side of the heat exchanger a pressure loss is subtracted from the inlet pressure. The pressure drop is taken from the manufactures calculation tools and are given for the selected heat exchanger and refrigerant. For R600 the pressure loss equals to 51,8 kPa and 52,4 kPa for R600a. The pressure loss on the liquid side is not taken into account.

7.5 Pressure Loss in the Heat Exchangers

The measured pressure drop in the heat exchangers consists of several components. The total pressure drop in the evaporator is calculated by (Amalfi et al., 2016a):

$$\Delta P_{tot,evap} = \Delta P_G + \Delta P_{acc} + \Delta P_{fric} + \Delta P_p \quad (7.27)$$

And the total pressure drop in the condenser (Longo, 2010):

$$\Delta p_{tot,cond} = -\Delta P_G - \Delta P_{acc} + \Delta P_{fric} + \Delta P_p \quad (7.28)$$

Where ΔP_G is the pressure loss due to gravity, ΔP_{acc} is pressure loss due to acceleration(or deceleration), ΔP_p is pressure loss across the inlet and outlet ports in addition to the frictional pressure loss ΔP_{fric} which is calculated in (7.21) and (7.25). The ΔP_G is negative in the condenser because it's chosen that the refrigerant flows downwards, increasing the pressure. In the condenser the refrigerant decelerate when it is transitioning from gas to liquid, increasing the pressure. The different components are defined by:

$$\Delta P_G = \rho_m \, g \, L_{plate} \quad (7.29)$$

$$\Delta P_{acc} = G^2 \Delta x \left(\frac{1}{\rho_g} - \frac{1}{\rho_l} \right) \quad (7.30)$$

$$\Delta P_p = 0{,}75 \, N_{pass} \left[\left(\frac{G_p^2}{2\rho} \right)_{in} + \left(\frac{G_p^2}{2\rho} \right)_{out} \right] \quad (7.31)$$

Where L_{plate} is the length of the plate. The number of passes N_{pass} is chosen to be 1 in the model.

7.6 Compressor

The compressor work is calculated using isentropic efficiency and a heat loss. The isentropic efficiency is calculated using (7.32) using the pressure ratio (Eikevik et al., 2016). The formula is based on measurements done on a piston compressor, it is not measured on the chosen compressors for this system. However, it does take the change in efficiency based on pressure ratio into account, instead of using a constant efficiency for all pressure ratios. The heat loss is constant and equal to 10% of the compressor work.

$$\eta_{is} = -0{,}00000461\,PR^6 + 0{,}00027131\,PR^5 - 0{,}00628605\,PR^4 + 0{,}07370258\,PR^3 - 0{,}46054399\,PR^2 + 1{,}40653347\,PR - 0{,}87811477 \quad (7.32)$$

The volumetric efficiency is calculated using (7.33), which is made from the same measurements.

$$\lambda = 0{,}0011\,PR^2 - 0{,}0487\,PR + 0{,}9979 \quad (7.33)$$

7.7 Piping

The piping is used to connect the different components in the system. While the refrigerant is flowing through the pipes a pressure loss will occur due to friction between the pipe wall and the fluid, which in turn increases the work needed to be done by the compressor. This pressure loss is calculated by calling the built in function $Pipeflow$ (Klein, 2015). It returns the pressure drop for a given mass flow rate through a circular tube with a given length and diameter. The pressure drop is used to find the temperature fall by assuming that the flow has a constant enthalpy.

Another important aspect to take into account when designing the system is having sufficient flow velocity in the pipes, this is to ensure sufficient oil return. An insufficient oil return is one of the most important practical problems that needs to be solved when designing a heat pump system. Choosing an oil that can withstand the required temperatures, that mixes good with the refrigerant and that gives a sufficient oil return is important if the system should operate properly over several years. Insufficient oil return can result in oil holdup in the heat exchangers, especially in the evaporator, reducing the heat transfer. When the oil is not reaching the compressor to lubricate it and to remove heat, the result could be overheating or damage to the compressor.

To have a sufficient transportation of oil in vertical pipes Bäckström (1946) suggested that:

$$\rho_g u_g^2 \geq 126 \qquad (7.34)$$

u_g is gas velocity. For the liquid return lines a sufficient flow velocity would be $u_l > 0{,}5\ m/s$ (Eikevik, 2016).

The Norwegian Refrigeration and Heat Pump Norm recommends $9 - 10\ m/s$ in the suction pipeline, $6 - 7\ m/s$ in the pressure pipeline and $5\ m/s$ in the return pipeline (Haukås, 2015). This values are meant to give efficient oil return and moderate pressure/temperature loss in pipelines.

On the basis of the suggested flow velocities, diameters for the pipes have been chosen. The length and diameter of the different pipes can be found in Table 7.3, Table 7.4 and Table 7.5. This results in velocities around $9 - 10\ m/s$ in the suction line, $6 - 7\ m/s$ in the pressure pipeline and $2 - 3{,}5\ m/s$ in the return lines for the 3 systems. Which should give a sufficient oil return. The roughness is chosen to be $0{,}15\ mm$, this is equal to commercial galvanized steel pipes (Nellis and Klein, 2009).

Table 7.3 Pipe dimensions for R600

Pipe	Diameter [m]	Length [m]
L_{1-2}	0,10	1,5
L_{3-4}	0,11	1,5
L_{5-6}	0,06	0,75
L_{8-9}	0,03	1,5
L_{10-11}	0,03	1,5

Table 7.4 Pipe dimensions for R600a

Pipe	Diameter [m]	Length [m]
L_{1-2}	0,10	1,5
L_{3-4}	0,10	1,5
L_{5-6}	0,06	0,75
L_{8-9}	0,03	1,5
L_{10-11}	0,03	1,5

Table 7.5 Pipe dimensions for R1234ze(Z)

Pipe	Diameter [m]	Length [m]
L_{1-2}	0,11	1,5
L_{3-4}	0,11	1,5
L_{5-6}	0,06	0,75
L_{8-9}	0,03	1,5
L_{10-11}	0,03	1,5

7.8 Iterative Optimization

A set of error functions are used to find the correct input values that corresponds with the different operating conditions. A guess is made and the program will run an iterative process, minimizing the error function finding the correct values.

Mass flow rate

The mass flow rate of the system is decided by the boundary conditions of the system. The temperature of the water flows in condenser and evaporator are given in the case and the mass flow rate are decided upon. By minimizing the wanted and the actual temperature difference of the water exiting the condenser by varying the mass flow rate of the refrigerant. This is done using EES' inbuilt MIN/MAX function on the following error function:

$$\mathrm{err_{temp;cond}} = \mathrm{abs(T_{w;real;out} - T_{water;out;cond})} \quad (7.35)$$

This function is used for the different fluids at $T_e = 40\ °C$ and $T_c = 100\ °C$ and the mass flow rate is then kept constant for other operating conditions. It will cause a slight deviation for the water temperatures in heat exchangers but it is done to keep operating conditions similar for the 3 systems.

Condensation pressure

Due to a pressure drop in the pipe between the compressor exit and the condenser inlet an error function is made to account for the loss. It is done by guessing the pressure drop in the pipe and adding this to the compressor outlet pressure:

$$\mathrm{P_{guess;comp}} = \mathrm{X\ [Pa]} \quad (7.36)$$

$$P_{out;comp} = P_{ref;cond} + P_{guess;comp} \quad (7.37)$$

The error function is then minimized using MIN/MAX:

$$err_{comp} = abs(P_{guess;comp} - \Delta P_{56}) \quad (7.38)$$

Where ΔP_{56} is the pressure drop in the pipe between the compressor and evaporator.

Number of Plates in Evaporator and Condenser

The number of plates used in the heat exchangers is decided by two error functions that compares the calculated length of the heat exchanger versus the length of the plates. If it is not possible to get the exact length the number of plates is increased so the length out of the heat exchangers is shorter than the plate. This is done by varying the number of channels in the heat exchangers. The error functions used is:

$$err_{length;cond} = abs(L_{plate;cond} - L_{out;cond}) \quad (7.39)$$

$$err_{length;evap} = abs(L_{plate;evap} - L_{out;evap}) \quad (7.40)$$

8 Economic model

An economic model has been created to compare the operational and investment costs of the different heat pump solutions in addition to comparing them with a traditional heating solution, namely a natural gas boiler. The annual cost for the different solutions is calculated by summing the annual capital cost, the annual operational cost and the annual maintenance cost as shown in (8.1):

$$AC = \sum (I_0\ a)_n + \sum (W_e\ e) + \sum MC \qquad (8.1)$$

Where I_0 is the additional investment cost for each subsystem, a is the annuity factor, W_e is the energy demand, e is the energy price and MC is the maintenance costs. The maintenance cost is calculated as a percentage of the investment cost. The annuity factor is calculated by:

$$a = \frac{r}{1 - (1 + r)^{-n}} \qquad (8.2)$$

Where r is the real interest rate and n is the depreciation time.

To assess if it is profitable to invest in the different heat pump solutions over a natural gas boiler a profitability analysis is conducted. This is done using the Present Value Method and Pay-Off Time (Stene, 2016). The Present Value Method shows the absolute profitability of an investment. If a heat pump project has a $PV > 0$ then its regarded as a profitable investment. PV is calculated by:

$$PV = \frac{B}{a} - I_0 \qquad (8.3)$$

Where B is the net annual earnings/saving and I_0 is the additional investment cost compared to competing heating systems. B gives the annual cost reduction for operation and maintenance compared to other heating solutions. B is calculated by:

$$B = (annual\ savings - annual\ costs) \qquad (8.4)$$

Pay-Off Time will result in the number of years it takes before the sum of net annual savings equals to the additional investment cost, while taking account the real interest rate. This makes the method more accurate than "Pay-Back Time". Pay-off time is calculated by:

$$PO = \frac{ln\left[\left(1 - \left(\frac{I_0}{B}\right) r\right)^{-1}\right]}{ln(1+r)} \quad (8.5)$$

In addition to this the specific heating cost is calculated:

$$SHC = (\frac{AC}{Q_h}) \quad (8.6)$$

The specific heating cost does not say anything about the profitability of the investment, but will give the cost per kWh.

Lastly a sensitivity analysis is conducted by varying the electricity prices and natural gas prices.

The electricity and natural gas prices was based on the average prices for the second half of 2013 in member countries of the European Union. The prices for natural gas was 0,04 Euro/kWh and 0,118 Euro/kWh for electricity (Eurostat, 2016). An exchange rate of 1 Euro equal to 9,3 NOK was used in the calculations. Resulting in a price of 0,37 NOK/kWh for natural gas and 1,10 NOK/kWh for electricity. Inputs can be seen in Table 8.1.

Table 8.1 Inputs used in economic calculations

Inputs	**Value**
Real interest rate r	5 [%]
Depreciation time n	25 [years]
Running time	4400 [hours]
Heat Duty Q	210 [kW]
Energy demand	924 000 [kWh]
Annual maintenance cost heat pump	6 [%]
Annual maintenance cost gas boiler	3 [%]
Efficiency gas boiler η_{gas}	0,95 [-]
Gas price e_{gas}	0,37 [NOK/kWh]
Electricity price e_{el}	1,10 [NOK/kWh]

9 Simulation Results

The effect of varying the operating conditions for the 3 heat pump cycles is assessed in the following chapter. The condensation temperature was kept constant while the evaporation temperature was varied, and opposite when the evaporation temperature was kept constant and condensation temperature was varied. The mass flow rate was also kept constant for all operating condition. This was done to reduce the degrees of freedom, easing the process of finding the amount of plates and operating pressure for the given conditions. This will also highlight the effect of the individual parameter.

The results were then used to do economic evaluations for the different systems, including finding a suitable compressor and calculate the total investment cost and operating cost. This was then used to do investment analysis for the different solutions comparing them against a natural gas boiler.

9.1 The Effect of Changing the Evaporation Temperature

The effect on the systems COP by varying the evaporation temperature is seen in Figure 9.1. The condensation temperature was kept at 100 ºC. The system using R1234ze(Z) has the highest COP, and by increasing the evaporation temperature the COP increases from 3 to 3,8. The COP for R600 and R600a is lower mainly due to an additional pressure drop of approximately 50 kPa in the suction gas heat exchanger due to the need for additional superheating. Increasing the evaporation temperature still have a beneficial effect, increasing the COP to 3,5 for R600 and 3,4 for R600a from 2,8.

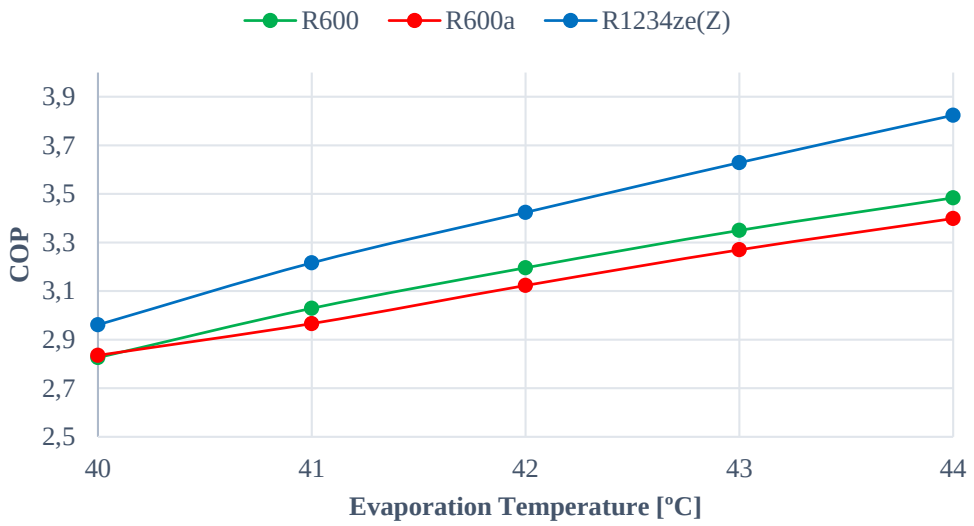

Figure 9.1 COP vs evaporation temperature

One of the main reasons for the increase in COP is the reduction of pressure drop in the evaporator. The pressure drop is plotted against the evaporation temperature in Figure 9.2. The reduction of pressure drop in the evaporator has several beneficial consequences; it reduces the pressure ratio for the system, increasing the compressors isentropic and volumetric efficiency in addition to reducing the required work need to be done by the compressor. It also reduces the required compressor volume at the compressor inlet due to increase vapor density. This reduces the required size of the compressor, potentially decreasing the investment cost. As seen in the figure, R1234ze(Z) have the highest overall pressure drop of the refrigerants, but the difference will be reduced at increasing temperatures. R600a show similar pressure drops to R1234ze(Z) but slightly lower overall. R600 have the lowest pressure drops, especially at 40 ºC but the difference is smaller at 44 ºC. When comparing the pressure drop Figure 9.2 with the corresponding number of channels in Figure 9.3, an significant reduction in pressure drop

can be observed by a relatively small increase in heat exchanger channels. R1234ze(Z) requires the most channels, while R600a requires the fewest.

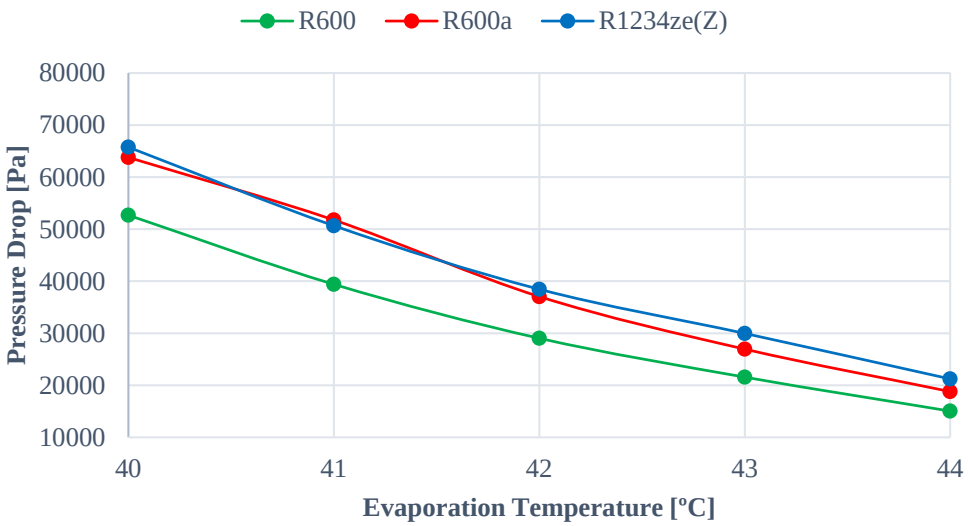

Figure 9.2 Pressure drop in evaporator at different evaporation temperatures

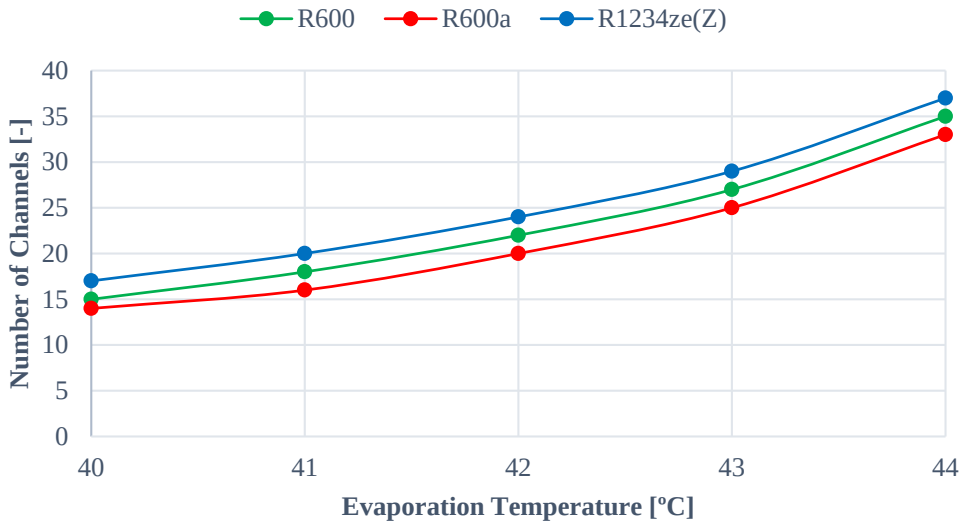

Figure 9.3 Number of channels required in the evaporator for different evaporation temperatures

The required compressor volume for the different systems can be seen in Figure 9.4. R600a requires a significantly smaller compressor volume, compared to the other refrigerants. The required compressor volume is similar for R600 and R1234ze(Z) mainly due to the additional pressure loss in the R600 system from the suction gas heat exchanger. Without the additional pressure drop, the required compressor volume would be even smaller for R600 and R600a.

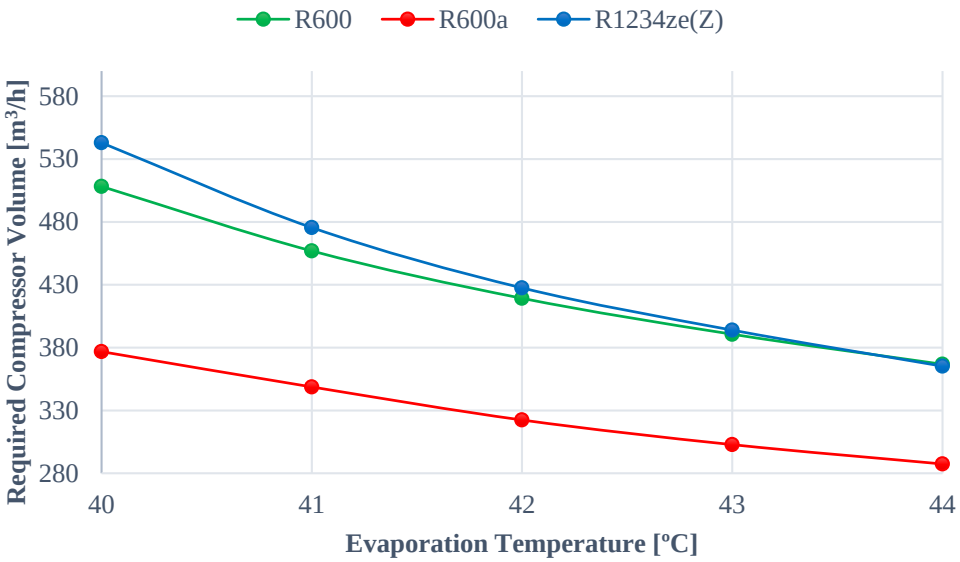

Figure 9.4 Required compressor volume at different evaporation temperatures

The required compressor work for the given evaporation temperatures is shown in Figure 9.5. R600 has the highest required work input at 40 °C but R600a will surpass it, requiring the highest work input of the systems at higher temperatures. This is reflected in the COP in Figure 9.1.

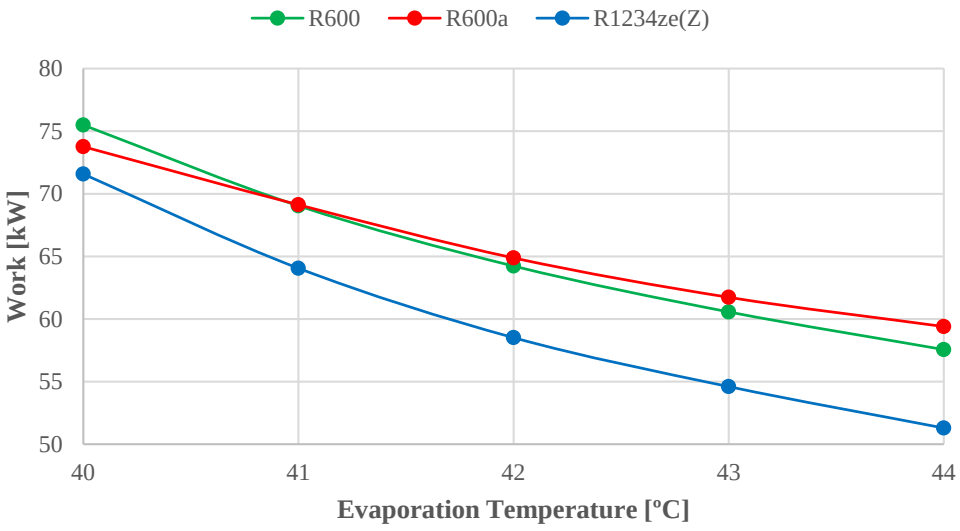

Figure 9.5 Required compressor work at different evaporation temperatures

In Figure 9.6 the pressure drop in the condenser is plotted to the corresponding evaporation temperature. R1234ze(Z) has the lowest pressure drop and R600a has the highest. All of these values are quite small and do not affect the performance much.

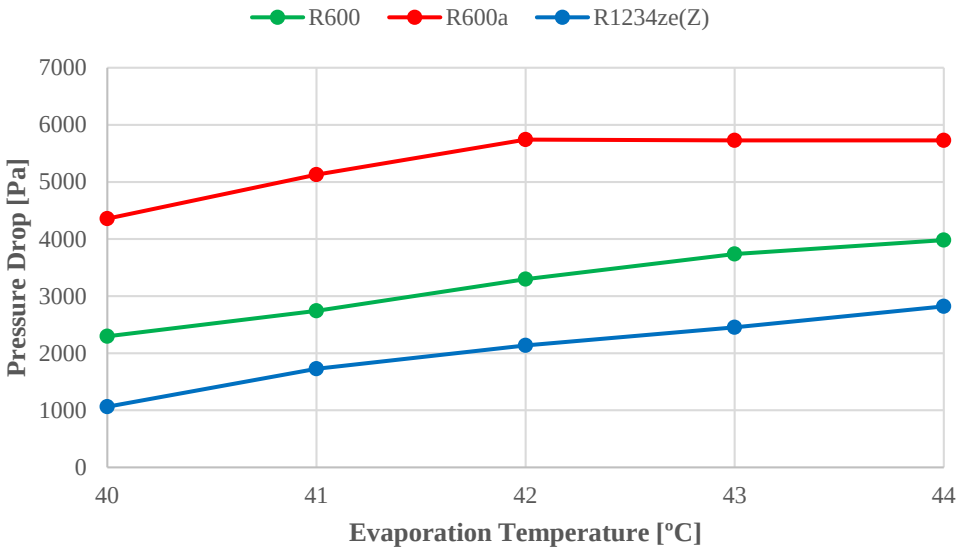

Figure 9.6 Pressure drop in the condenser at different evaporation temperatures

Results in tabular form can be found in Appendix A.

The heat transfer coefficient and pressure drop through the evaporator for R600 is shown in Figure 9.7 and Figure 9.8 respectively. The solid line represents an evaporation temperature of 40 ºC, while the dashed line represents 44 ºC. The blue lines represent the heat transfer coefficient during evaporation while the red lines represent the superheated region. Most of the heat transfer area is occupied by evaporation, only 6 cm of the plate is used for superheating. A large part of the heat exchanger is occupied for the region between $0{,}9 < x < 1$. During the superheating of the refrigerant, the biggest increase of pressure loss occurs, as seen in the Figure 9.8. This is seen for all of the refrigerants. The heat distribution through the heat exchanger and corresponding P-h diagrams can be found in Appendix A.

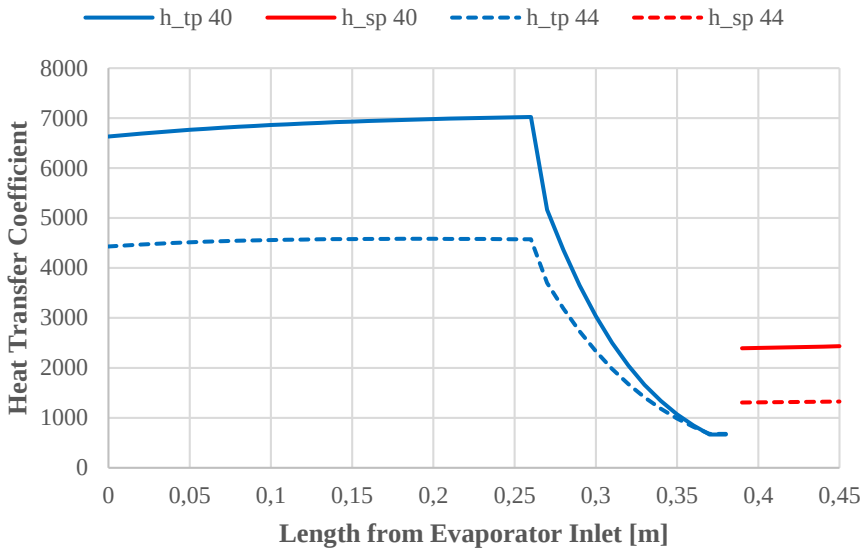

Figure 9.7 Heat transfer coefficient through evaporator for R600 for evaporation temperatures of 40 ºC and 44 ºC

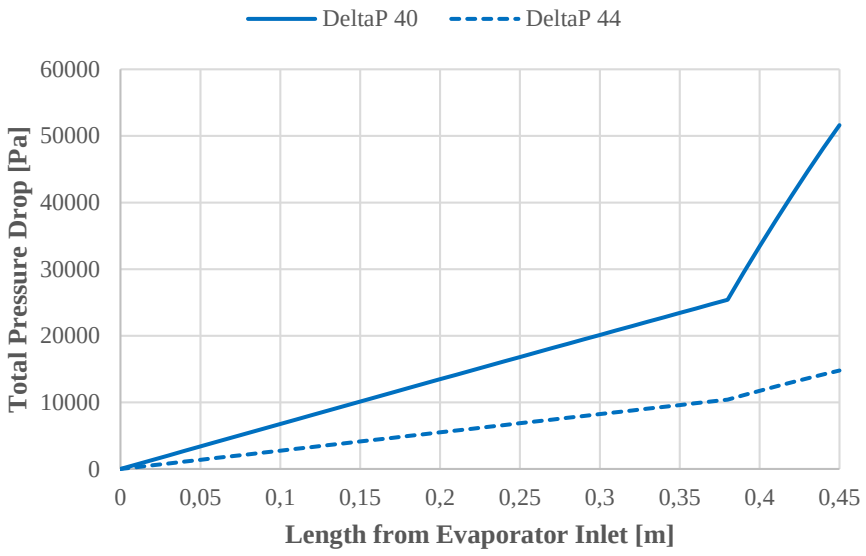

Figure 9.8 Total pressure drop through evaporator for R600 for evaporation temperatures of 40 ºC and 44 ºC

The heat transfer coefficient and pressure drop through the evaporator for R600a is shown in Figure 9.9 and Figure 9.10 respectively. The heat transfer coefficient is larger for R600a than R600. It can be noted that the required length for superheating is 1 cm larger at 44 ºC than for 40 ºC. The increase in pressure drop is larger than for R600 during both evaporation and superheating. A slightly larger area of the heat exchanger is occupied for the region between $0{,}9 < x < 1$ than for R600. The heat distribution through the heat exchanger and corresponding P-h diagrams can be found in Appendix A.

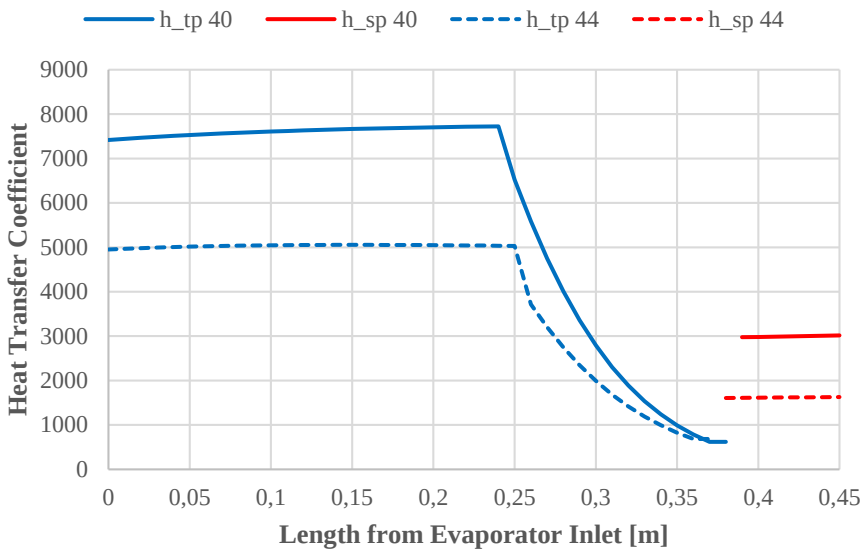

Figure 9.9 Heat transfer coefficient through evaporator for R600a for evaporation temperatures of 40 ºC and 44 ºC

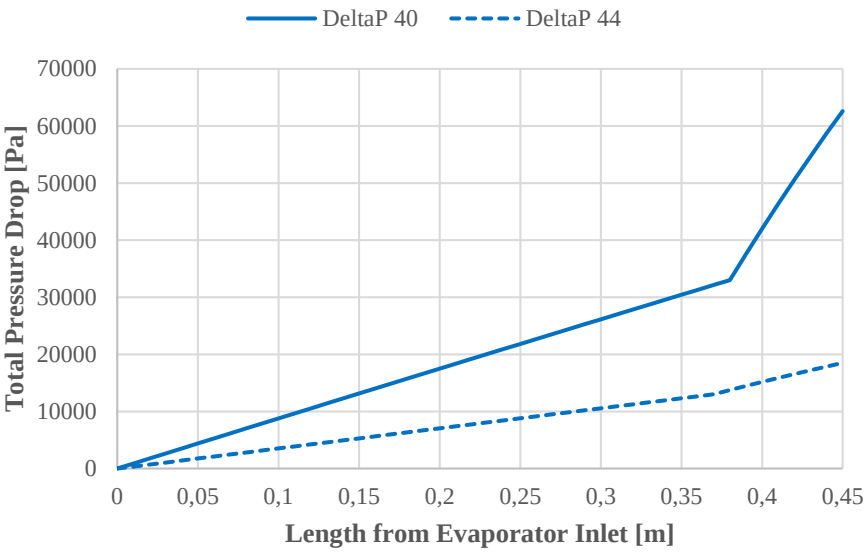

Figure 9.10 Total pressure drop through evaporator for R600a for evaporation temperatures of 40 ºC and 44 ºC

The heat transfer coefficient and pressure drop through the evaporator for R1234ze(Z) is shown in Figure 9.11 and Figure 9.12 respectively. R1234ze(Z) has the lowest heat transfer coefficient of the refrigerants. For an evaporation temperature of 40 ºC the heat exchanger is slightly over-dimensioned and the refrigerant reaches the wanted superheat 1 cm before the end of the plate. R1234ze(Z) has the smallest length required for superheating compared to the other refrigerants. However, the greatest increase in pressure loss for the selected refrigerants occurs for R1234ze(Z) when it is being superheated. The heat exchanger area occupied for the region between $0{,}9 < x < 1$ is slightly larger than R600 but lower than R600a. The heat distribution through the heat exchanger and corresponding P-h diagrams can be found in Appendix A.

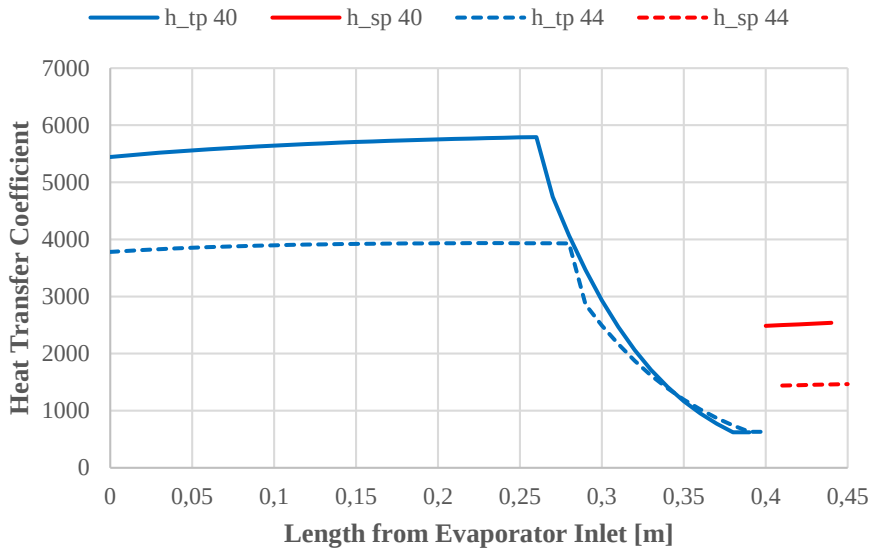

Figure 9.11 Heat transfer coefficient through evaporator for R1234ze(Z) for evaporation temperatures of 40 ºC and 44 ºC

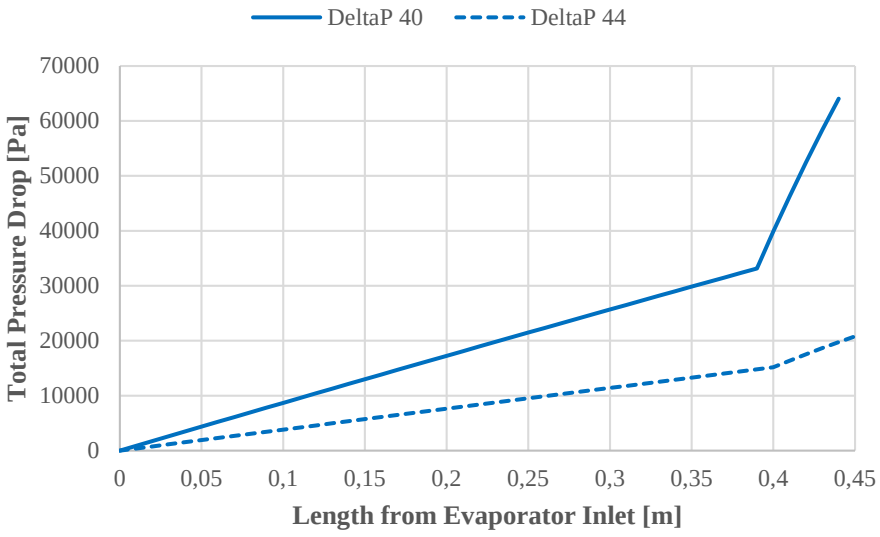

Figure 9.12 Total pressure drop through evaporator for R1234ze(Z) for evaporation temperatures of 40 ºC and 44 ºC

The effect of raising the evaporation temperature on the heat transfer coefficient in the condenser can be seen in Figure 9.13 for R600, in Figure 9.14 for R600a and Figure 9.15 for R1234ze(Z). The area used for desuperheating is significantly reduced due to a lower discharge gas temperature. The temperature distribution through the condenser for R1234ze(Z) can be seen in Figure 9.16 for 40 ºC and 44 ºC. At 44 ºC required temperature at the inlet of the evaporator is 12 K less than at 40 ºC. The result is a reduction in required heat transfer area.

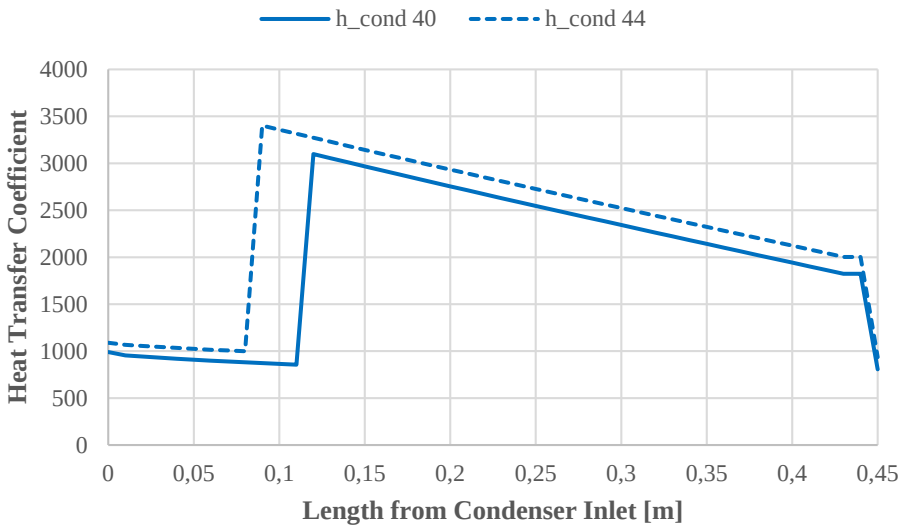

Figure 9.13 Heat transfer coefficient through the condenser for R600 for evaporation temperatures of 40 ºC and 44 ºC

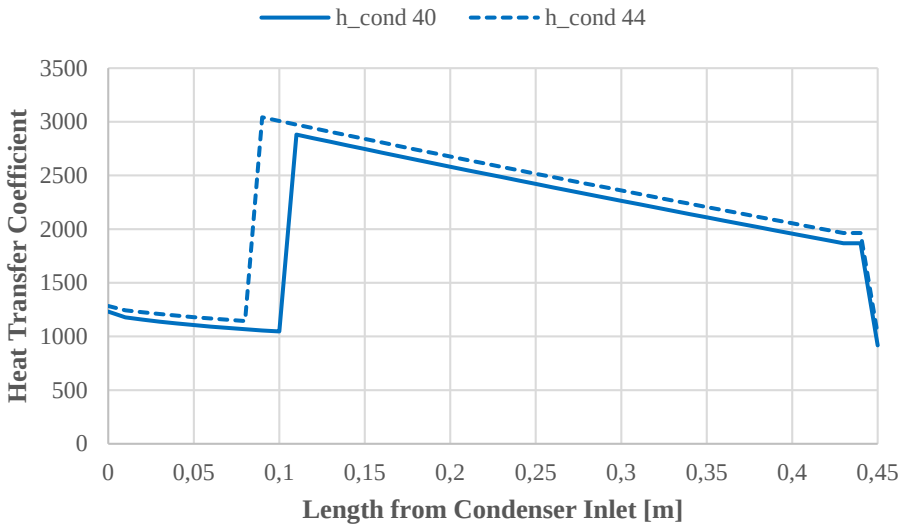

Figure 9.14 Heat transfer coefficient through the condenser for R600a for evaporation temperatures of 40 ºC and 44 ºC

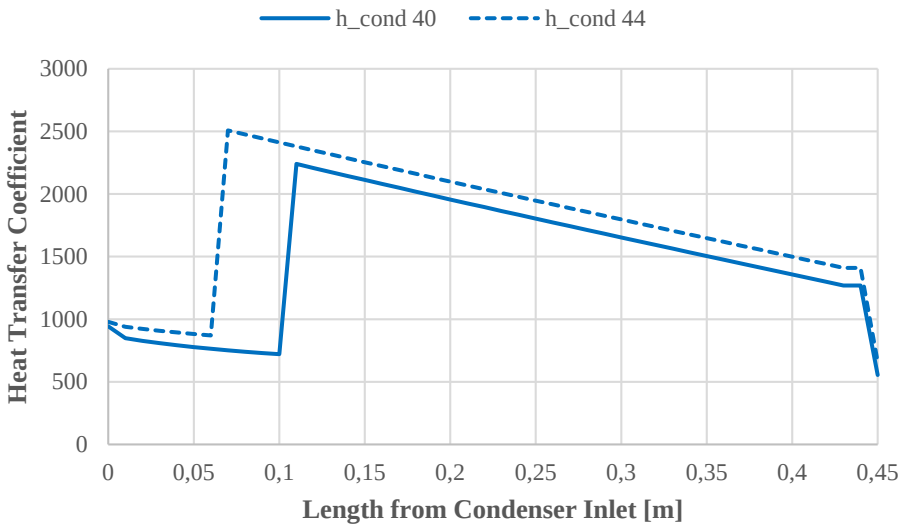

Figure 9.15 Heat transfer coefficient through the condenser for R1234ze(Z) for evaporation temperatures of 40 ºC and 44 ºC

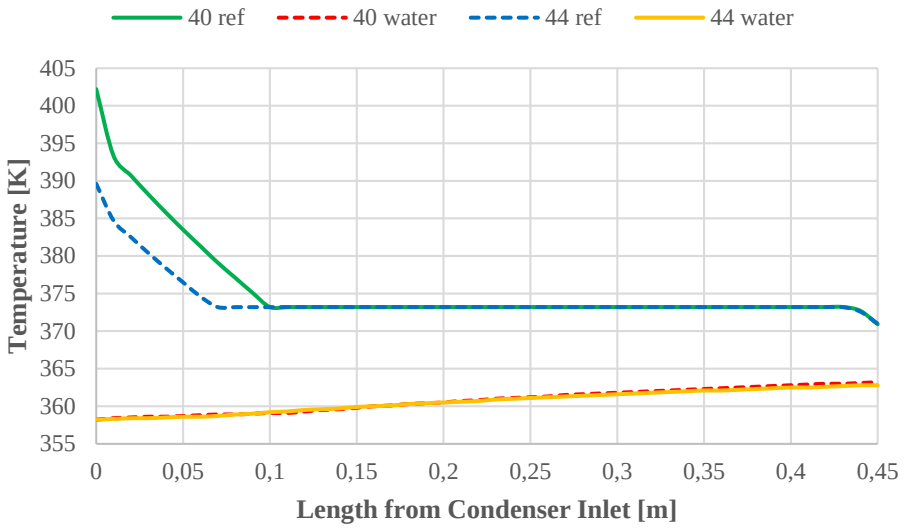

Figure 9.16 Temperature distribution in condenser for R1234ze(Z) for evaporation temperatures of 40 ºC and 44 ºC

The effect of changing the chevron angle in the evaporator for R1234ze(Z) at an evaporation temperature of 44 ºC is shown in Figure 9.17 and Figure 9.18. Having a large chevron angle will cause large pressure losses, increasing the heat transfer coefficient, reducing the number of required plates. When the chevron angle is 65º over half of the total pressure loss occurs when superheating the refrigerant. It can be noted that the increase in heat transfer coefficient between a chevron angle of 65º and 55º is around 20%, but the total pressure drop for 55º is about 40% of the pressure drop with an angle of 65º. The heat exchanger area occupied for the region between $0{,}9 < x < 1$ is increasing at increasing chevron angles. The total number of channels is not a problem at any angle for the chosen heat exchangers see Table 9.1.

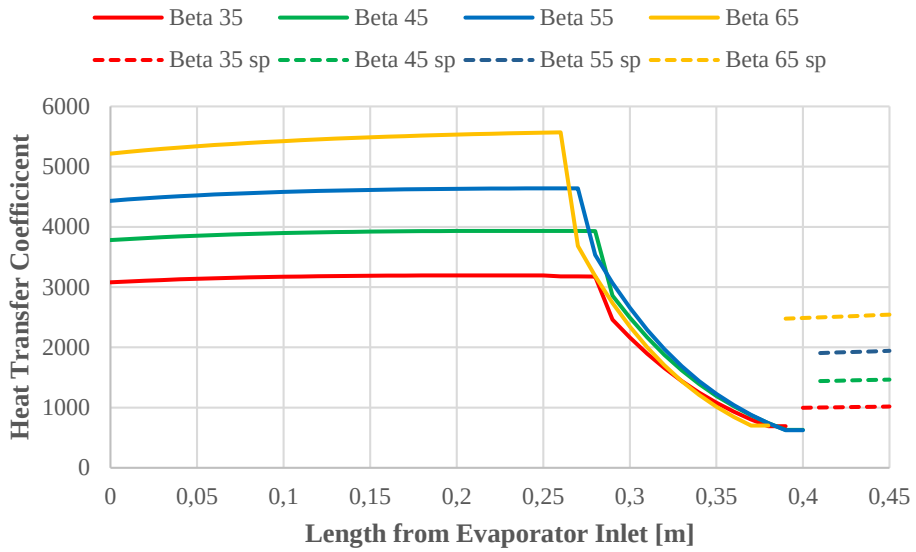

Figure 9.17 Heat transfer coefficient through evaporator for R1234ze(Z) at 44 ºC with different chevron angles

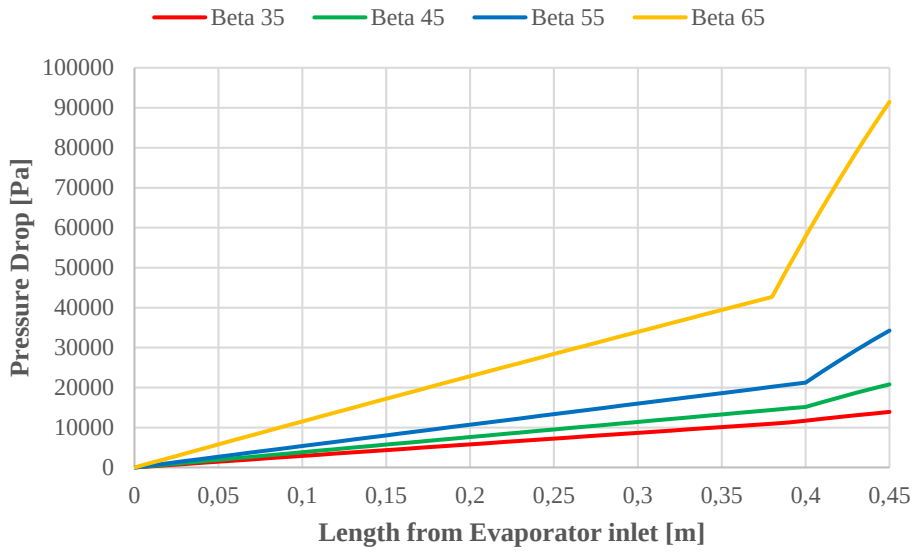

Figure 9.18 Total pressure drop through evaporator for R1234ze(Z) at 44 ºC with different chevron angles

Table 9.1 Chevron Angles and corresponding number of channels in evaporator

Chevron Angle β	**Number of channels**
35 º	47
45 º	37
55 º	31
65 º	25

9.2 The Effect of Changing the Condensation Temperature

The effect on the systems COP by varying the condensation temperature is seen in Figure 9.19. The evaporation temperature was kept at 40 ºC. The system using R1234ze(Z) will continue to have the highest COP. The increase in COP when reducing the condensation temperature is slightly lower for R1234ze(Z) than by increasing the evaporation temperature, but for R600 and R600a the effect is greater than changing the evaporation temperature. The COP for R600 and R600a is lower mainly due to an additional pressure drop of approximately 50 kPa in the suction gas heat exchanger due to the need for additional superheating.

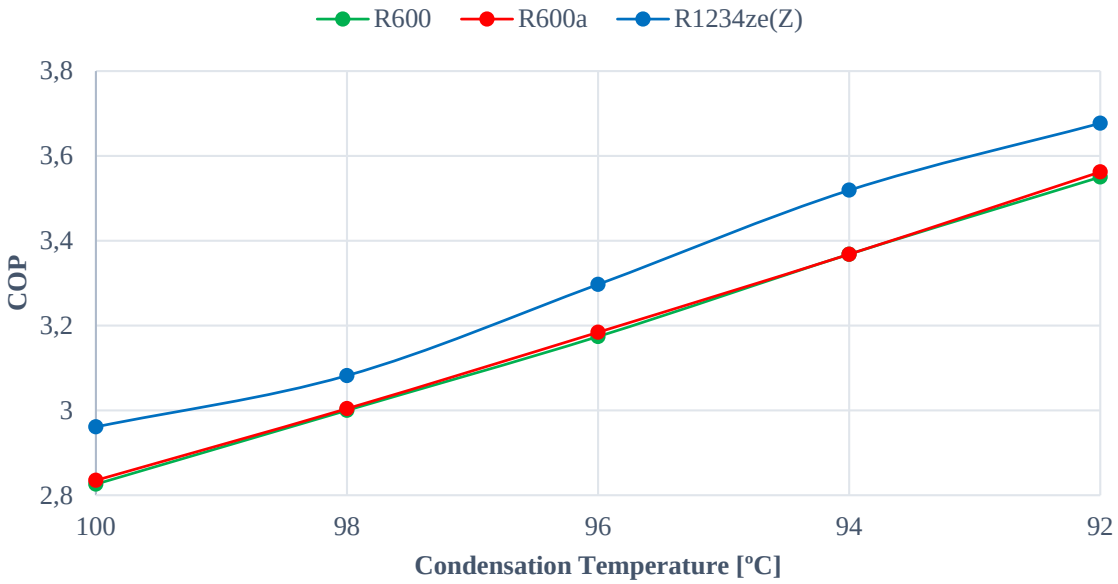

Figure 9.19 COP vs condensation temperature

However, it is important to note that by lowering the condensation temperature, the required heat transfer area increases exponentially. The number of channels required for the different condensation temperatures is shown in Figure 9.20. The maximum allowed number of plates for the chosen heat exchanger is 250, meaning a maximum of 125 channels. None of the

refrigerants were able to reach a condensation temperature lower or equal to 94 ºC with 40 ºC evaporation temperature. The results are plotted for all temperatures but the results for R600 and R600a below 96 ºC are therefore not valid for the current system. R1234ze(Z) was not able to have a condensation temperature of 96 ºC, due to requiring slightly more plates. This is due to a high pressure loss through the evaporator at 40 ºC giving a low compressor efficiency resulting in a high superheat on the vapor entering the condenser. By increasing the chevron angle in the condenser to 65 degrees it was possible to reduce the number of plates required as seen in Figure 9.20 for the lines with B=65. The increase heat transfers for B=65 is mainly due to an increase in heat transfer coefficient for water but also due to an increase in the enlargement factor for the refrigerants heat transfer correlation (1,24 instead of 1,20).

For the rest of the results the angle is assumed to be 45 degrees.

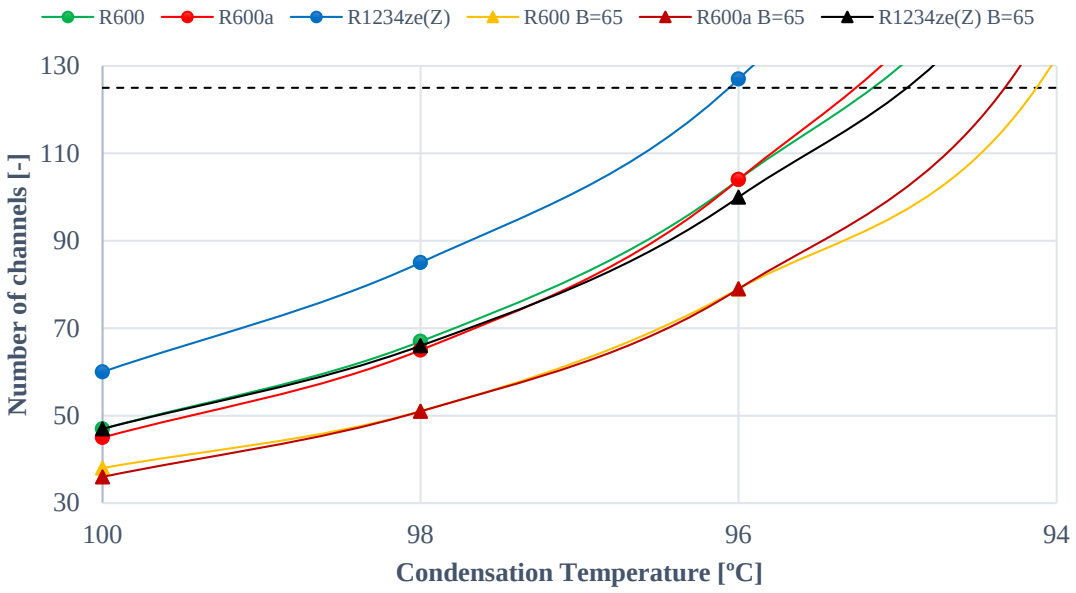

Figure 9.20 Number of channels required at different condensation temperatures and different chevron angles

The pressure drop in the evaporator corresponding to the different condensation temperatures is shown in Figure 9.21. There is an irregularity for R1234ze(Z) at 98 ºC, this is due to the calculation being slightly unstable at the chosen calculation step size, giving a larger value than it should have. The effect is however quite small, and is therefore ignored.

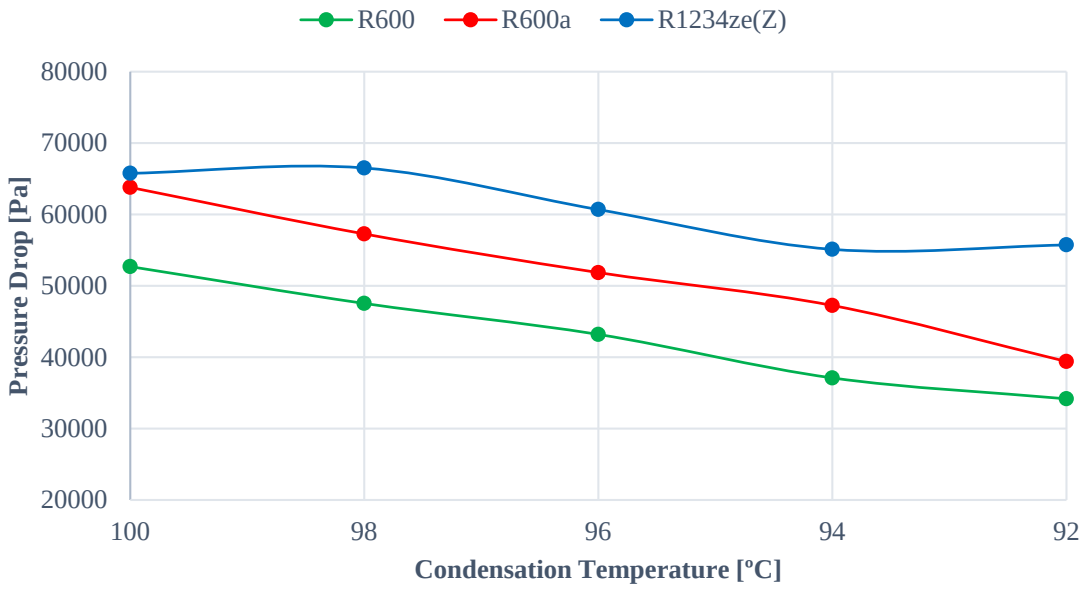

Figure 9.21 Pressure drop in the evaporator for different condensation temperatures

In Figure 9.22 the work is plotted against the condensation temperature. In the area were the results are valid for the system, the reduction in work for R1234ze(Z) is small, R600 and R600a have a slightly larger reduction in compressor work, approximately 8 kW for R600 and 7 kW for R600a when comparing 100 °C and 96 °C.

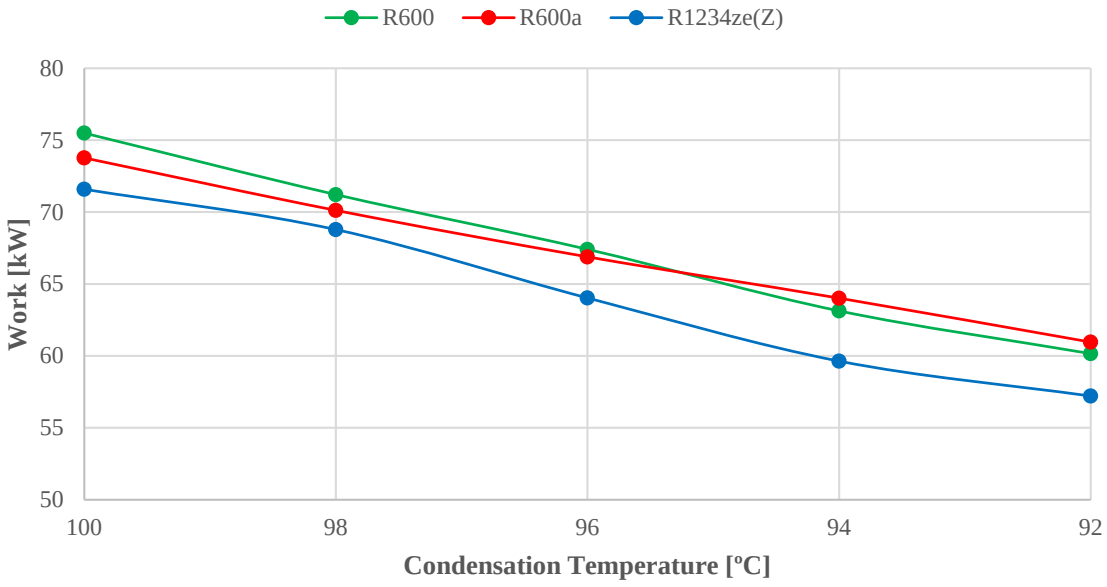

Figure 9.22 Work for different condensation temperatures

The effect of changing condensation temperature on the required compressor volume is shown in Figure 9.23. The reduction is minimal, due to a small reduction in pressure drop in the evaporator. The pressure drop in the condenser is shown in Figure 9.24. The pressure drop is

very small. The reason it goes below 0 is due to the contribution from the friction (7.25) gets smaller than the negative contribution from gravity (7.29) in (7.28). Which means that the pressure would increase through the condenser. The total pressure drop or gain is so small that it is almost negligible.

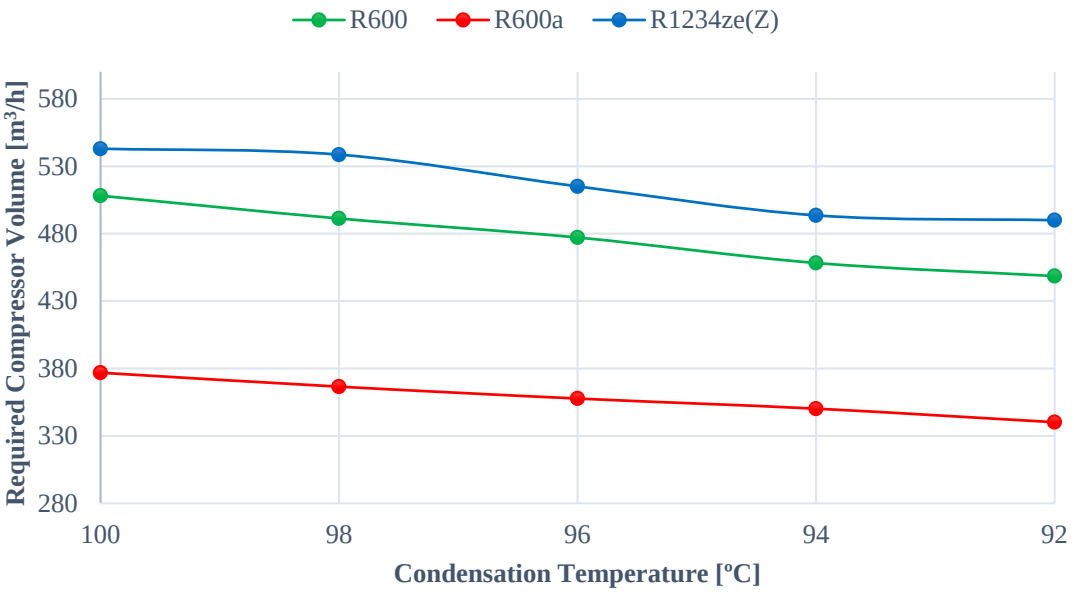

Figure 9.23 Required compressor volume for different condensation temperatures

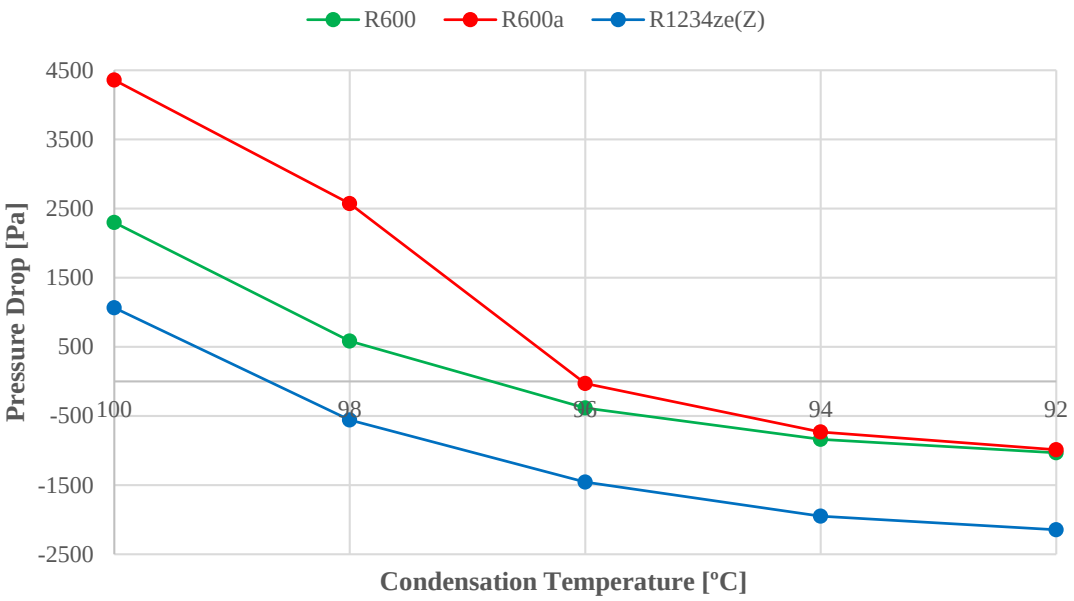

Figure 9.24 Pressure drop in condenser for different condensation temperatures

Results in tabular form can be found in Appendix A.

9.3 Economic Evaluations

In the first 2 subchapters the electricity and natural gas prices was based on the average prices for the second half of 2013 in member countries of the European Union. The last 2 subchapters show the effect of varying electricity and natural gas prices for the most cost efficient cycle.

9.3.1 Changing the Evaporation Temperature

As seen in (8.1) the annual cost consists of the capital cost, maintenance cost which is tied to the investment cost and the operational costs. When increasing the evaporation temperature, the amount of plates required in the evaporator increases, which in turn increases the investment cost. The increase in plates can be seen in Figure 9.3. However, the required number of channels is reduced in the condenser, due to a reduction in heat exchanger area required for desuperheating. The increase in number of plates in the evaporator will result in a smaller pressure loss through the evaporator, increasing the vapor density at the compressor inlet which reduces the required compressor volume. A reduction in the required compressor volume can lead to a smaller investment cost for the compressor. The variation in investment cost at different evaporation temperatures can be seen in Figure 9.25. The drops are due to smaller and cheaper compressor and a reduction in number of plates in the condenser, while requiring more plates in the evaporator.

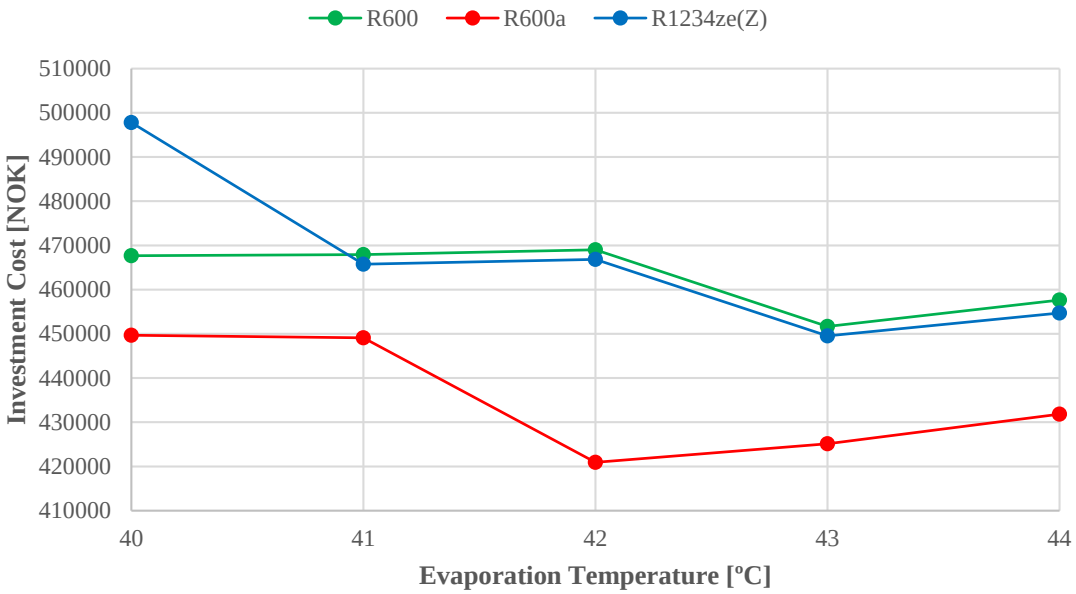

Figure 9.25 Investment cost at different evaporation temperatures

The reduction in investment cost will reduce the annual capital and maintenance cost and due to a reduction in compressor work the operational cost will decrease. Leading to a reduction of

total annual costs. The annual costs for the different heat pump solutions is shown in Figure 9.26. The annual cost of a gas boiler is also included in the plot. The gas boiler solution has the lowest annual cost of the 3 systems at 40 ºC, the R1234ze(Z) system will have a lower annual cost at 41 ºC while both R600 and R600a have a lower annual cost at 42 ºC.

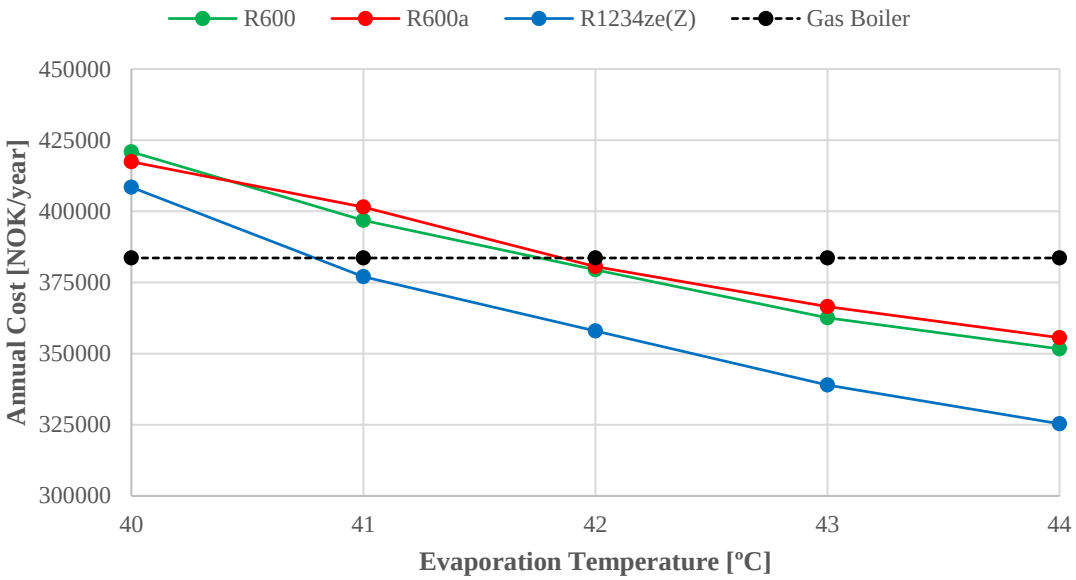

Figure 9.26 Annual cost vs evaporation temperature

The specific heating cost shown in Figure 9.27, gives the cost per kWh for the different heating solutions. It does not say anything about the investments profitability alone, but it shows that the cost per unit of energy is decreasing at increasing evaporation temperature for the 3 heat pump systems. Giving a lower energy cost per unit energy than the natural gas boiler.

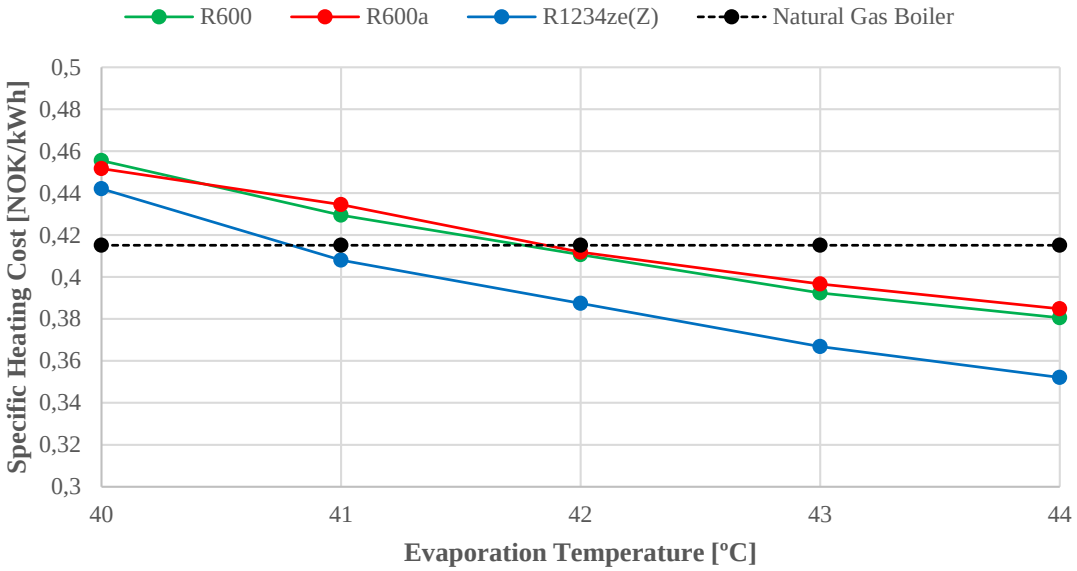

Figure 9.27 Specific heating cost vs evaporation temperature

The present value for the different heat pumps compared to a gas boiler solution is given in Figure 9.28. The higher the present value is, the more profitable the investment is. The R1234ze(Z) heat pump has a positive present value at evaporation temperature of 41 ºC, it also has the highest present value of the 3 systems. R600 and R600a can be regarded as profitable at 42 ºC, but their present value is close to 50% of R1234ze(Z).

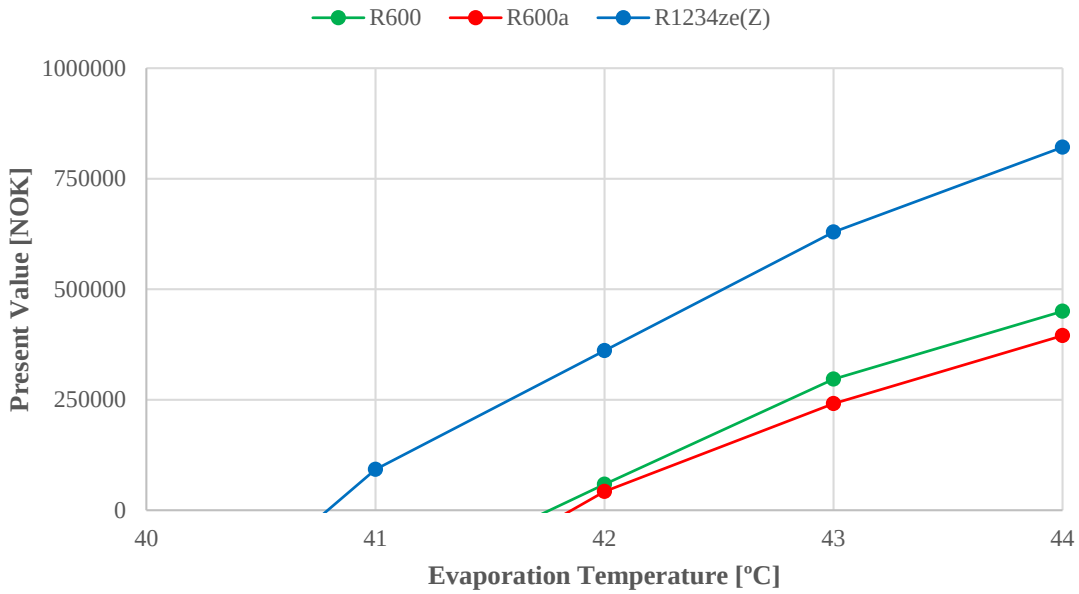

Figure 9.28 Present value at varying evaporation temperatures

The pay-off time is plotted against evaporation temperatures in Figure 9.29. When the value is negative the savings will not pay back the additional investment and the investment is not reasonable. Only positive values are plotted in the figure. It can be noted that for R1234ze(Z) at 41 ºC, R600 and R600a at 42 ºC that the amount of years before it becomes profitable is too long, even though it will pay itself back during its expected lifetime. The investment is more reasonable when the pay-off time is low, especially down to only a few years.

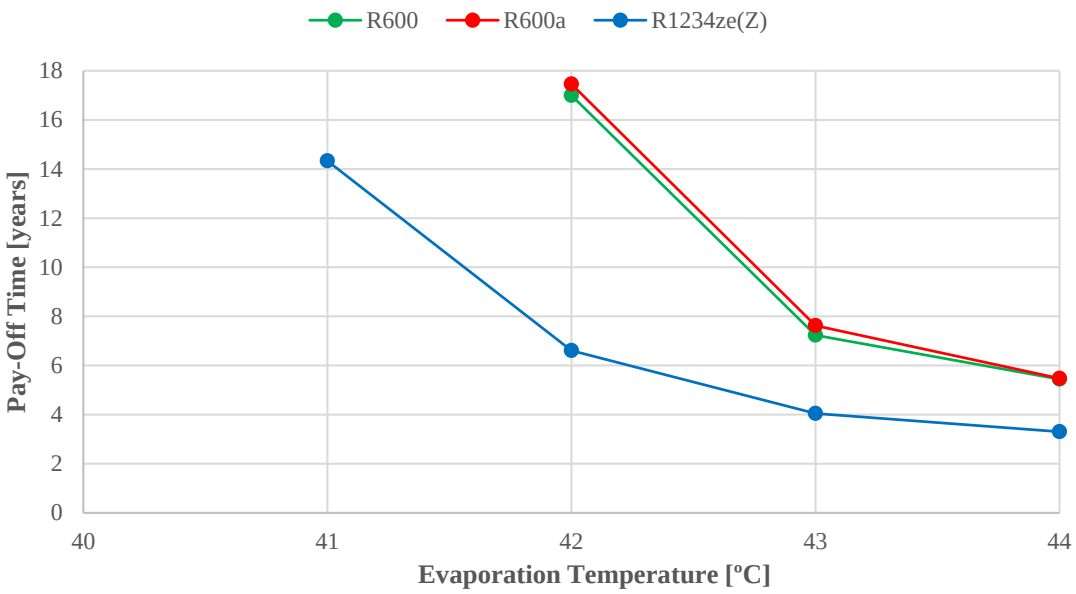

Figure 9.29 Pay-Off Time for different heat pump solution against a natural gas boiler

Results in tabular form can be found in Appendix A.

9.3.2 Changing the Condensation Temperature

When reducing the condensation temperature, the amount of plates required increases exponentially, which in turn increases the investment cost. The increase in plates can be seen in Figure 9.20, and as seen the maximum amount of plates is 250, limiting the reduction in condensation temperature. Only valid plate combinations are taken into account when doing the economic analyzes of the systems. The investment cost for the different heat pumps can be seen in Figure 9.30. The investment costs are only affected by an increase in plates for the system, the same compressor size is used for different condensation temperatures. The result is an increased investment cost, compared to the reduction that occurred when lowering the evaporation temperature.

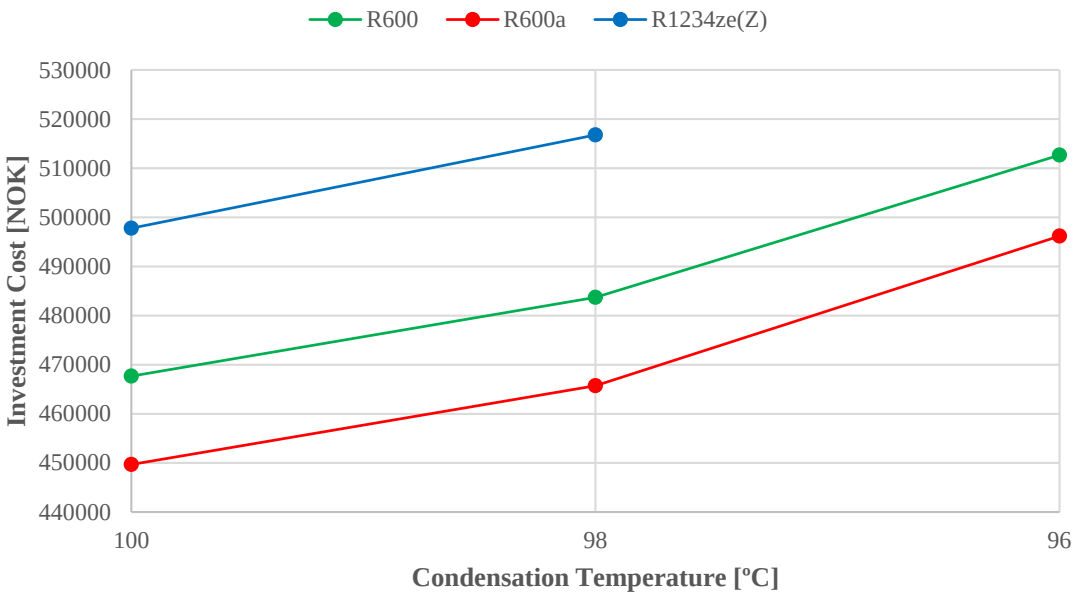

Figure 9.30 Investment cost for different condensation temperatures

The increase in investment cost, results in an increased annual capital and maintenance cost for the system, reducing the effect of a lower annual operating cost. The operational cost is not reduced as much when lowering the condensation temperature, due to a smaller reduction in required compressor work. The result is that the annual cost is higher for all heat pump solution compared to the natural gas boiler as seen in Figure 9.31.

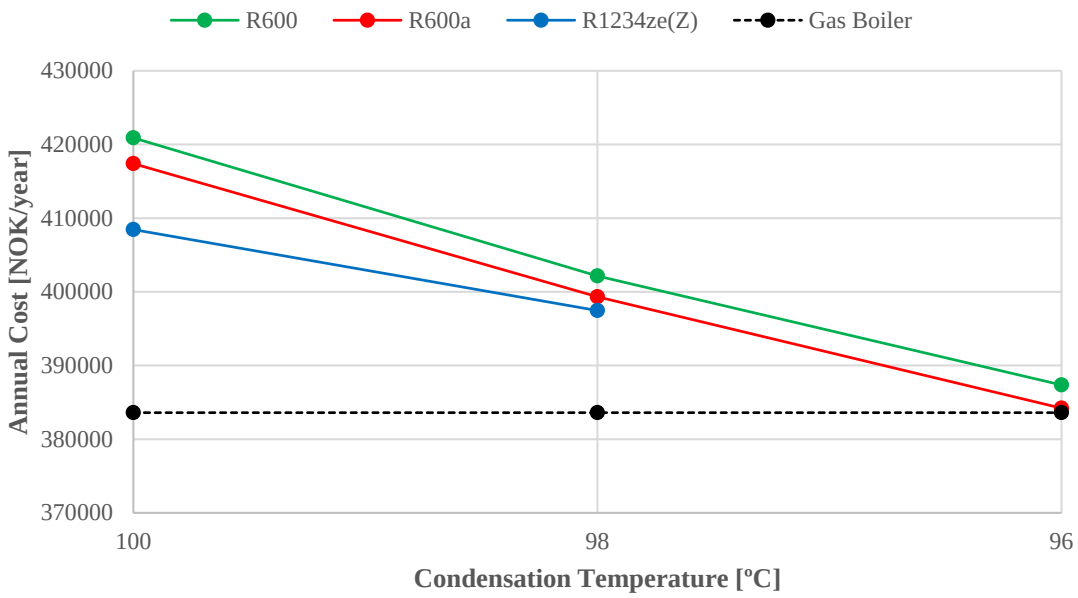

Figure 9.31 Annual cost for different condensation temperatures

This is also shown in Figure 9.32 where the specific heating cost for the different heat pumps is higher than the cost for the natural gas boiler.

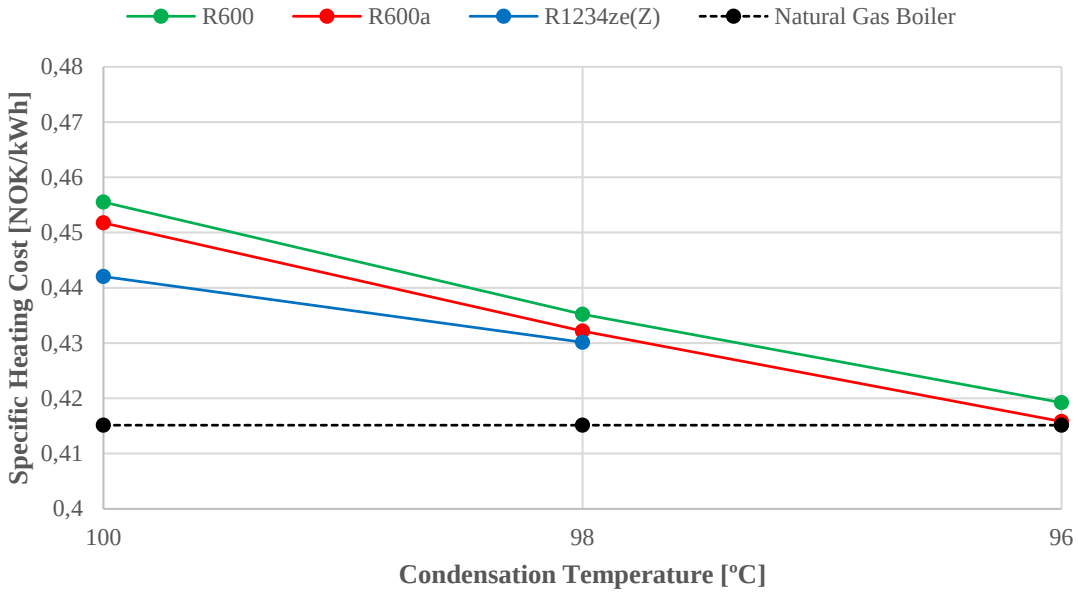

Figure 9.32 Specific heating cost for the different systems

The result of the high annual cost can be seen when calculating the present value in Figure 9.33. It is negative for all the system at the available condensation temperatures. Buying a heat pump and trying to optimizing it by reducing the condensation temperature for the chosen scenario is not a profitable investment, due to the high losses caused at the base evaporation temperature.

The R600a has a value of -8480 at 96 ºC, if it would be above 0, it would by definition be a profitable investment. The R1234ze(Z) and R600 is also below 0.

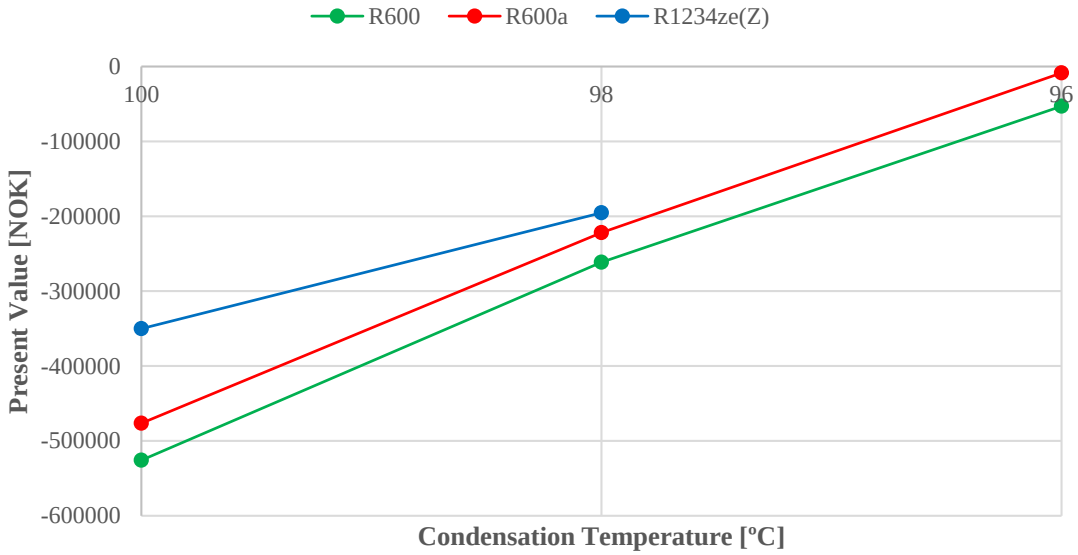

Figure 9.33 Present value at different condensation temperatures

The savings from using R600 and R600a heat pumps at a condensation temperature of 96 ºC will eventually pay for the additional investment, but this will happen after the expected lifetime of the investment as shown in Figure 9.34. 26,7 years for R600a and 42 years for R600. The result is still, that doing this is not a profitable investment for the given scenario.

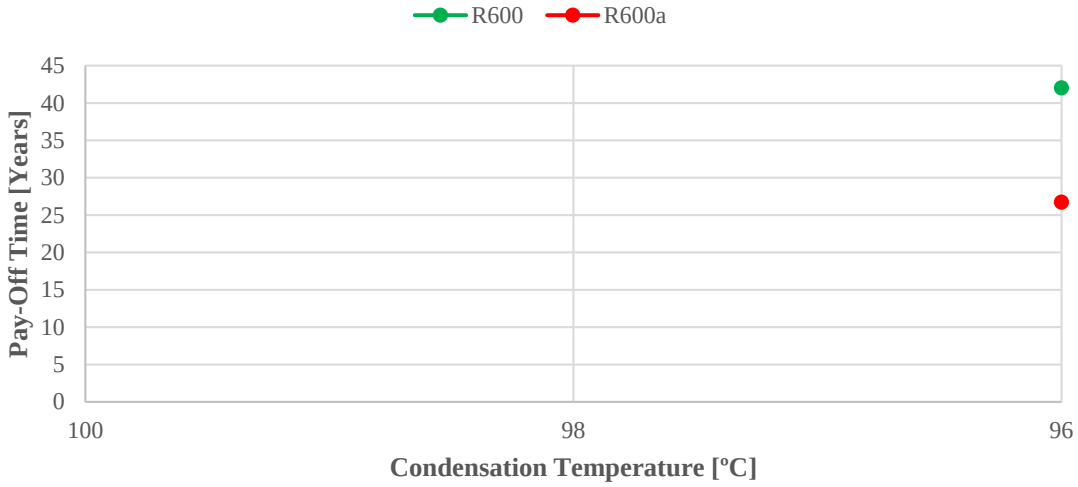

Figure 9.34 Pay-Off Time at different condensation temperatures

Results in tabular form can be found in Appendix A.

9.3.3 Effect of Reduced Electricity Prices

The effect of a reduction in electricity price was investigated for R1234ze(Z). The change in annual cost for the R1234ze(Z) heat pump at changing evaporation temperature can be seen in Figure 9.35. As it is shown in the figure, the electricity price has a large impact of on the annual cost of the system. With a reduction of 0,4 NOK/kWh the annual costs have a reduction of approximately 125 000 NOK at 40 ºC and close to 100 000 NOK at 44 ºC.

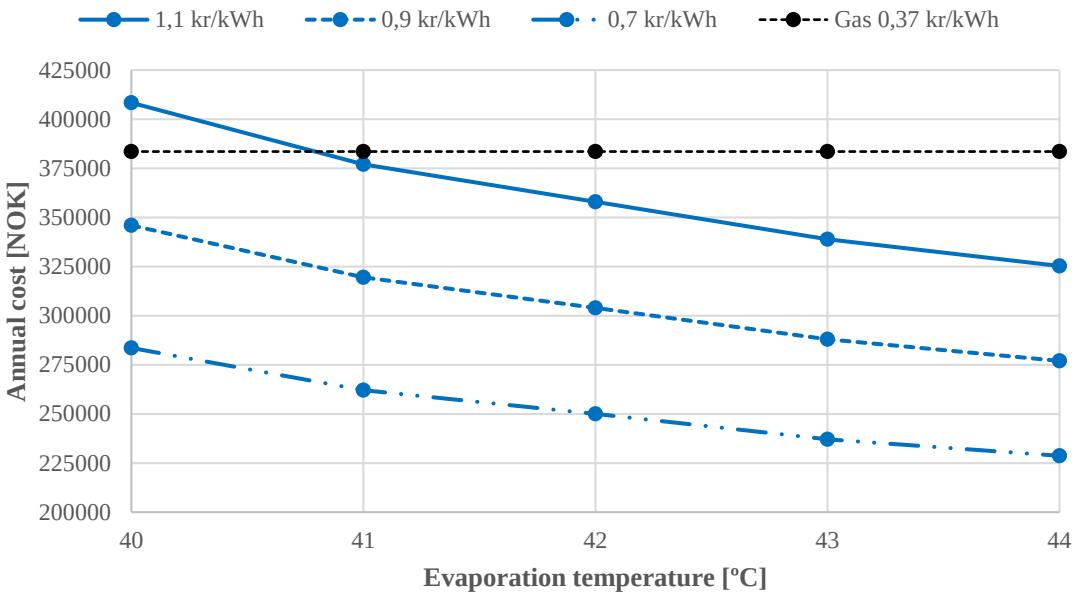

Figure 9.35 Annual cost for R1234ze(Z) heat pump at changing electricity price

The effect on the present value can be seen in Figure 9.36. The present value has a large increase, indicating a profitable investment, even at 40 ºC when the electricity price is 0,9 NOK/kWh. The investment gets a lot more profitable at lower electricity prices. The annual costs have a large effect on the profitability of the system.

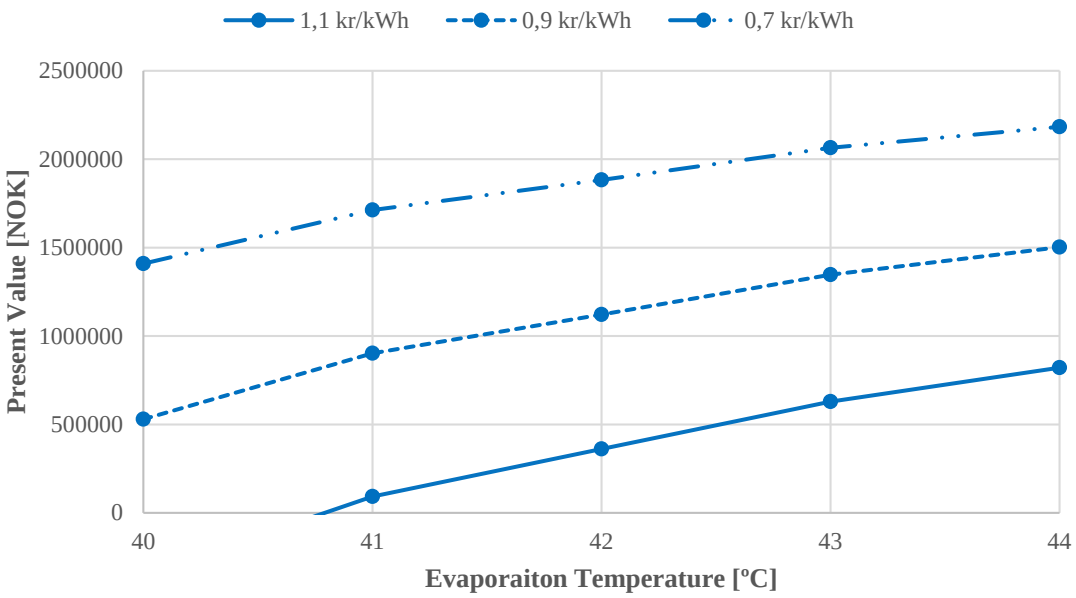

Figure 9.36 Present value for R1234ze(Z) heat pump at changing electricity price

This is further shown when calculating the pay-off time in Figure 9.37. Only positive values are plotted in the figure. The yearly saving is larger than the additional investment cost after only 3 years at 41 ºC with an electricity price of 0,9 NOK/kWh, this is lower than the original case even with an evaporation temperature of 44 ºC. For a price 0,7 NOK/kWh the system is pay-off time is 2,4 years at 40 ºC and 1,4 years at 44 ºC. This shows that the profitability of the investment is larger the closer the electricity prices is to the natural gas prices.

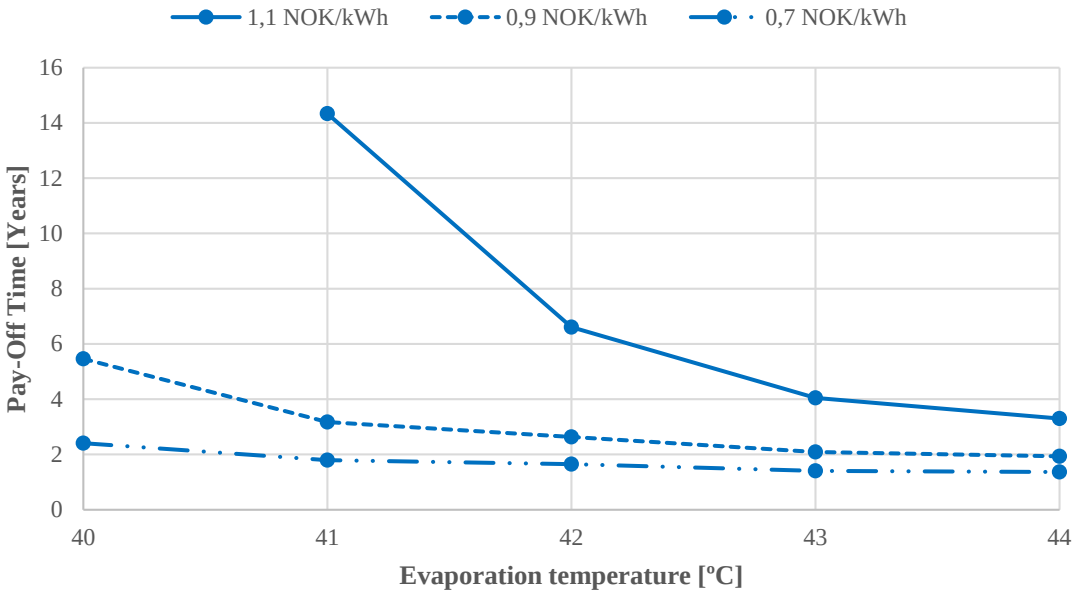

Figure 9.37 Pay-Off Time at varying electricity prices

Results in tabular form can be found in Appendix A.

9.3.4 Effect of Reduced Natural Gas Prices

When reducing the natural gas price, while keeping the same electricity price the opposite effect occurs. The difference in annual cost for the R1234ze(Z) heat pump gets smaller and smaller compared to the natural gas boiler at increasing evaporation temperatures. This can be seen in Figure 9.38. This reduces the savings for choosing a heat pump over a gas boiler, and can make the investment in a heat pump unfeasible. The reduction in natural gas prices is not large, but it has a large effect on the annual cost of the system.

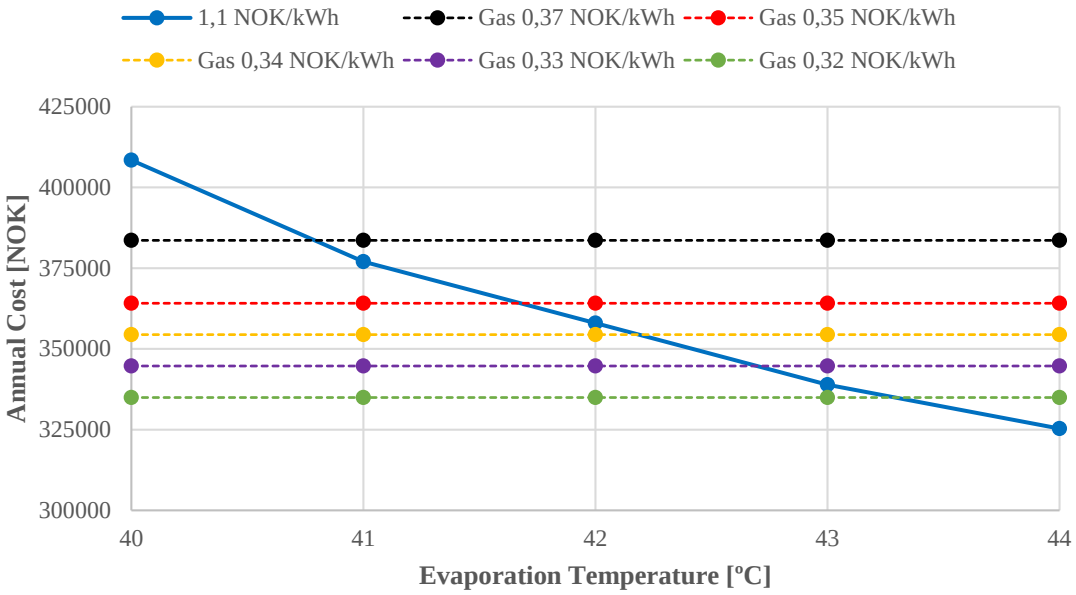

Figure 9.38 Annual Cost for R1234ze(Z) heat pump and gas boiler at different natural gas prices

The bar chart in Figure 9.39 shows the present value for the R1234ze(Z) heat pump at different evaporation temperatures with an electricity price of 1,1 NOK/kWh. As it shown in the chart, the present value is reduced significantly. A low, but positive present value indicates that the investment might be profitable, but not by much. At an evaporation temperature of 41 ºC the heat pump is only profitable for a price of 0,37 NOK/kWh, while the lower natural gas prices get more profitable at increasing evaporation temperatures. With a natural gas price of 0,32 NOK/kWh the investment is deemed profitable by definition at 44 ºC having a present value of 135660 NOK.

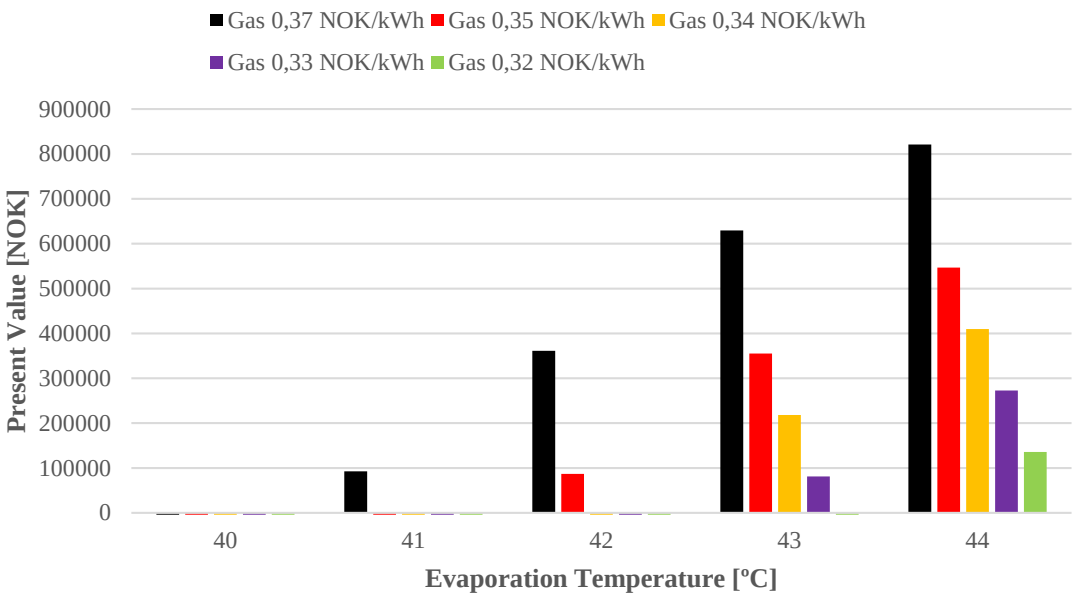

Figure 9.39 Present value for R1234ze(Z) heat pump at different natural gas prices

The effect on the pay-off time for a R1234ze(Z) heat pump is shown in Figure 9.40. The low savings from using a heat pump over a boiler, makes the amount of years before the additional investment is saved in longer, reducing the profitability of the heat pump. Even at 44 ºC, the Pay-Off Time starts to become large when the natural gas price is close to 0,33 NOK/kWh, where it is close to 7,7 years. The pay-off time for 0,34 NOK/kWh at 42 ºC is equal to 47 years and for 0,32 kWh at 43ºC is equal to 63 years. Far above the economic life time of 25 years. Results in tabular form can be found in Appendix A.

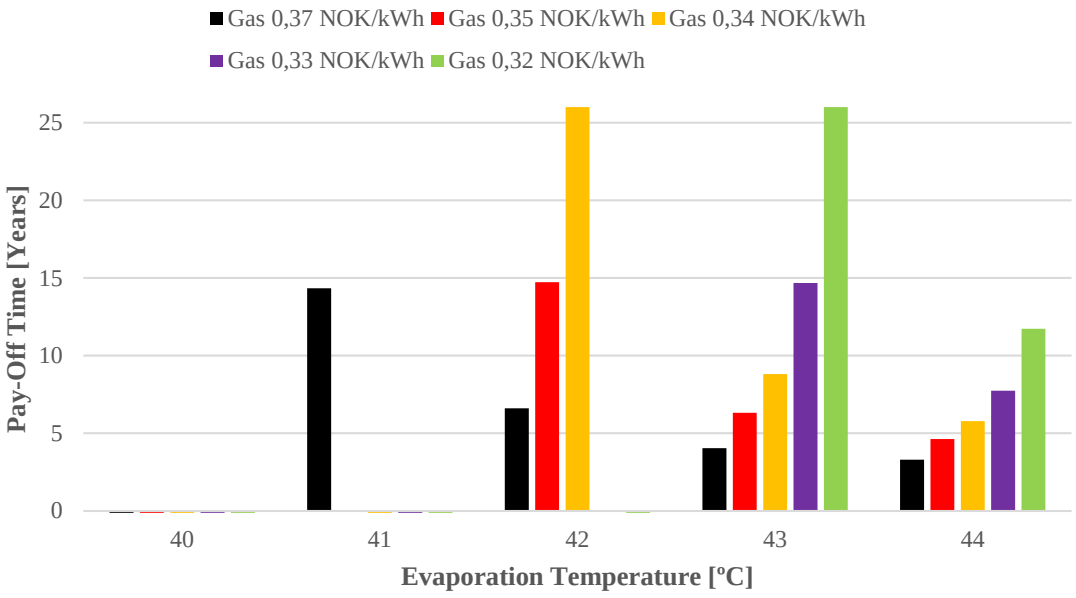

Figure 9.40 Pay-Off Time for R1234ze(Z) heat pump at different natural gas prices

9.4 Discussion

The results show that it is possible to save large amounts of energy by using a heat pump solution over competing heating solutions. At the base operating conditions, the COP for the cycle is close to 3 for R1234ze(Z) and 2,8 for R600 and R600a, which equals an energy saving of close to 67% and 62% respectively. By further optimizing the operating conditions, the energy saving will be close to 74% for R1234ze(Z), 71,5 % for R600 and 70,6 % for R600a. The most efficient way to do this is by reducing the pressure drop over the evaporator, this is done by increasing the evaporation temperature, increasing the size of the heat exchanger. The best result was achieved with an evaporation temperature of 44 ºC which gives a pinch point temperature of 1 K at the outlet of the evaporator, due to the 5 K superheat.

The reduction in pressure drop results in a reduction in the required compressor work of close to 30% from 40 ºC to 44 ºC. This is because of a reduced temperature lift and an increase is isentropic efficiency, due to a reduction in pressure ratio in (7.32). An efficient compressor reduces discharge temperature, reducing the required area for desuperheating in the condenser, resulting in a reduction in the condenser size. Another positive effect of a reduction in pressure ratio is an increase in volumetric efficiency in (7.33) and an increase in vapor density, reducing the required compressor volume, reducing the size of the compressor. The compressor work and size has a large contributing factor on the annual cost of the system. Optimizing the compressor work is essential, when wanting an efficient system.

By increasing the evaporation temperature, the increase in number of required channels is moderate compared to decreasing the condensation temperature, where the increase of required channels is exponential. The end result is that optimizing the cycle by just decreasing the condensation temperature will end up being restricted by maximum number of plates allowed in the exchanger. At an evaporation temperature of 40 ºC, R1234ze(Z) gets restricted before 96 ºC while R600 and R600a can operate at 96 ºC. This is due to a large required area for desuperheating, due to the high pressure losses at 40 ºC. However, the performance increase for reducing the condensation temperature is larger for R600 and R600a, due to having a lower pressure drop in the evaporator compared to R1234ze(Z) and due to them having a smaller superheat than R1234ze(Z). By increasing the evaporation temperature and reducing the pressure loss in evaporator is possible to reach a lower condensation temperature, but this is not assessed in the thesis.

When evaluating the results, it is important to take into account that basis of the model. The correlations used for heat transfer and friction factor calculations in both the evaporator and condenser is based on experimental data that is measured in the temperature range of 10-20 ºC for the evaporator and 20-40 ºC for the condenser. The measurements are done for several different refrigerants, including HFCs, HFOs(R1234ze(E) and yf) and natural refrigerants (R600a, R290, etc.), but not for R600 and R1234ze(Z). Longo et al. (2014) suggested that R1234ze(Z) should have higher heat transfer coefficients than the other refrigerants, including R600a and a frictional pressure drop equal to R600a. The results from the model used in this thesis is that the heat transfer coefficients are smaller but the pressure drop is of similar magnitude.

Another important factor that would affect the results is the geometry and the flow conditions inside the heat exchanger. Similar hydraulic diameter and chevron angle is however chosen to minimize this effect. As seen in the results, the chevron angle has a large effect on the pressure drop and heat transfer in the evaporator. In the condenser correlations this effect is not taken into consideration other than a change in enlargement factor and increased heat transfer from the water.

The heat exchangers are modelled as parallel-flow heat exchangers, resulting in a large temperature difference at the inlet of the condenser. Using a counter-flow configuration could increase the heat exchanger efficiency.

With the chosen step size the control volume length is 1 cm and for instance if the wanted subcooling is not reach the iteration will run 1 more step causing a lower exit temperature than wanted, this can be resolved by reducing the step size, increasing the accuracy of the calculation. However, the effect on the results are small and the chosen step size gives a sufficient accuracy overall.

In regards to the economic evaluations, it can be seen that the annual costs are heavily affected by the annual operating costs. None of the cycle improvements added more to the investment costs than it saved in operating costs. This could be different if the COP was a lot higher, since the reduction in energy saving per COP will be smaller at increasing COP. When the difference in electricity and natural gas prices is as large as it is, it is important to optimize the heat pump solution to have get a profitable investment. The bigger the difference in annual costs between the two system, the more profitable an investment will be.

The most cost efficient way to optimize the heat pump was in this case to increase the evaporation temperature, increasing the heat transfer area, thus reducing the pressure loss. This resulted in a smaller temperature lift, an increased compressor efficiency and a smaller required compressor volume. The importance of reducing the losses can also be seen in the results when only reducing the condensation temperature, where the annual cost was not reduced enough to make the system profitable. It can be noted that the R600 and R600a cycles both had an additional pressure loss that was constant due to the need of a suction gas heat exchanger, which resulted in reduced efficiency and slightly added investment cost. A larger suction gas heat exchanger with reduced pressure loss could increase the cycles efficiency and make them more profitable.

From the sensitivity analysis it can be seen that for low electricity prices has a large effect on the annual costs, and countries with cheap electricity, like Norway, have a higher chance of making heat pumps a profitable investment than countries with high electricity prices. A lower electricity price also opens up for a larger investment, making it possible to increase the efficiency even further. The gas prices could not decrease much before the R1234ze(Z) heat pump would be unprofitable. With increased awareness on global warming, it is not unreasonable to assume an increase in the price for fossil fuels or increased taxation on CO_2, which will further favor a heat pump solution using environmental friendly refrigerants.

R600a has the lowest compressor volume of the 3 refrigerants, and in the economic evaluations the compressor price is therefore lower for it than for R600 and R1234ze(Z). However, for the chosen compressor series the compressor had to run at a 1000 RPM with R600a instead of 1500 RPM as it does with R600 which the price is based on. Resulting in larger and more expensive compressors for R600a than for R600, further reducing the advantages of R600a compared to R600 and R1234ze(Z). The suppliers that were contacted had no compressors that was available for R1234ze(Z) as of now, so the compressor cost was assumed to be similar to a R600 compressor.

The results of this thesis shows that both R600 and R1234ze(Z) has a better operating efficiency than R600a, and in reality the investment costs might be higher for R600a than they are for R600 as discussed above. Resulting in lower annual costs for R600 and R1234ze(Z). Ommen et al. (2015) results indicate that R600a is the most suitable of refrigerants they investigate for high sink temperatures. This would imply that both R600 and R1234ze(Z) are an even better choice for high sink temperatures.

Another thing to be noted is that the investment costs calculated only contains the components costs and not additional costs that could increase the total cost of the systems; installation costs, safety measures due to flammability, refrigerant cost, valves, control system etc. It is also possible to invest in in two smaller systems that covers the heat duty together, for increased flexibility and safety at the cost of increased annual costs. This would decrease the profitability against the natural gas boiler, but with a properly optimized cycle it should be possible. Another alternative is two separate systems that can cover the entire load for increased operational reliability.

All of the selected refrigerants are regarded as flammable, however R1234ze(Z) is considered to be mildly flammable. This might be the deciding factor when it comes to getting acceptance by the consumer. Required safety measures are however, not assessed in this thesis, and therefore suggested for further investigation.

10 Conclusion

Heat pumps have the potential to reduce the energy consumption in industrial heating processes and at the same time being a profitable investment, even in markets where the electricity prices are a lot higher than fossil alternatives. However, the importance of optimizing the cycle is increasingly important when the electricity prices are high. A heat pump might cost less to operate yearly than a natural gas boiler, but if the savings are minimal the additional investment might result in an unprofitable investment. It is therefore important to do economic evaluations when considering in investing in a heat pump solution.

A heat pump model using environmental friendly refrigerants were developed for a given case and used to investigate different operating conditions, and their effect on the systems profitability when compared to a natural gas boiler.

The main results from the simulation are:

- R1234ze(Z) achieves the highest COP of 3,8 with an evaporation temperature of 44 ºC, this results in an annual cost of 325 000 NOK/year and a Pay-Off Time of 3,3 years compared to a gas boiler.
- R1234ze(Z) achieves the second highest COP of 3,6 at 43 ºC this results in an annual cost of 339 000 NOK/year and a Pay-Off Time of 4 years compared to a gas boiler.
- R600 achieves the third highest COP of 3,5 with an evaporation temperature of 44 ºC this results in an annual cost of 352 000 NOK/year and a Pay-Off Time of 5,4 years compared to a gas boiler.
- R600a achieves the lowest performance of the 3 refrigerants, maximum COP of 3,4 with an evaporation temperature of 44 ºC, this results in an annual cost of 356 000 NOK/year and a Pay-Off Time of 5,5 years compared to a gas boiler.
- Using R1234ze(Z) or R600 would be a better choice than R600a for high temperature heat pumps.
- The operational cost is the biggest contribution to the annual cost. All tested cycle improvements saved more money from operational cost than it added to the capital costs.
- When there is a big difference in natural gas and electricity prices a poorly optimized heat pump is not a profitable investment compared to a natural gas boiler. A heat pump that is better optimized will be able to handle an even larger price difference and still be profitable.

- The profitability of a heat pump investment will be a lot higher at reduced electricity prices, allowing for larger investments.
- Pressure drop in the evaporator has a significant impact of the performance and profitability of the system.
- Keeping a high pressure drop over the evaporator and only reducing the condensation resulted in a system that was not profitable.

11 Suggestions for Further Work

Based on the work carried out, the following are suggested to be investigated further:

- Investigate the effect of using flooded evaporators in regards to increased evaporation temperatures and the effect on the annual cost.
- Investigate the effect of using counter-flow heat exchangers over parallel-flow heat exchangers.
- Optimize the size of the suction gas heat exchanger to find the most efficient size in regards to pressure drop and investment cost.
- Optimize the heat pump cycle in regards to finding the optimal evaporation and condensation temperature.
- Investigate required safety measures for the different refrigerants and their cost.
- Do simulations with other refrigerants (i.e. HFO1336mzz(Z), ammonia) when property data and new correlations are available.

12 Bibliography

AMALFI, R. L., VAKILI-FARAHANI, F. & THOME, J. R. 2016a. Flow boiling and frictional pressure gradients in plate heat exchangers. Part 1: Review and experimental database. *International Journal of Refrigeration,* 61**,** 166-184.

AMALFI, R. L., VAKILI-FARAHANI, F. & THOME, J. R. 2016b. Flow boiling and frictional pressure gradients in plate heat exchangers. Part 2: Comparison of literature methods to database and new prediction methods. *International Journal of Refrigeration,* 61**,** 185-203.

ASSAF, K., ZOUGHAIB, A., SAPORA, E., PEUREUX, J.-L. & CLODIC, D. 2010. Experimental Simulation of a Heat Recovery Heat Pump System in Food Industries. *International Refrigeration and Air Conditioning Conference.* Purdue University: Purdue e-Pubs.

AUSTIN, B. T. & SUMATHY, K. 2011. Transcritical carbon dioxide heat pump systems: A review. *Renewable and Sustainable Energy Reviews,* 15**,** 4013-4029.

BERGLAND, M., EIKEVIK, T. M. & TOLSTOREBROV, I. 2015. OPTIMIZING THE COMPRESSION/ABSORPTION HEAT PUMP SYSTEM AT HIGH TEMPERATURES. *ICR 2015.* Yokohama, Japan.

BERTINAT, M. P. 1986. Fluids for high temperature heat pumps. *International Journal of Refrigeration,* 9**,** 43-50.

BOBELIN, D., BOURIG, A. & PEUREUX, J. L. 2012. Experimental results of a new developed very high temperature industrial heat pump (140°C) equipped with scroll compressors and working with a new blend refrigerant. *International Refrigeration and Air Conditioning Conference.* Purdue University, USA: Purdue e-Pubs.

BROBERG VIKLUND, S. & JOHANSSON, M. T. 2014. Technologies for utilization of industrial excess heat: Potentials for energy recovery and CO2 emission reduction. *Energy Conversion and Management,* 77**,** 369-379.

BROWN, J. S., ZILIO, C. & CAVALLINI, A. 2009. The fluorinated olefin R-1234ze(Z) as a high-temperature heat pumping refrigerant. *International Journal of Refrigeration,* 32**,** 1412-1422.

BRÜCKNER, S., LIU, S., MIRÓ, L., RADSPIELER, M., CABEZA, L. F. & LÄVEMANN, E. 2015. Industrial waste heat recovery technologies: An economic analysis of heat transformation technologies. *Applied Energy,* 151**,** 157-167.

BÄCKSTRÖM, M. 1946. *Kylteknikern del 1,* Stockholm, Svenska Kyltekniska Föreningen.

CALM, J. M. 2008. The next generation of refrigerants – Historical review, considerations, and outlook. *International Journal of Refrigeration,* 31**,** 1123-1133.

CAVALLINI, A., COL, D. D., DORETTI, L., MATKOVIC, M., ROSSETTO, L., ZILIO, C. & CENSI, G. 2006. Condensation in Horizontal Smooth Tubes: A New Heat Transfer Model for Heat Exchanger Design. *Heat Transfer Engineering,* 27**,** 31-38.

CHAMOUN, M., RULLIERE, R., HABERSCHILL, P. & PEUREUX, J.-L. 2012. Experimental Investigation of a New High Temperature Heat Pump Using Water as Refrigerant for Industrial Heat Recovery. *International Refrigeration and Air Conditioning Conference.* Purdue University, USA: Purdue e-Pubs.

CHAMOUN, M., RULLIERE, R., HABERSCHILL, P. & PEUREUX, J.-L. 2014. Experimental and numerical investigations of a new high temperature heat pump for

industrial heat recovery using water as refrigerant. *International Journal of Refrigeration,* 44**,** 177-188.

CHRISTENSEN, S. W., ELMEGAARD, B., MARKUSSEN, W. B., ROTHUIZEN, E. & MADSEN, C. 2015. MODELLING OF AMMONIA HEAT PUMP DESUPERHEATERS. *ICR 2015.* Yokohama, Japan.

CHUA, K. J., CHOU, S. K. & YANG, W. M. 2010. Advances in heat pump systems: A review. *Applied Energy,* 87**,** 3611-3624.

DANFOSS 2016. Coolselector®2.

DEVOTTA, S. & RAO PENDYALA, V. 1994. Thermodynamic screening of some HFCs and HFEs for high-temperature heat pumps as alternatives to CFC114. *International Journal of Refrigeration,* 17**,** 338-342.

EIKEVIK, T. M. 13.05 2016. *RE: Personal communication.*

EIKEVIK, T. M., TOLSTOREBROV, I., BREDESEN, A. M., REKSTAD, H., PETTERSEN, J., AFLEKT, K. & ELGSÆTHER, M. 2016. *TEP 4255 - Heat pumping processes and systems,* NTNU, NTNU EPT.

EKROTH, I. & GRANRYD, E. 2009. The vapor compression cycle. *Refrigerating Engineering.* Royal Institute of Technology, KTH.

ELDEEB, R., AUTE, V. & RADERMACHER, R. 2016. A survey of correlations for heat transfer and pressure drop for evaporation and condensation in plate heat exchangers. *International Journal of Refrigeration,* 65**,** 12-26.

EUROSTAT. 2016. *Energy Price Statistics* [Online]. Luxembourg: Eurostat Available: http://ec.europa.eu/eurostat/statistics-explained/index.php/Energy_price_statistics [Accessed 24.05 2016].

FUKUDA, S., KONDOU, C., TAKATA, N. & KOYAMA, S. 2014. Low GWP refrigerants R1234ze(E) and R1234ze(Z) for high temperature heat pumps. *International Journal of Refrigeration,* 40**,** 161-173.

GARCÍA-CASCALES, J. R., VERA-GARCÍA, F., CORBERÁN-SALVADOR, J. M. & GONZÁLVEZ-MACIÁ, J. 2007. Assessment of boiling and condensation heat transfer correlations in the modelling of plate heat exchangers. *International Journal of Refrigeration,* 30**,** 1029-1041.

GRANRYD, E. 2001. Hydrocarbons as refrigerants — an overview. *International Journal of Refrigeration,* 24**,** 15-24.

HAUKÅS, H. T. 2015. *Norsk Kulde- og Varmepumpenorm,* Norsk Kjøleteknisk Forening.

IEA-HPC 2014a. Application of Industrial Heat Pumps, Part 1. *IEA HPP ANNEX 35.* International Energy Agency Heat Pump Centre.

IEA-HPC 2014b. Application of Industrial Heat Pumps, Part 2. *IEA HPP ANNEX 35.* International Energy Agency Heat Pump Centre.

JANA, A. K. & MAITI, D. 2013. Assessment of the implementation of vapor recompression technique in batch distillation. *Separation and Purification Technology,* 107**,** 1-10.

JENSEN, J. K., MARKUSSEN, W. B., REINHOLDT, L. & ELMEGAARD, B. 2015a. On the development of high temperature ammonia-water hybrid absorption-compression heat pumps. *International Journal of Refrigeration.*

JENSEN, J. K., OMMEN, T., MARKUSSEN, W. B., REINHOLDT, L. & ELMEGAARD, B. 2015b. Technical and economic working domains of industrial heat pumps: Part 2 –

Ammonia-water hybrid absorption-compression heat pumps. *International Journal of Refrigeration,* 55**,** 183-200.

JOHNSON CONTROLS NORWAY. 26.05 2016. *RE: Email communication: Forespørsel om priser til masteroppgave ved NTNU.*

KAZEMI, A., HOSSEINI, M., MEHRABANI-ZEINABAD, A. & FAIZI, V. 2016. Evaluation of different vapor recompression distillation configurations based on energy requirements and associated costs. *Applied Thermal Engineering,* 94**,** 305-313.

KIM, J., PARK, S.-R., BAIK, Y.-J., CHANG, K.-C., RA, H.-S., KIM, M. & KIM, Y. 2013. Experimental study of operating characteristics of compression/absorption high-temperature hybrid heat pump using waste heat. *Renewable Energy,* 54**,** 13-19.

KIM, M.-H., PETTERSEN, J. & BULLARD, C. W. 2004. Fundamental process and system design issues in CO2 vapor compression systems. *Progress in Energy and Combustion Science,* 30**,** 119-174.

KLEIN, S. 2015. Engineering Equation Solver Professional 9.935-3D. Madison, WI: F-Chart Software.

KONDOU, C. & KOYAMA, S. 2015. Thermodynamic assessment of high-temperature heat pumps using Low-GWP HFO refrigerants for heat recovery. *International Journal of Refrigeration,* 53**,** 126-141.

KONTOMARIS, K. 2012. A ZERO-ODP, LOW GWP WORKING FLUID FOR HIGH TEMPERATURE HEATING AND POWER GENERATION FROM LOW TEMPERATURE HEAT: DR-2. *THE INTERNATIONAL SYMPOSIUM on NEW REFRIGERANTS and ENVIRONMENTAL TECHNOLOGY 2012.* Kobe, Japan: The Japan Refrigeration and Air Conditioning Industry Association.

KONTOMARIS, K. 2014. HFO-1336mzz-Z: High Temperature Chemical Stability and Use as A Working Fluid in Organic Rankine Cycles. *International Refrigeration and Air Conditioning Conference.* Purdue University: Purdue e-Pubs.

KONTOMARIS, K. 2016. Low GWP Refrigerants for Efficient Cooling, Heating and Power Generation. *IEA Heat Pump Centre Newsletter.* IEA Heat Pump centre.

LEMMON, E., HUBER, M. & MCLINDEN, M. Refprop 9.0, NIST standard reference database 23, Version 9.0 2010. USA.

LONGO, G. A. 2010. Heat transfer and pressure drop during hydrocarbon refrigerant condensation inside a brazed plate heat exchanger. *International Journal of Refrigeration,* 33**,** 944-953.

LONGO, G. A., MANCIN, S., RIGHETTI, G. & ZILIO, C. 2015a. A new model for refrigerant boiling inside Brazed Plate Heat Exchangers (BPHEs). *International Journal of Heat and Mass Transfer,* 91**,** 144-149.

LONGO, G. A., RIGHETTI, G. & ZILIO, C. 2015b. A new computational procedure for refrigerant condensation inside herringbone-type Brazed Plate Heat Exchangers. *International Journal of Heat and Mass Transfer,* 82**,** 530-536.

LONGO, G. A., ZILIO, C., RIGHETTI, G. & BROWN, J. S. 2014. Experimental assessment of the low GWP refrigerant HFO-1234ze(Z) for high temperature heat pumps. *Experimental Thermal and Fluid Science,* 57**,** 293-300.

MA, Y., LIU, Z. & TIAN, H. 2013. A review of transcritical carbon dioxide heat pump and refrigeration cycles. *Energy,* 55**,** 156-172.

MADSBOELL, H., WEEL, M. & KOLSTRUP, A. 2015. DEVELOPMENT OF A WATER VAPOR COMPRESSOR FOR HIGH TEMPERATURE HEAT PUMP APPLICATIONS. *ICR 2015.* Yokohama, Japan.

MARTIN, H. 1996. A theoretical approach to predict the performance of chevron-type plate heat exchangers. *Chemical Engineering and Processing: Process Intensification,* 35**,** 301-310.

MCLINDEN, M. O., KAZAKOV, A. F., STEVEN BROWN, J. & DOMANSKI, P. A. 2014. A thermodynamic analysis of refrigerants: Possibilities and tradeoffs for Low-GWP refrigerants. *International Journal of Refrigeration,* 38**,** 80-92.

NEKSÅ, P., REKSTAD, H., ZAKERI, G. R. & SCHIEFLOE, P. A. 1998. CO2-heat pump water heater: characteristics, system design and experimental results. *International Journal of Refrigeration,* 21**,** 172-179.

NELLIS, G. & KLEIN, S. 2009. *Heat transfer,* Cambridge, Cambridge University Press.

NORDTVEDT, S. R. 2005. *Experimental and theoretical study of a compression/absorption heat pump with ammonia/water as working fluid.* Norwegian University of Science and Technology.

NORDTVEDT, S. R., HORNTVEDT, B. R., EIKEFJORD, J. & JOHANSEN, J. 2013. Hybrid heat pump for waste heat recovery in norwegian food industry. *Thermally driven heat pumps for heating and cooling.* Berlin: Universitätsverlag der TU Berlin.

OLULEYE, G., JOBSON, M., SMITH, R. & PERRY, S. J. 2016. Evaluating the potential of process sites for waste heat recovery. *Applied Energy,* 161**,** 627-646.

OMMEN, T., JENSEN, J. K., MARKUSSEN, W. B., REINHOLDT, L. & ELMEGAARD, B. 2015. Technical and economic working domains of industrial heat pumps: Part 1 – Single stage vapour compression heat pumps. *International Journal of Refrigeration,* 55**,** 168-182.

PACHAI, A. C. & HARRAGHY, P. 2013. Practical experience of applying ammonia and hydrocarbon refrigeration systems for standard refrigeration and air conditioning applications – part two. *Ecolibrium***,** 46-51.

PALM, B. 2014. Köldmedier med låg GWP (HFO). KTH.

PAN, L., WANG, H., CHEN, Q. & CHEN, C. 2011. Theoretical and experimental study on several refrigerants of moderately high temperature heat pump. *Applied Thermal Engineering,* 31**,** 1886-1893.

PEARSON, A. 2012. High temperature heat pumps with natural refrigerants. *IEA HEAT PUMP CENTRE IEA NEWSLETTER VOL. 30 1/2012.* IEA.

QU, M. & ABDELAZIZ, O. 2015. IMPROVING WATER AND ENERGY EFFICIENCY OF POWER PLANT THROUGH ABSORPTION HEAT PUMP. *ICR 2015.* Yokohama, Japan.

SARKAR, J., BHATTACHARYYA, S. & GOPAL, M. R. 2004. Optimization of a transcritical CO2 heat pump cycle for simultaneous cooling and heating applications. *International Journal of Refrigeration,* 27**,** 830-838.

SARKAR, J., BHATTACHARYYA, S. & RAM GOPAL, M. 2007. Natural refrigerant-based subcritical and transcritical cycles for high temperature heating. *International Journal of Refrigeration,* 30**,** 3-10.

SHAH, R. K. & SEKULIĆ, D. P. 2007. Heat Exchanger Design Procedures. *Fundamentals of Heat Exchanger Design.* John Wiley & Sons, Inc.

SOROKA, B. 2015. Application Note – Industrial Heat Pumps. *Leonardo Energy*.

STENE, J. 1993. *VARMEPUMPER - Industrielle anvendelser*, NTH-SINTEF Kuldeteknikk.

STENE, J. 1997. *Varmepumper Grunnleggende varmepumpeteknikk,* SINTEF Energiforskning AS.

STENE, J. 2016. Investment Analysis for Heat Pump Systems. *TEP4260 Presentation.* NTNU.

SWEP 2016. SSP G7. 7.0.3.54 ed.

UDAY BHASKAR BABU, G. & JANA, A. K. 2014. Impact of vapor recompression in batch distillation on energy consumption, cost and CO2 emission: Open-loop versus closed-loop operation. *Applied Thermal Engineering,* 62**,** 365-374.

WANG, L., SUNDÉN, B. & MANGLIK, R. M. 2007. *Plate heat exchangers : design, applications and performance*, Southampton, WITPress.

Appendix A Supplements

P-h diagrams and temperature distributions in the heat exchangers for the different refrigerants for evaporation temperatures of 40 ºC and 44 ºC and condensation temperature of 100 ºC can be seen below. Results from the simulations is also found in tables below.

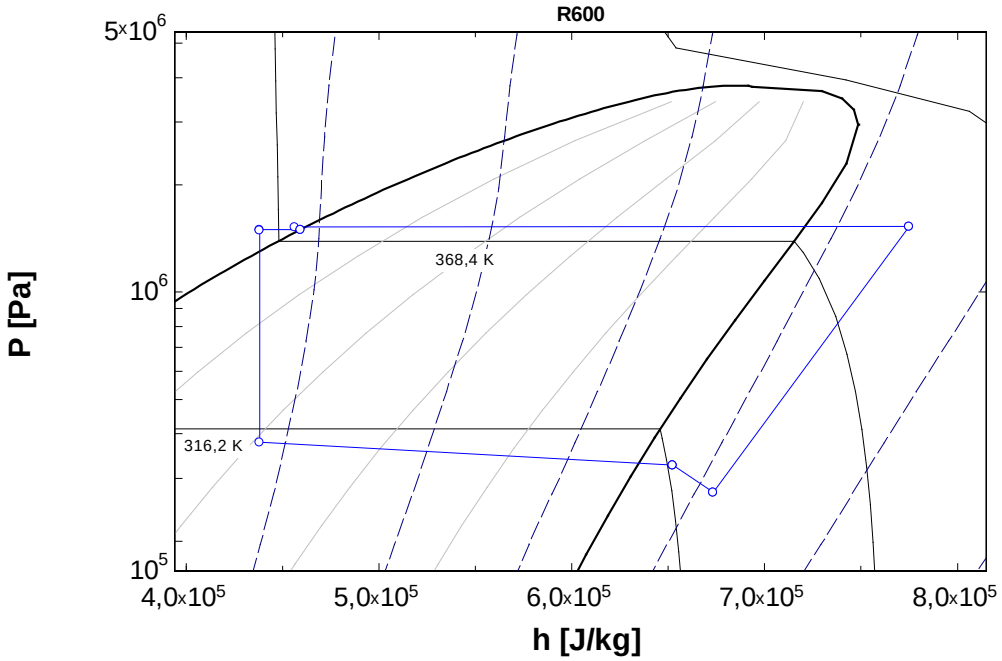

Figure A.1 P-h diagram for R600 at 40/100 ºC

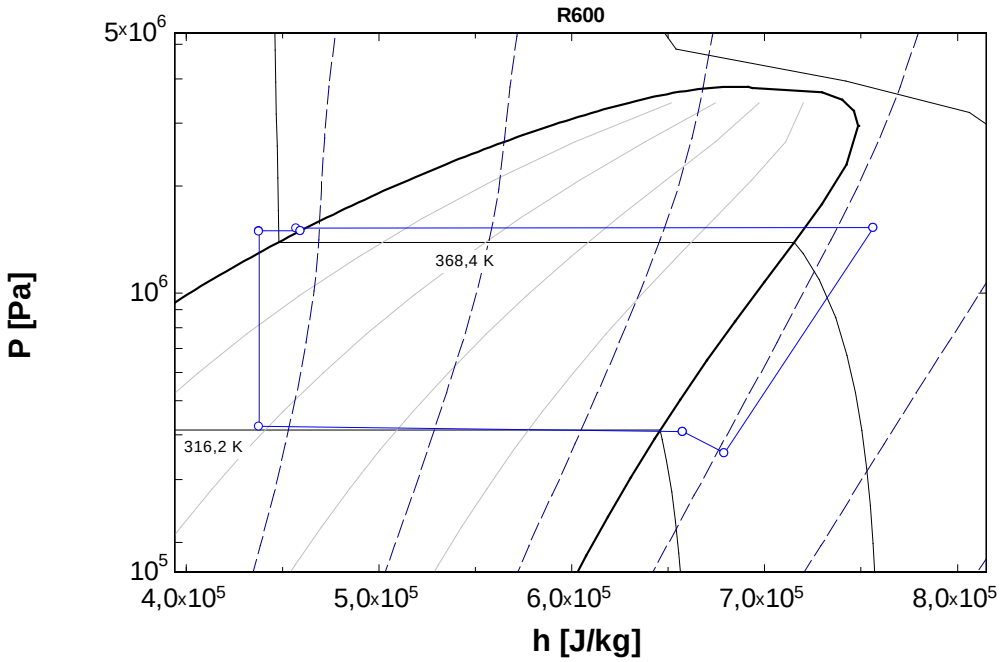

Figure A.2 P-h diagram for R600 at 44/100 ºC

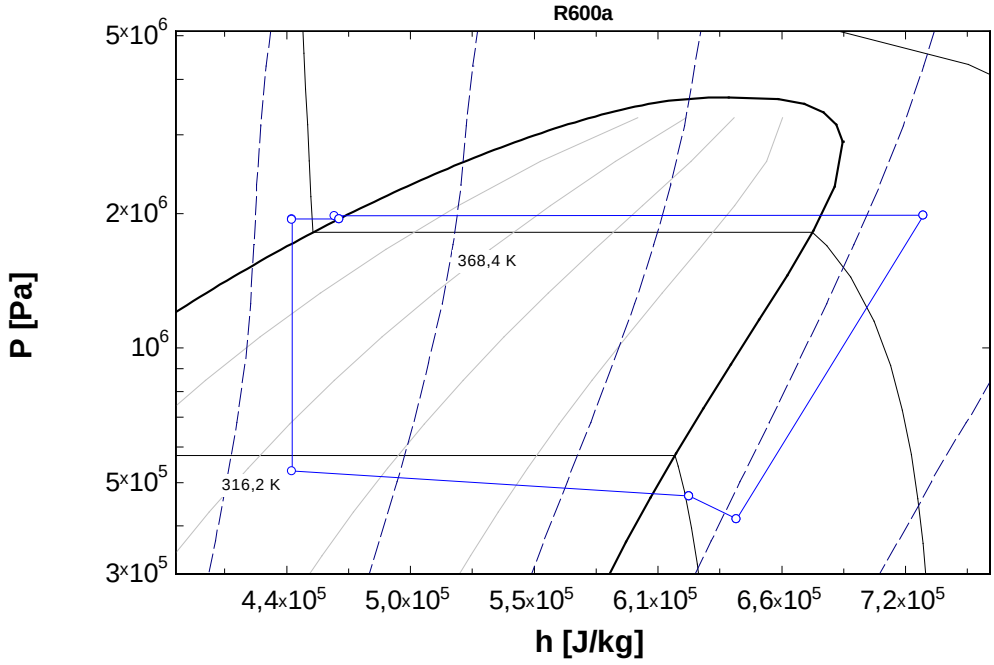

Figure A.3 P-h diagram for R600a at 40/100 ºC

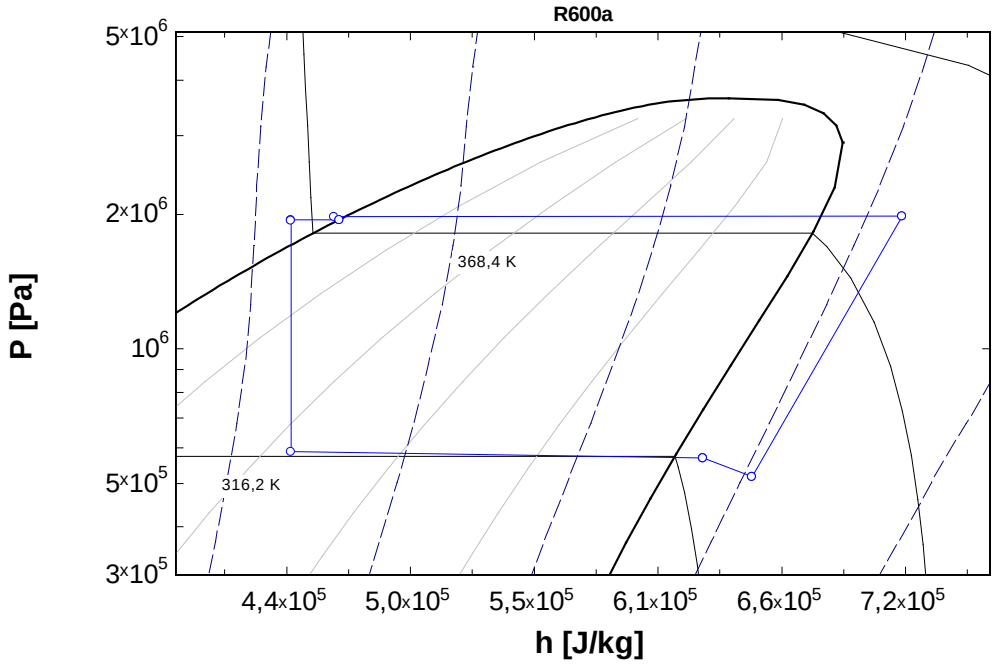

Figure A.4 P-h diagram for R600a at 44/100 ºC

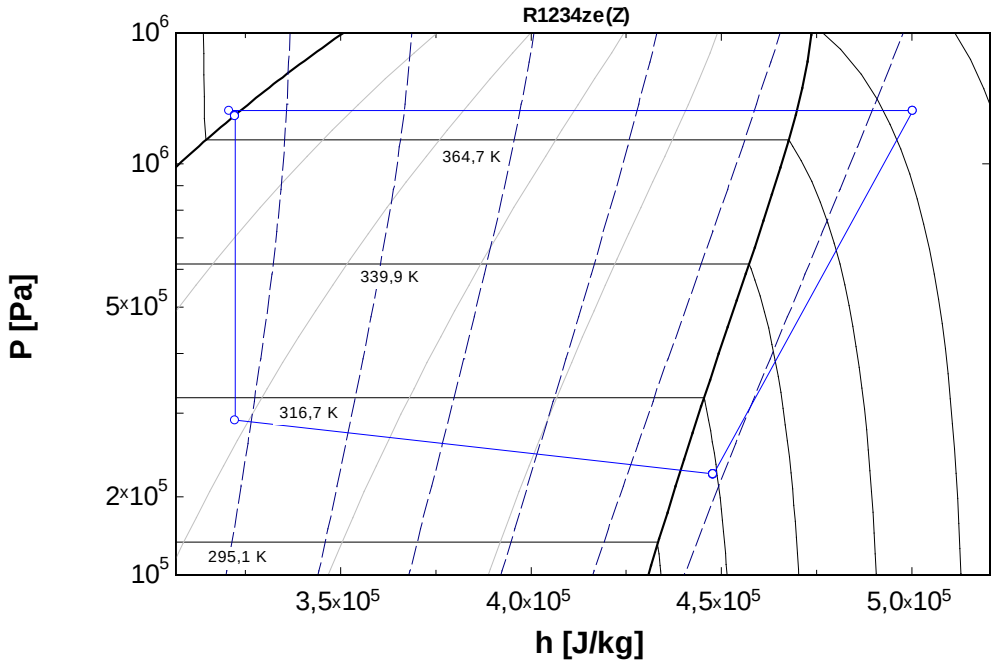

Figure A.5 P-h diagram for R1234ze(Z) at 40/100 ºC

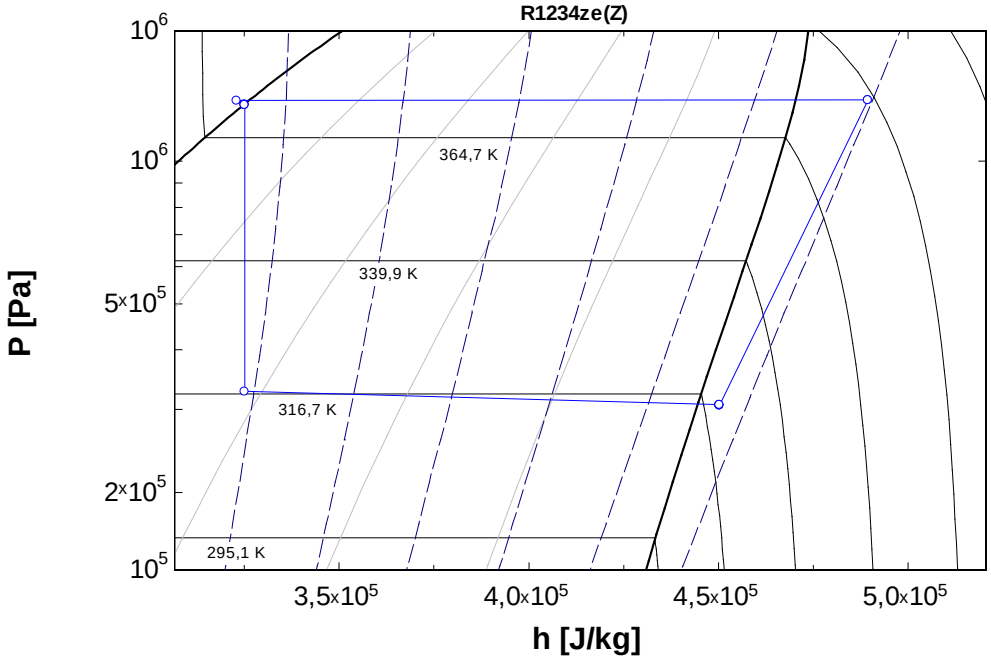

Figure A.6 P-h diagram for R1234ze(Z) at 44/100 ºC

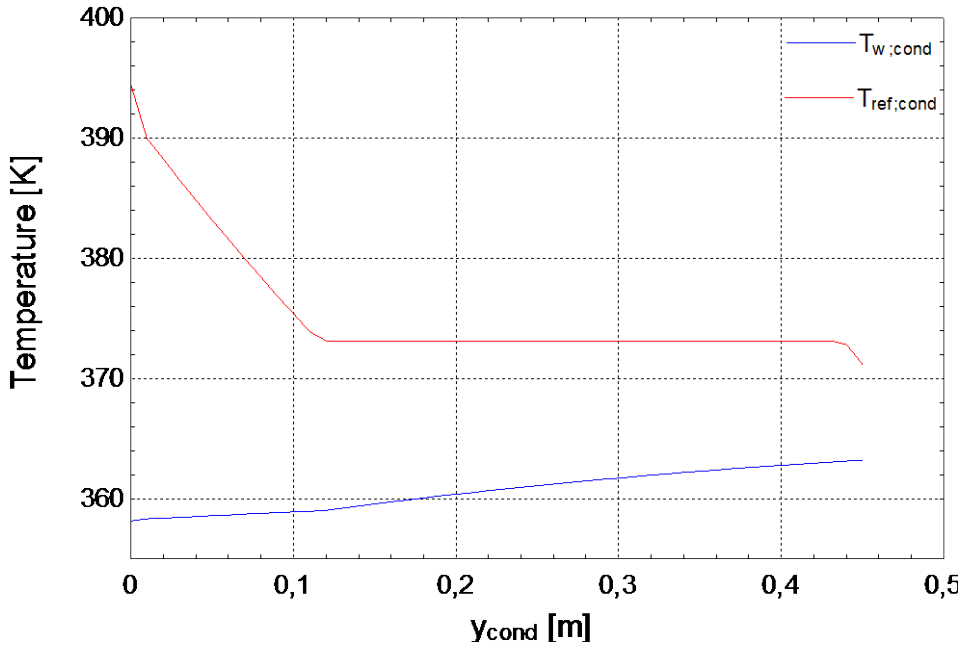

Figure A.7 Temperature distribution in condenser for R600 at 40 ºC

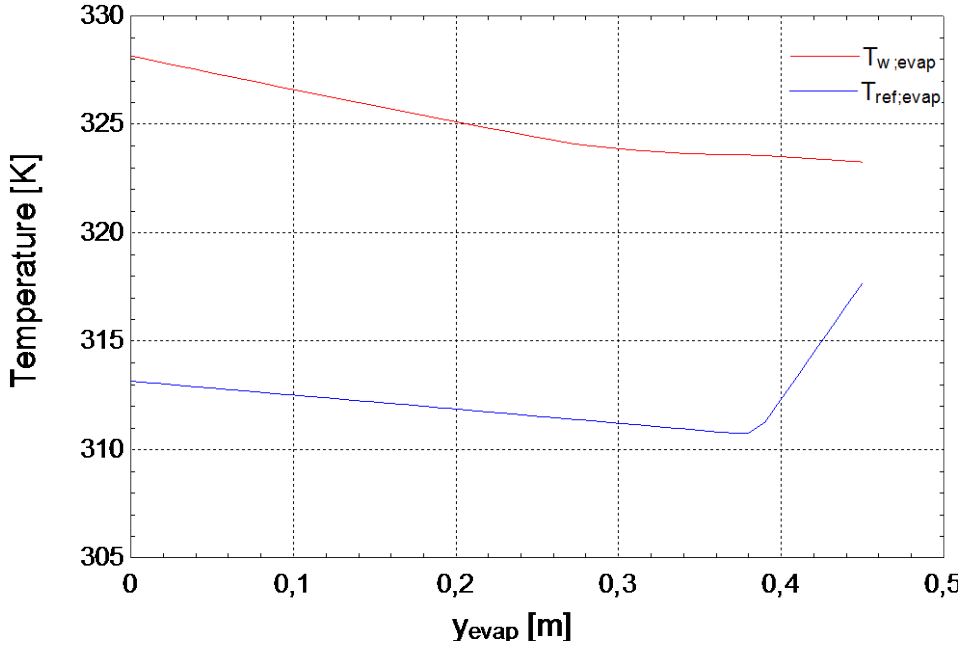

Figure A.8 Temperature distribution in evaporator for R600 at 40 ºC

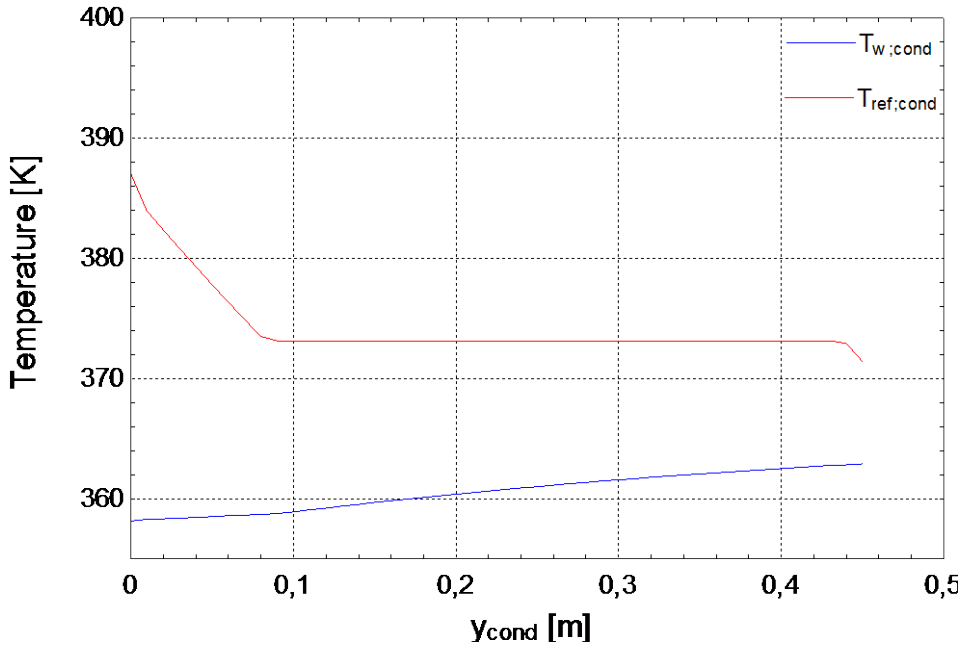

Figure A.9 Temperature distribution in condenser for R600 at 44 ºC

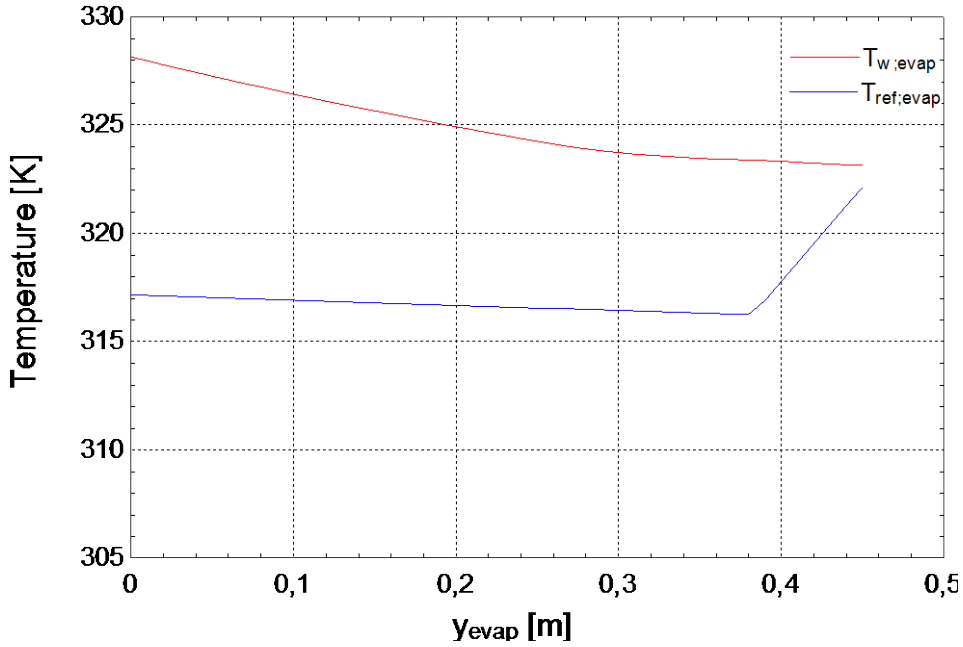

Figure A.10 Temperature distribution in evaporator for R600 at 44 ºC

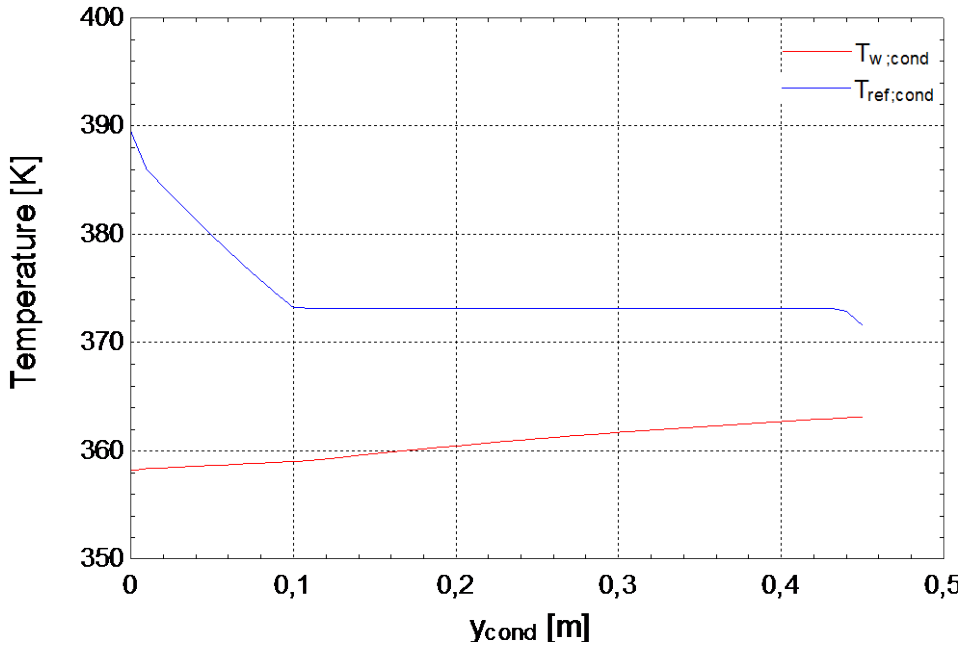

Figure A.11 Temperature distribution in condenser for R600a at 40 ºC

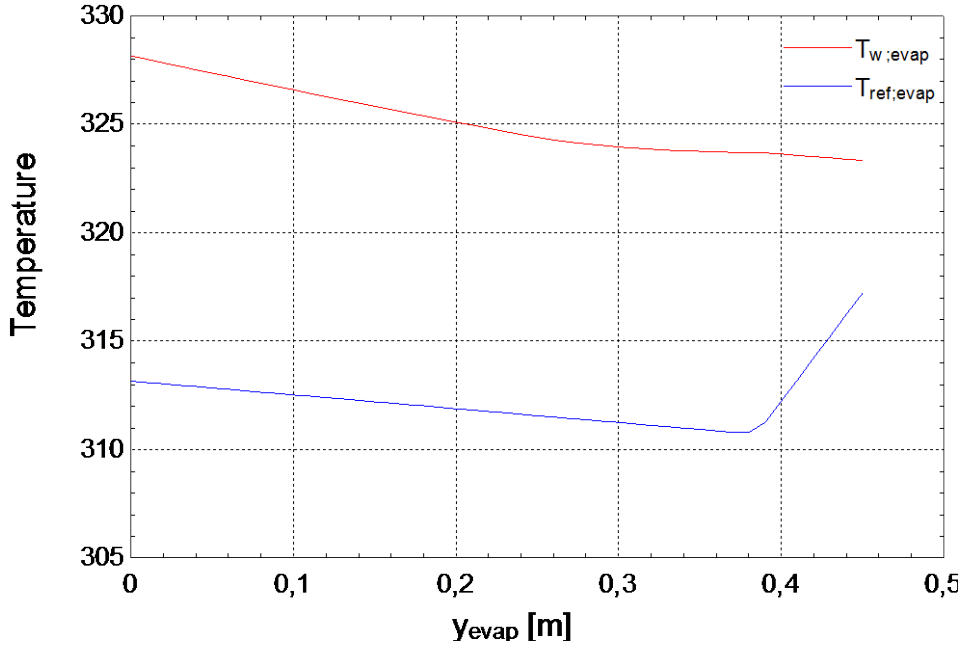

Figure A.12 Temperature distribution in evaporator for R600a at 40 ºC

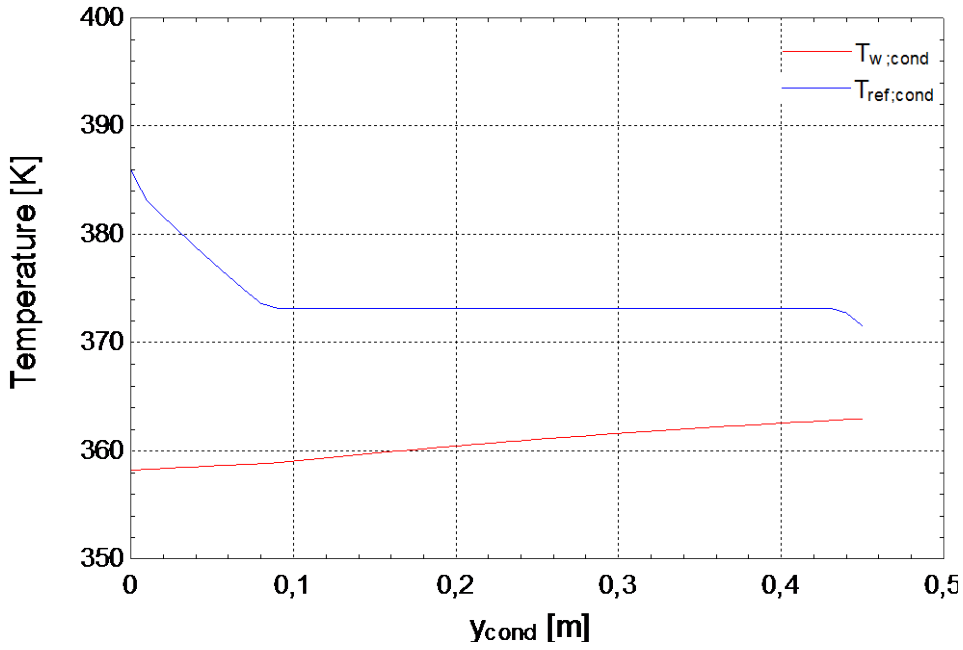

Figure A.13 Temperature distribution in condenser for R600a at 44 ºC

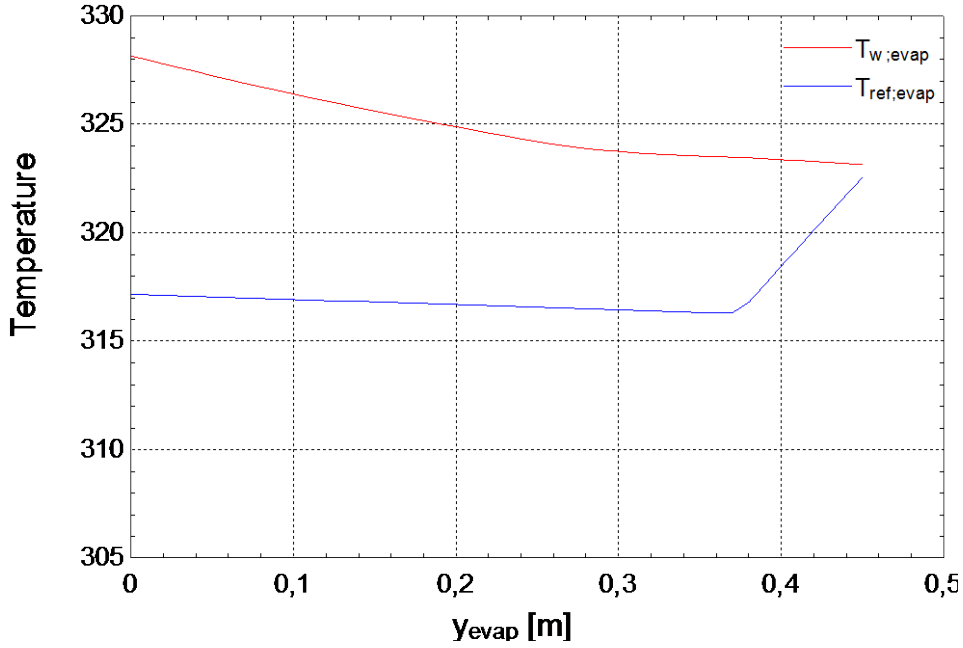

Figure A.14 Temperature distribution in evaporator for R600a at 44 ºC

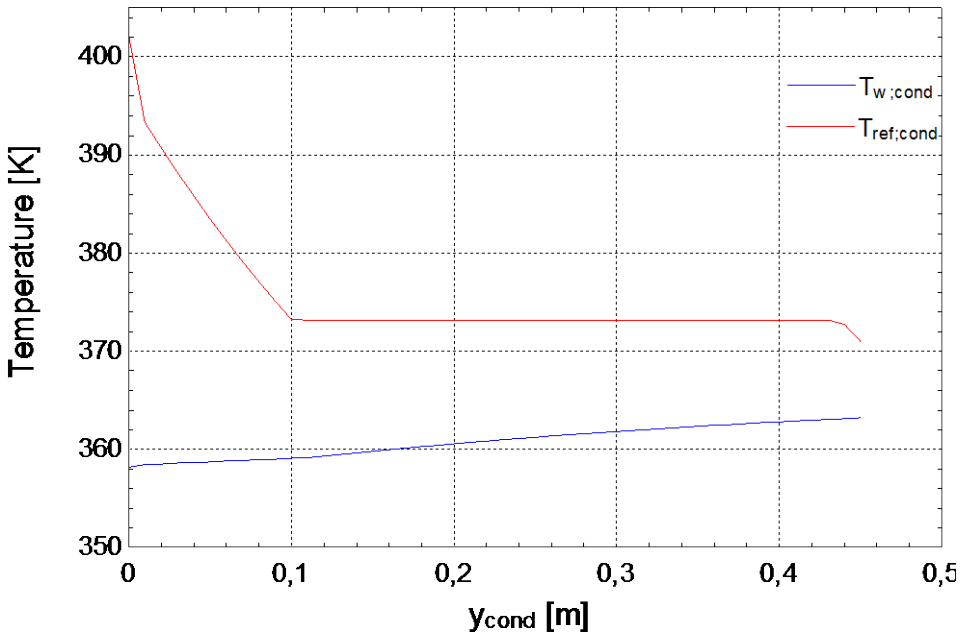

Figure A.15 Temperature distribution in condenser for R1234ze(Z) at 40 ºC

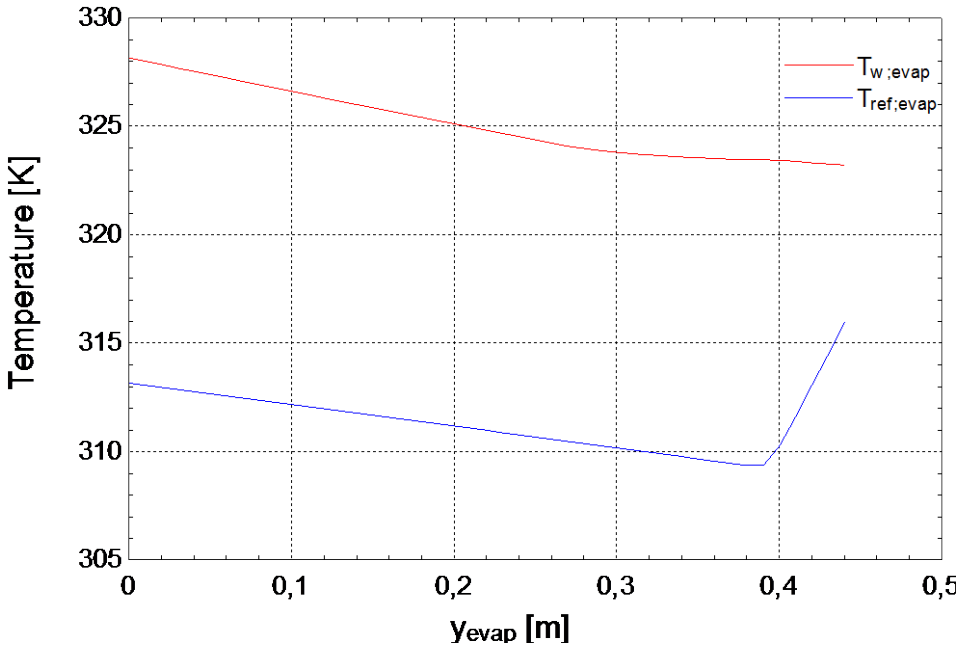

Figure A.16 Temperature distribution in evaporator for R1234ze(Z) at 40 ºC

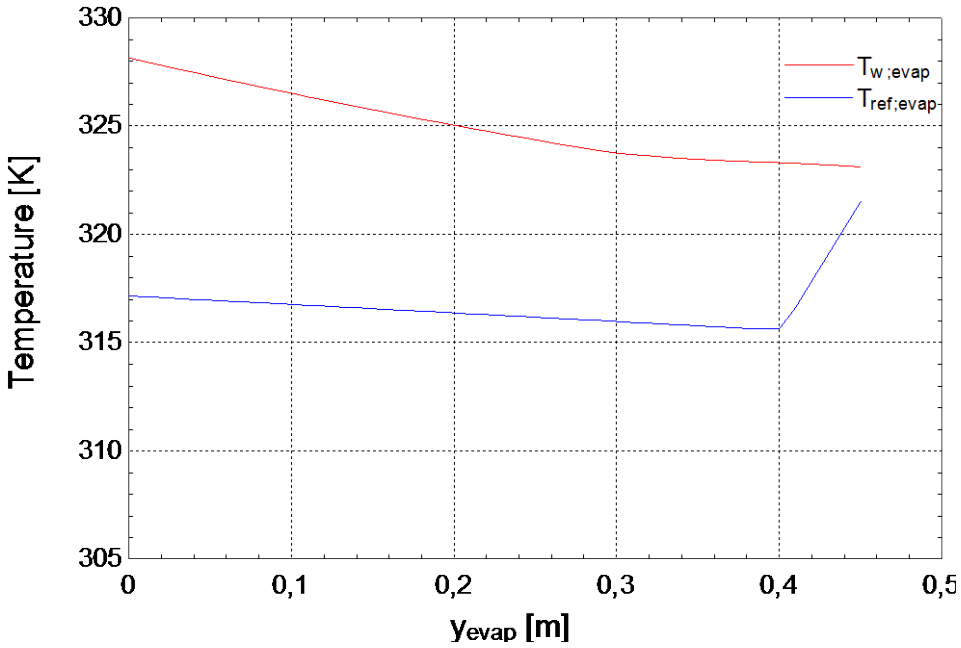

Figure A.17 Temperature distribution in condenser for R1234ze(Z) at 44 ºC

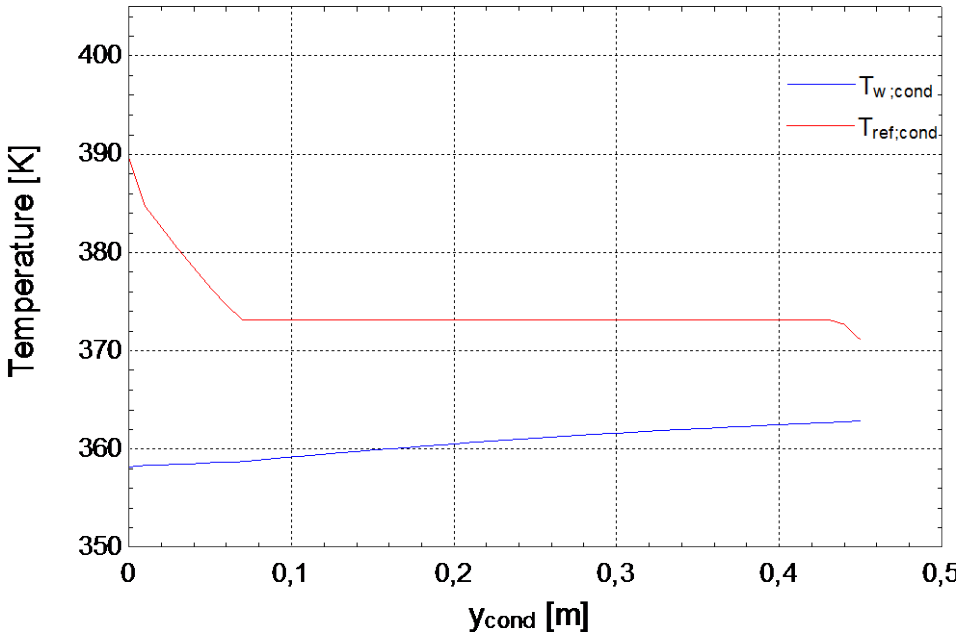

Figure A.18 Temperature distribution in evaporator for R1234ze(Z) at 44 ºC

Red numbers indicate invalid results, since the number of channels is above the maximum number of allowed plates ($N_{ch} > 125$).

Table A.1 Simulation results R600

T_{evap}	W	V_s	COP	$N_{ch;evap}$	$N_{ch;cond}$	U_{cond}	U_{evap}	ΔP_{Evap}	ΔP_{Cond}	PR	ΔP_{comp}	$\dot{m}_{ref}$
40	75487	508,2	2,826	15	47	1108	4637	52684	2297	5,563	300,1	0,67
41	69037	456,9	3,029	18	44	1232	4544	39398	2742	5,116	295,4	0,67
42	64226	419,2	3,196	22	41	1330	4476	29025	3298	4,775	292	0,67
43	60564	390,6	3,35	27	39	1434	4381	21558	3738	4,512	289,3	0,67
44	57553	366,7	3,484	35	38	1466	4598	15028	3981	4,285	287,5	0,67
$\beta_{cond} = 45°$												
T_{cond}	W	V_s	COP	$N_{ch;evap}$	$N_{ch;cond}$	U_{cond}	U_{evap}	ΔP_{Evap}	ΔP_{Cond}	PR	ΔP_{comp}	$\dot{m}_{ref}$
100	75487	508,2	2,826	15	47	1108	4637	52684	2297	5,563	300,1	0,67
98	71211	491,3	3	16	67	909,3	4580	47526	581,6	5,251	311	0,67
96	67405	477,2	3,174	17	104	700,3	4520	43183	-385,3	4,971	322,7	0,67
94	63124	458,3	3,368	18	178	538,8	4162	37087	-840	4,676	332,9	0,67
92	60153	448,6	3,55	19	425	348,2	4084	34158	-1034	4,446	346,3	0,67
$\beta_{cond} = 65°$												
T_{cond}	W	V_s	COP	$N_{ch;evap}$	$N_{ch;cond}$	U_{cond}	U_{evap}	ΔP_{Evap}	ΔP_{Cond}	PR	ΔP_{comp}	$\dot{m}_{ref}$
100	75487	508,2	2,821	15	38	1386	4637	52684		5,563	300,1	0,67
98	71211	491,3	2,994	16	51	1176	4580	47526		5,251	311	0,67
96	67405	477,2	3,178	17	79	932,4	4520	43183		4,971	322,7	0,67
94	63124	458,3	3,364	18	132	714,2	4162	37087		4,676	332,9	0,67
92	60153	448,6	3,543	19	317	431,6	4084	34158		4,446	346,3	0,67

Table A.2 Simulation results R600a

T_{evap}	W	V_s	COP	$N_{ch;evap}$	$N_{ch;cond}$	U_{cond}	U_{evap}	ΔP_{Evap}	ΔP_{Cond}	PR	ΔP_{comp}	$\dot{m}_{ref}$
40	73760	376,8	2,835	14	45	1218	4724	63781	4358	4,789	298,9	0,8
41	69122	348,7	2,966	16	42	1308	4629	51757	5128	4,505	295,2	0,8
42	64878	322,4	3,123	20	40	1386	4510	37039	5741	4,226	292,8	0,8
43	61733	302,8	3,27	25	40	1429	4423	26936	5728	4,015	290,9	0,8
44	59398	287,4	3,399	33	40	1426	5711	18782	5729	3,836	291	0,8
$\beta_{cond} = 45°$												
T_{cond}	W	V_s	COP	$N_{ch;evap}$	$N_{ch;cond}$	U_{cond}	U_{evap}	ΔP_{Evap}	ΔP_{Cond}	PR	ΔP_{comp}	$\dot{m}_{ref}$
100	73760	376,8	2,835	14	45	1218	4724	63781	4358	4,789	298,9	0,8
98	70113	366,5	3,004	15	65	979,4	4677	57260	2571	4,542	310,6	0,8
96	66882	357,7	3,184	16	104	748,3	4602	51848	-31,66	4,318	323	0,8
94	64010	350,2	3,368	17	189	541	4542	47240	-731,9	4,112	336,4	0,8
92	60954	340,2	3,562	19	476	305,5	4460	39385	-989,1	3,886	350,6	0,8
$\beta_{cond} = 65°$												
T_{cond}	W	V_s	COP	$N_{ch;evap}$	$N_{ch;cond}$	U_{cond}	U_{evap}	ΔP_{Evap}	ΔP_{Cond}	PR	ΔP_{comp}	$\dot{m}_{ref}$
100	73760	376,8	2,846	14	36	1550	4724	63781		4,789	298,9	0,8
98	70113	366,5	3,01	15	51	1262	4677	57260		4,542	310,6	0,8
96	66882	357,7	3,178	16	79	971,7	4602	51848		4,318	323	0,8
94	64010	350,2	3,356	17	144	680,4	4542	47240		4,112	336,4	0,8
92	60954	340,2	3,566	19	356	420,5	4460	39385		3,886	350,6	0,8

Table A.3 Simulation results R1234ze(Z)

T_{evap}	W	V_s	COP	$N_{ch;evap}$	$N_{ch;cond}$	U_{cond}	U_{evap}	ΔP_{Evap}	ΔP_{Cond}	PR	ΔP_{comp}	$\dot{m}_{ref}$
40	71580	543	2,961	17	60	772,8	3756	65761	1064	6,026	555,6	1,18
41	64057	475,5	3,216	20	54	900,8	3730	50659	1728	5,439	541	1,18
42	58515	427,5	3,424	24	51	953,7	3633	38448	2136	5,006	530	1,18
43	54608	393,9	3,629	29	49	1042	3583	29960	2453	4,688	522,9	1,18
44	51300	365,2	3,824	37	47	1121	3715	21212	2822	4,41	517,2	1,18
$\beta_{cond} = 45°$												
T_{cond}	W	V_s	COP	$N_{ch;evap}$	$N_{ch;cond}$	U_{cond}	U_{evap}	ΔP_{Evap}	ΔP_{Cond}	PR	ΔP_{comp}	$\dot{m}_{ref}$
100	71580	543	2,961	17	60	772,8	3756	65761	1064	6,026	555,6	1,18
98	68778	538,6	3,082	17	85	621,9	3724	66513	-559,2	5,792	577,2	1,18
96	64028	515,1	3,297	18	127	507,3	3702	60687	-1456	5,404	596,3	1,18
94	59636	493,6	3,519	19	223	367,7	3708	55113	-1951	5,049	616,4	1,18
92	57209	490	3,677	19	515	227,4	3680	55732	-2148	4,842	642,2	1,18
$\beta_{cond} = 65°$												
T_{cond}	W	V_s	COP	$N_{ch;evap}$	$N_{ch;cond}$	U_{cond}	U_{evap}	ΔP_{Evap}	ΔP_{Cond}	PR	ΔP_{comp}	$\dot{m}_{ref}$
100	71580	543	2,96	17	47	984,7	3756	65761		6,026	555,6	1,18
98	68778	538,6	3,083	17	66	804,3	3724	66513		5,792	577,2	1,18
96	64028	515,1	3,296	18	100	642,9	3702	60687		5,404	596,3	1,18
94	59636	493,6	3,516	19	168	479,8	3708	55113		5,049	616,4	1,18
92	57209	490	3,675	19	385	300,6	3680	55732		4,842	642,2	1,18

Table A.4 Results for economic calculations R600

T_{evap}	IC	$Annual\ MC$	$Annual\ CC$	$Annual\ OC$	AC	SHC
40	467681,00	28060,86	33183,12	359660,30	420904,27	0,46
41	467921,00	28075,26	33200,14	335556,29	396831,69	0,43
42	469001,00	28140,06	33276,77	318022,53	379439,36	0,41
43	451681,00	27100,86	32047,88	303402,99	362551,72	0,39
44	457641,00	27458,46	32470,75	291733,64	351662,85	0,38
Investment analysis vs gas						
T_{evap}	I_0	ΔOC	ΔMC	PO	PV	
40	232681,00	213,39	-21010,86	-9,11	-525799,43	
41	232921,00	24317,40	-21025,26	#NUM!	-186521,83	
42	234001,00	41851,16	-21090,06	16,99	58604,74	
43	216681,00	56470,70	-20050,86	7,24	296618,19	
44	222641,00	68140,04	-20408,46	5,44	450085,31	
T_{cond}	IC	$Annual\ MC$	$Annual\ CC$	$Annual\ OC$	AC	SHC
100	467681,00	28060,86	33183,12	359660,30	420904,27	0,46
98	483721,00	29023,26	34321,19	338800,00	402144,45	0,44
96	512681,00	30760,86	36375,98	320226,84	387363,68	0,42
94	569761,00	34185,66	40425,94	301781,47	376393,08	0,41
92	758321,00	45499,26	53804,74	286309,86	385613,86	0,42
Investment analysis vs gas						
T_{cond}	I_0	ΔOC	ΔMC	PO	PV	
100	232681,00	213,39	-21010,86	-9,11	-525799,43	
98	248721,00	21073,68	-21973,26	-55,26	-261399,57	
96	277681,00	39646,84	-23710,86	42,01	-53080,17	
94	334761,00	58092,21	-27135,66	15,95	101538,92	
92	523321,00	73563,83	-38449,26	28,02	-28418,27	

Table A.5 Results for economic calculations R600a

T_{evap}	IC	$Annual\ MC$	$Annual\ CC$	$Annual\ OC$	AC	SHC
40	449676,00	26980,56	31905,62	358518,52	417404,70	0,45
41	449076,00	26944,56	31863,05	342683,75	401491,35	0,43
42	420916,00	25254,96	29865,02	325456,29	380576,28	0,41
43	425116,00	25506,96	30163,02	310825,69	366495,67	0,40
44	431836,00	25910,16	30639,83	299029,13	355579,11	0,38
Investment analysis vs gas						
T_{evap}	I_0	ΔOC	ΔMC	PO	PV	
40	214676,00	1355,17	-19930,56	-9,35	-476476,58	
41	214076,00	17189,94	-19894,56	-32,81	-252194,83	
42	185916,00	34417,39	-18204,96	17,46	42581,12	
43	190116,00	49048,00	-18456,96	7,63	241032,37	
44	196836,00	60844,56	-18860,16	5,47	394889,78	
T_{cond}	IC	$Annual\ MC$	$Annual\ CC$	$Annual\ OC$	AC	SHC
100	449676,00	26980,56	31905,62	358518,52	417404,70	0,45
98	465716,00	27942,96	33043,69	338348,87	399335,52	0,43
96	496196,00	29771,76	35206,33	319221,11	384199,19	0,42
94	561636,00	33698,16	39849,45	301781,47	375329,09	0,41
92	781436,00	46886,16	55444,80	285345,31	387676,28	0,42
Investment analysis vs gas						
T_{cond}	I_0	ΔOC	ΔMC	PO	PV	
100	214676,00	1355,17	-19930,56	-9,35	-476476,58	
98	230716,00	21524,82	-20892,96	#NUM!	-221810,66	
96	261196,00	40652,58	-22721,76	26,71	-8480,04	
94	326636,00	58092,21	-26648,16	15,02	116534,72	
92	546436,00	74528,37	-39836,16	31,75	-57485,88	

Table A.6 Results for economic calculations R1234ze(Z)

T_{evap}	IC	$Annual\ MC$	$Annual\ CC$	$Annual\ OC$	AC	SHC
40	497791,00	29867,46	35319,49	343262,41	408449,37	0,44
41	465751,00	27945,06	33046,18	316044,78	377036,01	0,41
42	466831,00	28009,86	33122,81	296845,79	357978,46	0,39
43	449511,00	26970,66	31893,91	280077,16	338941,73	0,37
44	454711,00	27282,66	32262,86	265794,98	325340,50	0,35
Investment analysis vs gas						
T_{evap}	I_0	ΔOC	ΔMC	PO	PV	
40	262791,00	16611,27	-22817,46	-23,30	-350260,66	
41	230751,00	43828,91	-20895,06	14,33	92477,38	
42	231831,00	63027,89	-20959,86	6,61	361073,48	
43	214511,00	79796,53	-19920,66	4,05	629376,16	
44	219711,00	94078,71	-20232,66	3,30	821071,07	
T_{cond}	IC	$Annual\ MC$	$Annual\ CC$	$Annual\ OC$	AC	SHC
100	497791,00	29867,46	35319,49	343262,41	408449,37	0,44
98	516791,00	31007,46	36667,59	329785,85	397460,90	0,43
96	549551,00	32973,06	38991,99	308280,25	380245,31	0,41
94	593351,00	35601,06	42099,71	288832,05	366532,83	0,40
92	815271,00	48916,26	57845,48	276421,00	383182,74	0,41
Investment analysis vs gas						
T_{cond}	I_0	ΔOC	ΔMC	PO	PV	
100	262791,00	16611,27	-22817,46	-23,30	-350260,66	
98	281791,00	30087,83	-23957,46	#NUM!	-195389,89	
96	314551,00	51593,43	-25923,06	19,44	47245,76	
94	358351,00	71041,63	-28551,06	11,22	240508,73	
92	580271,00	83452,69	-41866,26	24,52	5845,82	

Table A.7 Results sensitivity analysis for R1234ze(Z) for electricity

e_{el} = 1,1 NOK/kWh e_{gas} = 0,37 NOK/kWh				
T_{evap}	AC	PO	PV	$GAS\ AC$
40	408449,37	-23,30	-350260,66	383597,51
41	377036,01	14,33	92477,38	383597,51
42	357978,46	6,61	361073,48	383597,51
43	338941,73	4,05	629376,16	383597,51
44	325340,50	3,30	821071,07	383597,51
e_{el} = 0,9 NOK/kWh e_{gas} = 0,37 NOK/kWh				
T_{evap}	AC	PO	PV	$GAS\ AC$
40	346038,02	5,46	529361,41	383597,51
41	319573,33	3,18	902353,30	383597,51
42	304006,50	2,64	1121751,33	383597,51
43	288018,61	2,09	1347083,78	383597,51
44	277014,14	1,93	1502180,10	383597,51
e_{el} = 0,7 NOK/kWh e_{gas} = 0,37 NOK/kWh				
T_{evap}	AC	PO	PV	$GAS\ AC$
40	283626,67	2,41	1408983,49	383597,51
41	262110,64	1,79	1712229,22	383597,51
42	250034,54	1,65	1882429,18	383597,51
43	237095,49	1,41	2064791,41	383597,51
44	228687,78	1,37	2183289,14	383597,51

Table A.8 Results sensitivity analysis for R1234ze(Z) for gas price

e_{gas} = 0,35 NOK/kWh e_{el} = 1,1 NOK/kWh				
T_{evap}	AC	PO	PV	$GAS\ AC$
40	408449,37	-8,47	-624424,97	364144,88
41	377036,01	#NUM!	-181686,93	364144,88
42	357978,46	14,73	86909,17	364144,88
43	338941,73	6,32	355211,85	364144,88
44	325340,50	4,62	546906,76	364144,88
e_{gas} = 0,34 NOK/kWh e_{el} = 1,1 NOK/kWh				
T_{evap}	AC	PO	PV	$GAS\ AC$
40	408449,37	-6,47	-761507,12	354418,56
41	377036,01	-21,45	-318769,08	354418,56
42	357978,46	47,06	-50172,99	354418,56
43	338941,73	8,81	218129,70	354418,56
44	325340,50	5,79	409824,60	354418,56
e_{gas} = 0,33 NOK/kWh e_{el} = 1,1 NOK/kWh				
T_{evap}	AC	PO	PV	$GAS\ AC$
40	408449,37	-5,24	-898589,28	344692,25
41	377036,01	-11,14	-455851,24	344692,25
42	357978,46	#NUM!	-187255,14	344692,25
43	338941,73	14,68	81047,54	344692,25
44	325340,50	7,74	272742,44	344692,25
e_{gas} = 0,32 NOK/kWh e_{el} = 1,1 NOK/kWh				
T_{evap}	AC	PO	PV	$GAS\ AC$
40	408449,37	-4,40	-1035671,44	334965,93
41	377036,01	-7,60	-592933,39	334965,93
42	357978,46	-20,85	-324337,30	334965,93
43	338941,73	63,05	-56034,61	334965,93
44	325340,50	11,73	135660,29	334965,93

Appendix B EES CODE

The code for the EES-model for R600 will follow. R600a has the exactly the same code. R1234ze(Z) however is different in the SGHE where the inlet values are equal to the outlet values, since there are no SGHE in that system.

```
"--------------------EVAPORATOR PROCEDURE------------------"

PROCEDURE EVAP(T_water_in_evap;
T_water_out_evap;P_water_evap;P_ref_evap;T_ref_evap;W_evap$;R$
;m_dot_water_evap;N_ch_evap;W_evap;m_dot_ref;th_m_evap;
stepsize;b_evap;p_evap;A_cross_evap;Beta_evap;
i_ref_LT;T_evap_superheat : L_out_evap;
i_ref_out_evap;i_ref_evap[1];i_w_out_evap;P_evap_out;T_ref_out
_evap;DELTAP_evap_all;d_h_evap;T_w_evap_real_out )
$ARRAYS ON

y_evap[1] = 0                          "starting point"

"Water side"
T_w_evap[1] = T_water_in_evap      "inlet water temperature"
i_w_evap[1] = enthalpy(W_evap$;T=T_w_evap[1];P=P_water_evap
"inlet water enthalpy"

"Refrigerant side"
i_ref_evap[1] =i_ref_LT            "Inlet refrigerant enthalpy"
x_ref_evap[1] = quality(R$;T=T_ref_evap;h=i_ref_evap[1])
   "inlet refrigerant quality"

T_ref_evap[1] = T_ref_evap         "inlet refrigerant
temperature"
P_ref_evap_local[1] = P_ref_evap   "refrigerant pressure"


"Other"
q_dot_evap[1] = 0 "Starting point for heat transfer"
k_m_evap[1]=k_('Stainless_AISI316';(T_ref_evap[1]+T_w_evap[1])
/2)"metal conductivity at local average temperature at
starting point" c_water_evap[1] =
cP(W_evap$;P=P_water_evap;x=0)"water specific heat capacity at
starting point"
g = 9,81 [m/s^2] "gravity constant"
Beta_max = 70 [degrees] "max chevron angle"
CorX = b_evap*pi/p_evap "dimensionless corrugation parameter"
PhiAmp = (1/6)*((1+sqrt(1+CorX^2))+4*sqrt(1+(CorX^2
/2)))"enlargement factor "
d_h_evap = (2*b_evap)/PhiAmp "Hydraulic diameter"

"----------HEAT TRANSFER COEFFICIENTS---------"
"Martin correlation for one phase flow"
G_w_evap = m_dot_water_evap/(A_cross_evap*N_ch_evap) "mass
flux water"
mu_l_water[1]=viscosity(W_evap$;T=T_w_evap[1];x=0)
  "viscosity of liquid phase"
mu_wall_water_evap[1]=viscosity(W_evap$;T=((T_ref_evap[1]+T_w_
evap[1])/2);x=0) "viscosity at wall"
```

```
Re_w_evap[1] =  (G_w_evap*d_h_evap)/mu_l_water[1] "reynolds
number"
Pr_w[1]=Prandtl(W_evap$;T=T_w_evap[1];x=0)"prandtl number"

IF Re_w_evap[1] < 2000 THEN        "Parameter for friction
factor calculation"
f0_martin[1] = 64/Re_w_evap[1]
f1_martin[1] = (597/Re_w_evap[1] )+3,85
ELSE
f0_martin[1]=(1,8*log10(Re_w_evap[1])-1,5)^(-2)
f1_martin[1] = 39/(Re_w_evap[1]^0,289)
ENDIF

f_martin[1]=(1/(cos(beta_evap)/sqrt(0,18*tan(beta_evap)+0,36*s
in(beta_evap)+(f0_martin[1]/cos(beta_evap)))+((1-
cos(beta_evap))/(sqrt(3,8*f1_martin[1])))) )^2 "friction
factor"
Nusselt_w[1]=0,122*(Pr_w[1]^(1/3))*(((mu_l_water[1]/mu_wall_wa
ter_evap[1])^(1/6)))*(f_martin[1]*(
(Re_w_evap[1]^2)*sin(2*beta_evap)))^0,374"Nusselt number"
k_w[1] = conductivity(W_evap$;T=T_w_evap[1];x=0)
  "water conductivity"
h_water_evap[1]=(Nusselt_w[1]*k_w[1])/d_h_evap "heat transfer
coefficient water"

"General data for refrigerant"

rho_g[1] = density(R$;T=T_ref_evap[1];x=1)"density of vapour
phase"
rho_l[1] = density(R$;T=T_ref_evap[1];x=0)"density of liquid
phase"
mu_g[1] = viscosity(R$;T=T_ref_evap[1];x=1)"viscosity of
vapour phase"
mu_l[1] = viscosity(R$;T=T_ref_evap[1];x=0)"viscosity of
liquid phase"

G_evap= m_dot_ref/(A_cross_evap*N_ch_evap)"mass flux"
G_eq[1]=G_evap*((1-
x_ref_evap[1])+x_ref_evap[1]*(rho_l[1]/rho_g[1])^0,5)
"equivalent mass flux"
Re_eq[1]=(G_eq[1]*d_h_evap)/mu_l[1] "equivalent reynolds
number"
Pr[1]=prandtl(R$;T=T_ref_evap[1];x=0) "prandt number liquid
phase"
k_ref_evap[1]=Conductivity(R$;T=T_ref_evap[1];x=0)"conductivit
y refrigerant liquid phase"

"Boiling number, X_tt and Bond number"
x_m = (1+x_ref_evap[1])/2          "mean quality"
rho_m = 1 / ( (x_m/rho_g[1]) + ((1-x_m)/rho_l[1])) "homogenous
density"
```

```
DELTAT_evap[1]=T_w_evap[1] - T_ref_evap[1] "temperature
difference"
q_flux[1] = h_water_evap[1]*DELTAT_evap[1] "heat flux"
gamma_evap[1]=Enthalpy_vaporization(R$;T=T_ref_evap[1])
"latent heat of evaporation"
X_tt[1]=((1-
x_m)/x_m)^0,9*((rho_g[1]/rho_l[1])^0,5)*(mu_l[1]/mu_g[1])^0,1

"lockhart-Martinelli parameter"
sigma_evap[1]=SurfaceTension(R$;T=T_ref_evap[1])
  "surface tension"
Bo[1]= q_flux[1]/(G_evap*gamma_evap[1])"boiling number"
Bd_evap[1]=((rho_l[1]-rho_g[1])*g*(d_h_evap^2))/sigma_evap[1]
"Bond number"
Re_v[1]=((G_Evap* x_ref_evap[1] *d_h_evap)/mu_g[1]) "vapor
Reynoldsnumber"
Re_lo[1] = ((G_Evap*d_h_evap)/mu_l[1])"Renynoldsnumber liquid
only"
ro_ratio[1] = rho_l[1]/rho_g[1] "Ratio between liquid and
vapor densities "
Beta_ratio = Beta_evap/Beta_max "Ratio between chevron angle
and max angle in the correlations data set"
We_m[1] = ((G_evap^2 *d_h_evap)/(rho_m*sigma_evap[1]))
"Homogenus Weber number"

BoX_tt[1] = Bo[1]*X_tt[1] "Boiling check, Convective if BoX_tt
< 0,15 *10^(-3) ; Nucleate for larger values"

"Almalfi et al. 2015 correlation for boiling heat transfer"
IF Bd_evap[1] < 4 THEN "Bond number less than 4 means
microscale"
Nu_tp[1] = 982 * Beta_ratio^1,101 * We_m[1]^0,315 *
Bo[1]^0,320 * ro_ratio[1]^(-0,224)
ELSE  "Larger then 4 means macroscale"
Nu_tp[1] = 18,495 * Beta_ratio^0,248 * Re_v[1]^0,135 *
Re_lo[1]^0,351 *Bd_evap[1]^0,235 * Bo[1]^0,198 *
ro_ratio[1]^(-0,223)
ENDIF

h_tp[1]=(k_ref_evap[1] / d_h_evap) * Nu_tp[1]
  "Heat transfer coefficient for two phase flow"

"State equation"
dtWdy_evap[1] = -(2*N_ch_evap*(T_w_evap[1]-T_ref_evap[1]) )
/(m_dot_water_evap*c_water_evap[1] *
(1/(h_tp[1]*W_evap)+th_m_evap/(k_m_evap[1]*W_evap)+1/(h_water_
evap[1]*W_evap))) "state equation for T_water"

N_evap =300[-] "Number of integration steps, should be minimum
"
DELTAy_evap =stepsize /N_evap "step size"
```

```
"Pressure drop"
"Amalfi et al 2015 f_tp"
C_evap = 2,125*Beta_ratio^9,993 +0,955 "Coefficient for the
effect of the corrugation angle in degrees"
f_tp[1] =C_evap*15,698*We_m[1]^(-0,475) * Bd_evap[1]^0,255 *
ro_ratio[1]^(-0,571) "two phase friction factor Amalfi et al.
2015"

DELTAP_evap[1]=(2*f_tp[1]*(G_evap^2)*DELTAy_evap)/(d_h_evap*rh
o_m) "pressure drop"

"------------------WHILE-LOOP-----------------"
i = 2                                  "step variable"

REPEAT "While loop for calculating the heatransfer in the two
phase region"

y_evap[i] = y_evap[i-1] + DELTAy_evap "Heat exchanger
location"

"Water side"
T_w_evap[i] = T_w_evap[i-1] + dtWdy_evap[i-1]*DELTAy_evap
"Water temperature"
i_w_evap[i] = enthalpy(W_evap$;T=T_w_evap[i];P=P_water_evap)
"Water specific enthalpy"
q_dot_evap[i] = m_dot_water_evap*(i_w_evap[i-1] -
i_w_evap[i])/N_ch_evap "Heat transfered"

"Refrigerant side"
P_ref_evap_local[i] = P_ref_evap_local[i-1]-DELTAP_evap[i-1]
"Refrigerant local pressuret"
i_ref_evap[i] = i_ref_evap[i-1] +
q_dot_evap[i]/(m_dot_ref/N_ch_evap) "Refrigerant specific
enthalpy"
x_ref_evap[i] =
quality(R$;h=i_ref_evap[i];P=P_ref_evap_local[i]) "Refrigerant
quality"

"IF ELSE FOR SUPERHEATED VAPOUR temperature change"
IF x_ref_evap[i] = 100 THEN
T_ref_evap[i] =
temperature(R$;P=P_ref_evap_local[i];h=i_ref_evap[i])

ELSE
T_ref_evap[i] =
temperature(R$;P=P_ref_evap_local[i];x=x_ref_evap[i])
"refrigerant temperature"
ENDIF

"---------------START OF IF-SENTENCE----------------------"
```

```
"!If the refrigerant quality is above 0,9, we have to use
another correlation"

IF (x_ref_evap[i-1] < 0,9) THEN "Two phase region"

k_m_evap[i]=k_('Stainless_AISI316';(T_ref_evap[i]+T_w_evap[i])
/2) "metal conductivity at local average temperature"
c_water_evap[i]=cP(W_evap$;P=P_water_evap;x=0) "specific heat
capacity of water"

"Martin correlation for one-phase flow water"
G_w_evap= m_dot_water_evap/(A_cross_evap*N_ch_evap) "mass flux
water"
mu_l_water[i]=viscosity(W_evap$;T=T_w_evap[i];x=0)
  "viscosity of liquid phase"
mu_wall_water_evap[i]=viscosity(W_evap$;T=(T_w_evap[i]+T_ref_e
vap[i])/2;x=0)
Re_w_evap[i] =
(G_w_evap*d_h_evap)/mu_l_water[i]  "reynolds number"
Pr_w[i]=Prandtl(W_evap$;T=T_w_evap[i];x=0)"prandtl number"

IF Re_w_evap[i] < 2000 THEN "Parameter for friction factor
calculation"
f0_martin[i] = 64/Re_w_evap[i]
f1_martin[i] = (597/Re_w_evap[i])+3,85
ELSE
f0_martin[i]=(1,8*log10(Re_w_evap[i])-1,5)^(-2)
f1_martin[i]=39/(Re_w_evap[i]^0,289)

ENDIF

f_martin[i]=(1/(cos(beta_evap)/sqrt(0,18*tan(beta_evap)+0,36*s
in(beta_evap)+(f0_martin[i]/cos(beta_evap)))+((1-
cos(beta_evap))/(sqrt(3,8*f1_martin[i])))))^2"friction factor"
Nusselt_w[i]=0,122*(Pr_w[i]^(1/3))*((mu_l_water[i]/mu_wall_wat
er_evap[i])^(1/6))*(f_martin[i]*((Re_w_evap[i]^2)*sin(2*beta_e
vap)))^0,374 "Nusselt number"
k_w[i] = conductivity(W_evap$;T=T_w_evap[i];x=0) "water
conductivity"
h_water_evap[i]=(Nusselt_w[i]*k_w[i])/d_h_evap "heat transfer
coefficient water"

"General data for refrigerant"
rho_g[i]= density(R$;T=T_ref_evap[i];x=1)"density of vapor
phase"
rho_l[i]= density(R$;T=T_ref_evap[i];x=0)"density of liquid
phase"
mu_g[i] = viscosity(R$;T=T_ref_evap[i];x=1)"viscosity of vapor
phase"
mu_l[i] = viscosity(R$;T=T_ref_evap[i];x=0) "viscosity of
liquid phase"
```

```
Pr[i]=prandtl(R$;T=T_ref_evap[i];x=0) "prandt number liquid
phase"
k_ref_evap[i] = Conductivity(R$;T=T_ref_evap[i];x=0)
"conductivity refrigerant liquid phase"
G_eq[i] = G_evap*((1-x_ref_evap[i])+
x_ref_evap[i]*(rho_l[i]/rho_g[i])^0,5) "equivalent mass flux"
Re_eq[i] =(G_eq[i]*d_h_evap)/mu_l[i] "equivalent Reynolds
number"

"Boiling number and X_tt"
DELTAT_evap[i] = T_w_evap[i] - T_ref_evap[i] "Temperature
difference"
q_flux[i] = h_water_evap[i]*DELTAT_evap[i] "Heat flux"
gamma_evap[i]=Enthalpy_vaporization(R$;T=T_ref_evap[i])"latent
heat of evaporation"
X_tt[i]=((1-
x_m)/x_m)^0,9*((rho_g[i]/rho_l[i])^0,5)*(mu_l[i]/mu_g[i])^0,1
"Lockhart-Martinelli parameter"
sigma_evap[i]=SurfaceTension(R$;T=T_ref_evap[i]) "surface
tension"
Bo[i] = q_flux[i]/(G_evap*gamma_evap[i]) "Boiling number"
Bd_evap[i] = ((rho_l[i]-rho_g[i])*g*(d_h_evap^2))/
sigma_evap[i] "Bond number"
Re_v[i] = ((G_Evap* x_ref_evap[i] *d_h_evap)/mu_g[i]) "vapor
Reynoldsnumber"
Re_lo[i] = ((G_Evap*d_h_evap)/mu_l[i]) "Renynoldsnumber liquid
only"
ro_ratio[i] = rho_l[i]/rho_g[i] "Ratio between liquid and
vapor densities "
Beta_ratio = Beta_evap/Beta_max "Ratio between chevron angle
and max angle in the correlations data set"
We_m[i]= ((G_evap^2*d_h_evap)/(rho_m*sigma_evap[i]))"Homogenus
Weber number"

BoX_tt[i] = Bo[i]*X_tt[i] "Boiling check, Convective if BoX_tt
< 0,15 *10^(-3) ; Nucleate for larger values"

"Almalfi 2015 correlation for boiling heat transfer"
IF Bd_evap[i] < 4 THEN "Bond number less than 4 means
microscale"
Nu_tp[i] = 982 * Beta_ratio^1,101 * We_m[i]^0,315 *
Bo[i]^0,320 * ro_ratio[i]^(-0,224)
ELSE "Larger then 4 means macroscale"
Nu_tp[i] = 18,495 * Beta_ratio^0,248 * Re_v[i]^0,135 *
Re_lo[i]^0,351 *Bd_evap[i]^0,235 * Bo[i]^0,198 *
ro_ratio[i]^(-0,223)
ENDIF
h_tp[i]=(k_ref_evap[i] / d_h_evap) * Nu_tp[i] "Heat transfer
coefficient for twophase flow"
```

```
h_dummy = max(h_tp[i])"dummy variable which saves the heat
transfer coefficient. To be used later for the linear
equation"

"State equation for T_water, to calculate temperature change"
  dtWdy_evap[i] = -(2*N_ch_evap*(T_w_evap[i]-T_ref_evap[i]) )
/(m_dot_water_evap*c_water_evap[i] *
(1/(h_tp[i]*W_evap)+th_m_evap/(k_m_evap[i]*W_evap)+1/(h_water_
evap[i]*W_evap)))

"Pressure drop"
f_tp[i] =C_evap*15,698*We_m[i]^(-0,475) * Bd_evap[i]^0,255 *
ro_ratio[i]^(-0,571) "two phase friction factor"
DELTAP_evap[i]=(2*f_tp[i-
1]*(G_evap^2)*DELTAy_evap)/(d_h_evap*rho_m) "pressure drop"
DELTAP_evap_tot[1] = 0              "initializing array"
DELTAP_evap_tot[i] = DELTAP_evap_tot[i-1] + DELTAP_evap[i]
"pressure drop"

i = i +1                            "counter"

ELSE                                "If quality is higher than
0,9"
"----------HEAT TRANSFER COEFFICIENTS---------"

y_evap[i] = y_evap[i-1] + DELTAy_evap
  "Heat exchanger location"

"Water side"
T_w_evap[i] = T_w_evap[i-1] + dtWdy_evap[i-1]*DELTAy_evap
"Water temperature"
i_w_evap[i] = enthalpy(W_evap$;T=T_w_evap[i];P=P_water_evap)
"Water specific enthalpy"

q_dot_evap[i] = m_dot_water_evap*(i_w_evap[i-1] -
i_w_evap[i])/N_ch_evap "Heat transfered"

"Refrigerant side"
P_ref_evap_local[i] = P_ref_evap_local[i-1]-DELTAP_evap[i-1]
"pressure of refrigerant"
i_ref_evap[i]=i_ref_evap[i-1] +
q_dot_evap[i]/(m_dot_ref/N_ch_evap) "Refrigerant specific
enthalpy"
x_ref_evap[i]=quality(R$;h=i_ref_evap[i];P=P_ref_evap_local[i]
) "Refrigerant quality"

IF (x_ref_evap[i] = 100) THEN "if else sentence to give the
correct temperature while transitioning"
T_ref_evap[i] = T_ref_evap[i-1]
ELSE
```

```
T_ref_evap[i]=temperature(R$;P=P_ref_evap_local[i];x=x_ref_eva
p[i]) "refrigerant temperature"
ENDIF

"Martin correlation for one-phase flow water"
G_w_evap= m_dot_water_evap/(A_cross_evap*N_ch_evap) "mass flux
water"
mu_l_water[i]=viscosity(W_evap$;T=T_w_evap[i];x=0) "viscosity
of liquid phase"
mu_wall_water_evap[i]=viscosity(W_evap$;T=(T_w_evap[i]+T_ref_e
vap[i])/2;x=0)
Re_w_evap[i]=(G_w_evap*d_h_evap)/mu_l_water[i] "reynolds
number"
Pr_w[i]=Prandtl(W_evap$;T=T_w_evap[i];x=0)"prandtl number"

IF Re_w_evap[i] < 2000 THEN "Parameter for friction factor
calculation"
f0_martin[i] = 64/Re_w_evap[i]
f1_martin[i] = (597/Re_w_evap[i] )+3,85
ELSE
f0_martin[i] =(1,8*log10(Re_w_evap[i])-1,5)^(-2)
f1_martin[i]= 39/(Re_w_evap[i]^0,289)
ENDIF

f_martin[i]=(1/(cos(beta_evap)/sqrt(0,18*tan(beta_evap)+0,36*s
in(beta_evap)+(f0_martin[i]/cos(beta_evap))) + ((1-
cos(beta_evap))/(sqrt(3,8*f1_martin[i])))))^2 "friction
factor"
Nusselt_w[i]=0,122*(Pr_w[i]^(1/3))*(((mu_l_water[i]/mu_wall_wa
ter_evap[i])^(1/6)))*(f_martin[i]*((Re_w_evap[i]^2)*sin(2*beta
_evap)))^0,374 "Nusselt number"
k_w[i] = conductivity(W_evap$;T=T_w_evap[i];x=0)  "water
conductivity"
h_water_evap[i]=(Nusselt_w[i]*k_w[i])/d_h_evap "heat transfer
coefficient water"
"Two-phase heat transfer coefficient"
"Linear correlation for wall dry out"
y_1 = h_dummy
y_2 = 600
x_1 = 0,9
x_2 = 1,0

a = (y_2-y_1)/(x_2-x_1)
b = y_2 -a*x_2
IF (x_ref_evap[i] < 100) THEN      "if sentence to correctly
transition between correlations"
h_tp[i] = a*x_ref_evap[i] + b
ELSE
h_tp[i] = h_tp[i-1]
ENDIF
```

```
"Boiling number check"
rho_g[i] = density(R$;T=T_ref_evap[i];x=1)"density of vapour
phase"
rho_l[i] = density(R$;T=T_ref_evap[i];x=0)"density of liquid
phase"
mu_g[i] = viscosity(R$;T=T_ref_evap[i];x=1)"viscosity of
vapour phase"
mu_l[i] = viscosity(R$;T=T_ref_evap[i];x=0)"viscosity of
liquid phase"
Pr[i]=prandtl(R$;T=T_ref_evap[i];x=0)"prandt number liquid
phase"
k_ref_evap[i]= Conductivity(R$;T=T_ref_evap[i];x=0)
"conductivity refrigerant liquid phase"

IF (x_ref_evap[i] < 100) THEN "if else to prevent error given
by x less than zero"
G_eq[i]=G_evap*((1-x_ref_evap[i])+
x_ref_evap[i]*(rho_l[i]/rho_g[i])^0,5)  "equivalent mass flux"
ELSE
G_eq[i] = G_eq[i-1]
ENDIF

Re_eq[i] = (G_eq[i]*d_h_evap)/mu_l[i] "equivalent reynolds
number"
gamma_evap[i]=Enthalpy_vaporization(R$;T=T_ref_evap[i])"latent
heat of evaporation"
X_tt[i] = ((1-x_m)/x_m)^0,9*
((rho_g[i]/rho_l[i])^0,5)*(mu_l[i]/mu_g[i])^0,1 "Lockhart-
Martinelli parameter"

"Boiling number and X_tt"
DELTAT_evap[i] = T_w_evap[i] - T_ref_evap[i] "Temperature
difference"
q_flux[i] = h_water_evap[i]*DELTAT_evap[i] "Heat flux"
Bo[i] = q_flux[i]/(G_evap*gamma_evap[i])"Boiling number"
BoX_tt[i] = Bo[i]*X_tt[i] "convective boiling check"

"Misc"
k_m_evap[i]=k_('Stainless_AISI316';(T_ref_evap[i]+T_w_evap[i])
/2) "metal conductivity at local average temperature"
c_water_evap[i] = cP(W_evap$; P=P_water_evap;x=0)" specific
heat capacity of water"

"State equation for T_water, to calculate temperature change"
 dtWdy_evap[i] = -(2*N_ch_evap*(T_w_evap[i]-T_ref_evap))
/(m_dot_water_evap*c_water_evap[i] *
(1/(h_tp[i]*W_evap)+th_m_evap/(k_m_evap[i]*W_evap)+1/(h_water_
evap[i]*W_evap)))

"Pressure drop"
```

```
sigma_evap[i]=SurfaceTension(R$;T=T_ref_evap[i]) "surface
tension"
Bd_evap[i] = ((rho_l[i]-
rho_g[i])*g*(d_h_evap^2))/sigma_evap[i] "Bond number"
f_tp[i]=C_evap*15,698*((((G_evap^2*d_h_evap)/(rho_m*sigma_evap
[i]))^(-0,475))*(Bd_evap[i]^0,255)*((rho_l[i]/rho_g[i])^(-
0,571))) "two phase friction factor"
DELTAP_evap[i]=(2*f_tp[i-1]*(G_evap^2)*DELTAy_evap)
/(d_h_evap*rho_m) "pressure drop"
DELTAP_evap_tot[i] = DELTAP_evap_tot[i-1] + DELTAP_evap[i]
"cumulative pressure drop"

i = i+1 "counter"
ENDIF

UNTIL ( x_ref_evap[i-1] = 100)  "End condition, saturated
vapour"
"---------------While loop for superheated part--------------"
REPEAT

y_evap[i] = y_evap[i-1] + DELTAy_evap
  "Heat exchanger location"
L_out_evap = y_evap[i] "Final length of heat exchanger"

"Water side"
T_w_evap[i] = T_w_evap[i-1] + dtWdy_evap[i-1]*DELTAy_evap
"Water temperature"
i_w_evap[i] = enthalpy(W_evap$;T=T_w_evap[i];P=P_water_evap)
"Water specific enthalpy"
{i_w_out_evap = i_w_evap[i-1] "water outlet enthalpy"}
i_w_out_evap = i_w_evap[i] "water outlet enthalpy"
q_dot_evap[i] = m_dot_water_evap*(i_w_evap[i-1]-
i_w_evap[i])/N_ch_evap "Heat transfered"

T_w_evap_real_out = T_w_evap[i] "Outlet water tempeature"

"Refrigerant side"
P_ref_evap_local[i] = P_ref_evap_local[i-1]-DELTAP_evap[i-1]
"pressure of refrigerant"
i_ref_evap[i] = i_ref_evap[i-1] +
q_dot_evap[i]/(m_dot_ref/N_ch_evap)"Refrigerant specific
enthalpy"
T_ref_evap[i]=temperature(R$;P=P_ref_evap_local[i];h=i_ref_eva
p[i]) "Temperature refrigerant"
T_ref_out_evap = T_ref_evap[i]     "Refrigerant outlet
temperature"
i_ref_out_evap = i_ref_evap[i]     "specific enthalpy of
refrigerant out of the evaporator"

"Martin correlation for one-phase flow water"
```

```
G_w_evap= m_dot_water_evap/(A_cross_evap*N_ch_evap) "mass flux
water"
mu_l_water[i]=viscosity(W_evap$;T=T_w_evap[i];x=0) "viscosity
of liquid phase"
mu_wall_water_evap[i]=viscosity(W_evap$;T=(T_w_evap[i]+T_ref_e
vap[i])/2;x=0) "viscosity at wall"
Re_w_evap[i]=(G_w_evap*d_h_evap)/mu_l_water[i] "reynolds
number"
Pr_w[i]=Prandtl(W_evap$;T=T_w_evap[i];x=0) "prandtl number"

IF Re_w_evap[i] < 2000 THEN        "Parameter for friction
factor calculation"
f0_martin[i] = 64/Re_w_evap[i]
f1_martin[i] = (597/Re_w_evap[i] )+3,85
ELSE
f0_martin[i] = (1,8*log10(Re_w_evap[i])-1,5)^(-2)
f1_martin[i]=39/(Re_w_evap[i]^0,289)

ENDIF

f_martin[i]=(1/(cos(beta_evap)/sqrt(0,18*tan(beta_evap)+0,36*s
in(beta_evap)+(f0_martin[i]/cos(beta_evap))) + ((1-
cos(beta_evap))/(sqrt(3,8*f1_martin[i])))) )^2 "friction
factor"
Nusselt_w[i]=0,122*(Pr_w[i]^(1/3))*(((mu_l_water[i]/mu_wall_wa
ter_evap[i])^(1/6)))*(f_martin[i]*(
(Re_w_evap[i]^2)*sin(2*beta_evap)))^0,374 "Nusselt number"
k_w[i] = conductivity(W_evap$;T=T_w_evap[i];x=0) "water
conductivity"
h_water_evap[i]=(Nusselt_w[i]*k_w[i])/d_h_evap "heat transfer
coefficient water"

"Martin correlation for one-phase flow refrigerant"
rho_g[i] = density(R$;T=T_ref_evap[i];x=1)"density of vapour
phase"
rho_l[i] = density(R$;T=T_ref_evap[i];x=0)"density of liquid
phase"
mu_g[i] = viscosity(R$;T=T_ref_evap[i];x=1)"viscosity of
vapour phase"
mu_l[i] = viscosity(R$;T=T_ref_evap[i];x=0)"viscosity of
liquid phase"
Pr[i]=prandtl(R$;T=T_ref_evap[i];x=0) "prandt number liquid
phase"
G_ref_evap=m_dot_ref/(A_cross_evap*N_ch_evap) "mass flux
refrigerant"
mu_wall_ref_evap[i]=viscosity(R$;T=(T_ref_evap[i]+T_w_evap[i])
/2;x=1) "Viscosity at wall"

Re_ref_evap[i] =(G_ref_evap*d_h_evap)/mu_g[i]"reynolds number"
Pr_ref_evap[i]=Prandtl(R$;T=T_ref_evap[i];x=1)"prandtl number"
```

```
IF Re_ref_evap[i] < 2000 THEN "Parameter for friction factor
calculation"
f0_martin_ref_evap[i] = 64/Re_ref_evap[i]
f1_martin_ref_evap[i]= (597/Re_ref_evap[i] )+3,85
ELSE
f0_martin_ref_evap[i] =(1,8*log10(Re_ref_evap[i])-1,5)^(-2)
f1_martin_ref_evap[i]=39/(Re_ref_evap[i]^0,289)

ENDIF

f_martin_ref_evap[i]=(1/(cos(Beta_evap)/sqrt(0,18*tan(Beta_eva
p)+0,36*sin(Beta_evap)+(f0_martin_ref_evap[i]/cos(Beta_evap)))
+ ((1-cos(Beta_evap))/(sqrt(3,8*f1_martin_ref_evap[i])))) )^2
"friction factor"
Nusselt_ref_evap[i]=0,122*(Pr[i]^(1/3))*((mu_g[i]/mu_wall_ref_
evap[i])^(1/6))*(f_martin_ref_evap[i]*((Re_ref_evap[i]^2)*sin(
2*Beta_evap)))^0,374 "Nusselt
number"

k_ref_evap[i] = conductivity(R$;T=T_ref_evap[i];x=1)
"refrigerant conductivity"
h_ref[i]=(Nusselt_ref_evap[i]*k_ref_evap[i])/d_h_evap "heat
transfer coefficient"

"Misc"
k_m_evap[i]=k_('Stainless_AISI316';(T_ref_evap[i]+T_w_evap[i])
/2) "metal conductivity at local average temperature"
c_water_evap[i] = cP(W_evap$; P=P_water_evap;x=0)"specific
heat capacity of water"

"State equation for T_water, to calculate temperature change"
dtWdy_evap[i] = -(2*N_ch_evap*(T_w_evap[i]-T_ref_evap))
/(m_dot_water_evap*c_water_evap[i] *
(1/(h_ref[i]*W_evap)+th_m_evap/(k_m_evap[i]*W_evap)+1/(h_water
_evap[i]*W_evap)))

"Misc pressure drops except the frictional pressure drop"
DELTAP_evap[i]=(2*f_martin_ref_evap[i]*(G_ref_evap^2)*DELTAy_e
vap)/(d_h_evap*rho_g[i]) "pressure drop"
DELTAP_evap_tot[i] = DELTAP_evap_tot[i-1] + DELTAP_evap[i]
"cumulative pressure drop"

g = 9,81 [m/s^2] "gravitational constant"
DELTAPgravity_evap = rho_m*g*L_out_evap "gravity driven
acceleration"

DELTAx_ref_evap = abs(1 - x_ref_evap[1])"quality change"
DELTAPacc_evap = (G_evap^2)*DELTAx_ref_evap*( (1/rho_g[1]) -
(1/rho_l[1])) "acceleration pressure"
DELTAPmanifold_evap = 1,5*(rho_m*((G_evap/rho_m)^2)*0,5)
"inlet/outlet pressure loss"
```

```
DELTAP_evap_all = DELTAP_evap_tot[i] + DELTAPgravity_evap +
DELTAPacc_evap + DELTAPmanifold_evap "total pressure loss"
P_evap_out =P_ref_evap - DELTAP_evap_all "outlet pressure"

i = i +1

i_ref_evap_needed = enthalpy(R$;T=T_ref_evap +
T_evap_superheat;P=P_ref_evap) "needed rerigerant enthalpy to
reach the correct superheat temperature"

UNTIL ( i_ref_evap[i-1] > i_ref_evap_needed)
  "End condition"

END
"--------------END OF EVAPORATOR PROCEDURE------------------"

"---------------------CONDENSER PROCEDURE--------------------
"
PROCEDURE
COND(T_water_in_cond;P_water_cond;P_ref_cond;T_ref_cond;T_wate
r_out_cond;W_cond$;R$;m_dot_water_cond;W_cond;m_dot_ref;th_m_c
ond; stepsize;h_condenser_inlet;
N_ch_cond;b_cond;A_cross_cond;beta_cond;p_cond;T_condenser_inl
et;T_subcool :
i_ref_out_cond;x_ref_out_cond;T_w_real_out;L_out_cond;i_w_out_
cond;P_cond_out;T_ref_cond_out;d_h_cond)
$ARRAYS ON
"----DESUPERHEATER PART-------------------------------------"
"Initializing variables, starting points"
y_cond[1] = 0                        "Starting point"

"Water side"
T_w_cond[1] = T_water_in_cond      "Inlet water temperature"
i_w_cond[1] =enthalpy(W_cond$;T=T_w_cond[1];P=P_water_cond)
"Inlet water enthalpy"
i_w_out_wanted_cond=enthalpy(W_cond$;T=T_water_out_cond;P=P_wa
ter_cond)"wanted outlet enthalpy"

"Refrigerant side"
i_ref_cond[1] = h_condenser_inlet  "Inlet refrigerant enthalpy"
T_ref_cond[1] = T_condenser_inlet  "Inlet refrigerant
temperature"
P_ref_cond_local[1] = P_ref_cond   "local refrigerant pressure"
x_ref_cond[1]=quality(R$;h=i_ref_cond[1];P=P_ref_cond_local[1]
)"refrigerant quality"

"Other"
q_dot_cond[1] = 0                  "Starting point for heat
transfer"
```

```
k_m_cond[1]=k_('Stainless_AISI316';(T_ref_cond+T_w_cond[1])/2)
"Metal conductivity at local average temperature at starting
point"
phi = 1,20"Longo 2015 enlargement factor beta 45"
{phi = 1,24}"Longo 2015 for Beta 65"
c_water_cond[1] = cP(W_cond$; P=P_water_cond;x=0) "Water
specific heat capacity at starting point"

N_cond = 300 [-]"Number of integration steps"
DELTAy_cond = stepsize/N_cond
  "step size"

CorX = b_cond*pi/p_cond "dimensionless corrugation parameter"
PhiAmp = (1/6)*((1+sqrt(1+CorX^2))+4*sqrt(1+(CorX^2 /2)))
"enlargement factor "
d_h_cond = (2*b_cond)/PhiAmp "Hydraulic diameter"

"Variables related to pressure drop"
rho_g_cond[1] = density(R$;T=T_ref_cond[1];x=1) "density of
vapour phase"
rho_l_cond[1] = density(R$;T=T_ref_cond[1];x=0) "density of
liquid phase"
rho_m_cond = (rho_g_cond[1]+rho_l_cond[1])/2 "mean density"

"----------HEAT TRANSFER COEFFICIENTS---------"
"Martin correlation for one-phase flow"
G_w_cond = m_dot_water_cond/(A_cross_cond*N_ch_cond)"mass flux
water"
mu_l_water_cond[1] = viscosity(W_cond$;T=T_w_cond[1];x=0)
"viscosity of liquid phase"
mu_wall_water_cond[1]=viscosity(W_cond$;T=(T_w_cond[1]+T_ref_c
ond[1])/2;x=0) "viscosity at wall"
Re_w_cond[1] =(G_w_cond*d_h_cond)/mu_l_water_cond[1]"reynolds
number"
Pr_w_cond[1]=Prandtl(W_cond$;T=T_w_cond[1];x=0)"prandtl
number"

IF Re_w_cond[1] < 2000 THEN "Parameter for friction factor
calculation"
f0_martin_cond[1]= 64/Re_w_cond[1]
f1_martin_cond[1]= (597/Re_w_cond[1] )+3,85
ELSE
f0_martin_cond[1]= (1,8*log10(Re_w_cond[1])-1,5)^(-2)
f1_martin_cond[1]=39/(Re_w_cond[1]^0,289)

ENDIF

f_martin_cond[1]=(1/(cos(Beta_cond)/sqrt(0,18*tan(Beta_cond)+0
,36*sin(Beta_cond)+(f0_martin_cond[1]/cos(Beta_cond))) + ((1-
cos(Beta_cond))/(sqrt(3,8*f1_martin_cond[1])))) )^2 "friction
factor"
```

```
Nusselt_w_cond[1]=0,122*(Pr_w_cond[1]^(1/3))*((mu_l_water_cond
[1]/mu_wall_water_cond[1])^(1/6))*(f_martin_cond[1]*((Re_w_con
d[1]^2)*sin(2*Beta_cond)))^0,374 "Nusselt number. Should also
include the viscosity term later"
k_w_cond[1] = conductivity(W_cond$;T=T_w_cond[1];x=0)"water
conductivity"
h_water_cond[1] =(Nusselt_w_cond[1]*k_w_cond[1])/d_h_cond
"heat transfer coefficient water"

IF (x_ref_cond[1] = 100) THEN "SUPERHEATED VAPOUR"

"Martin correlation for one-phase flow refrigerant"
G_ref_cond=m_dot_ref/(A_cross_cond*N_ch_cond) "mass flux
refrigerant"
mu_g_ref_cond[1]=viscosity(R$;T=T_ref_cond[1];x=1) "viscosity
of liquid phase"
mu_wall_ref_cond[1]=viscosity(R$;T=(T_ref_cond[1]+T_w_cond[1])
/2;x=1) "viscosity at wall"
Re_ref_cond[1]
=(G_ref_cond*d_h_cond)/mu_g_ref_cond[1]"reynolds number"
Pr_ref_cond[1]=Prandtl(R$;T=T_ref_cond[1];x=1)"prandtl number"

IF Re_ref_cond[1] < 2000 THEN "Parameter for friction factor
calculation"
f0_martin_ref_cond[1] = 64/Re_ref_cond[1]
f1_martin_ref_cond[1]= (597/Re_ref_cond[1] )+3,85
ELSE
f0_martin_ref_cond[1] = (1,8*log10(Re_ref_cond[1])-1,5)^(-2)
f1_martin_ref_cond[1]=39/(Re_ref_cond[1]^0,289)

ENDIF

f_martin_ref_cond[1]=(1/(cos(Beta_cond)/sqrt(0,18*tan(Beta_con
d)+0,36*sin(Beta_cond)+(f0_martin_ref_cond[1]/cos(Beta_cond)))
+ ((1-cos(Beta_cond))/(sqrt(3,8*f1_martin_ref_cond[1])))))^2
"friction factor"
Nusselt_ref_cond[1]=0,122*(Pr_ref_cond[1]^(1/3))*((mu_g_ref_co
nd[1]/mu_wall_ref_cond[1])^(1/6))*(f_martin_ref_cond[1]*(
(Re_ref_cond[1]^2)*sin(2*Beta_cond)))^0,374 "Nusselt number.
Should also include the viscosity term"
k_ref_cond[1] = conductivity(R$;T=T_ref_cond[1];x=1)
  "Refrigerant conductivity"
h_ref_cond[1] = (Nusselt_ref_cond[1]*k_ref_cond[1])/d_h_cond
"heat transfer coefficient ref"
{DELTAP_cond[1]=(2*f_martin_ref_cond[1]*(G_ref_cond^2)*DELTAy_
cond)/(d_h_cond*rho_m_cond)
DELTAP_cond_tot[1] = 0}            "total pressure drop"
ELSE                               "Incase of no superheated
vapor at starting conditions"

"Longo 2015 correlation for condensation of saturated gas"
```

```
G_ref_cond = m_dot_ref/(A_cross_cond*N_ch_cond)"mass flux"
rho_g_cond[1] = density(R$;T=T_ref_cond[1];x=1)"density of
vapor phase"
rho_l_cond[1] = density(R$;T=T_ref_cond[1];x=0)"density of
liquid phase"
G_eq_cond[1] = G_ref_cond *((1-x_ref_cond[1] )+ x_ref_cond[1]
*(rho_l_cond[1]/rho_g_cond[1])^0,5)"equivalent mass flux"
mu_l_cond[1]=viscosity(R$;T=T_ref_cond[1];x=0)"viscosity of
liquid phase"
Re_eq_cond[1] =(G_eq_cond[1]*d_h_cond)/mu_l_cond[1]"equivalent
reynolds number"
Pr_l_cond[1]=Prandtl(R$;T=T_ref_cond[1];x=0)"prandtl number
liquid phase"
k_ref_cond[1]=conductivity(R$;T=T_ref_cond[1];x=0)"conductivit
y refrigerant"
h_ref_cond[1]=1,875*phi*(k_ref_cond[1]/d_h_cond)*(Re_eq_cond[1
]^0,445)*(Pr_l_cond[1]^(1/3)) "two phase heat trans coeff"

ENDIF
"State equation for T_water"
dtWdy_cond[1] = (2*N_ch_cond*(T_ref_cond[1]-T_w_cond[1]) )
/(m_dot_water_cond*c_water_cond[1]*(1/(h_ref_cond[1]*W_cond)+t
h_m_cond/(k_m_cond[1]*W_cond)+1/(h_water_cond[1]*W_cond)))

i = 2                                   "step counter"

REPEAT

y_cond[i] = y_cond[i-1] +DELTAy_cond "Location in heat
exchanger"
L_out_cond = y_cond[i] "plate length"

"Water side"
T_w_cond[i] = T_w_cond[i-1] + dtWdy_cond[i-1]*DELTAy_cond
"Water temperature"
i_w_cond[i] = enthalpy(W_cond$;T=T_w_cond[i];P=P_water_cond)
"Water specific enthalpy"

q_dot_cond[i] = m_dot_water_cond*(i_w_cond[i-1] -
i_w_cond[i])/N_ch_cond "Heat transfered"
T_w_real_out = T_w_cond[i-1]"Water temperature at outlet"
i_w_out_cond =i_w_cond[i-1]"water enthalpy at outlet"

"Refrigerant side"
P_ref_cond_local[i] = P_ref_cond "P_ref_cond_local[i-1] -
DELTAP_cond[i-1]" "local pressure"
i_ref_cond[i]=i_ref_cond[i-1]+q_dot_cond[i]/
(m_dot_ref/N_ch_cond) "Refrigerant specific enthalpy"
x_ref_cond[i]=quality(R$;h=i_ref_cond[i];P=P_ref_cond_local[i]
) "Refrigerant quality"
```

```
"--------------------START OF IF SENTENCE-------------------"
IF (x_ref_cond[i] = 100) THEN      "If superheated vapour"

T_ref_cond[i]=temperature(R$;P=P_ref_cond_local[i];h=i_ref_con
d[i])"Refrigerant temperature"

T_ref_cond_out =T_ref_cond[i-1] "outlet temperature of
refrigerant"

i_ref_out_cond = i_ref_cond[i-1] "refrigerant enthalpy at
condenser outlet"

x_ref_out_cond = x_ref_cond[i-1] "refrigerant quality at
condenser outlet"

c_water_cond[i] = cP(W_cond$;
T=T_ref_cond[i];P=P_ref_cond_local[i])"Specific heat capacity
water"
c_water_cond1[i]= cP(W_cond$; T=T_ref_cond[i];x=0) "Specific
heat liquid water"
k_m_cond[i]=k_('Stainless_AISI316';(T_ref_cond+T_w_cond[i])/2)
"Metal conductivity at local average temperature"

"----------HEAT TRANSFER COEFFICIENTS---------"

"Martin correlation water side"
G_w_cond = m_dot_water_cond/(A_cross_cond*N_ch_cond) "mass
flux water"
mu_l_water_cond[i] =viscosity(W_cond$;T=T_w_cond[i];x=0)
"viscosity of liquid phase"
mu_wall_water_cond[i]=viscosity(W_cond$;T=(T_w_cond[i]+T_ref_c
ond[i])/2;x=0) "viscosity at wall"
Re_w_cond[i] = (G_w_cond*d_h_cond)/mu_l_water_cond[i]"reynolds
number"
Pr_w_cond[i]=Prandtl(W_cond$;T=T_w_cond[i];x=0)
  "prandtl number"

IF Re_w_cond[i] < 2000 THEN "Parameter for friction factor
calculation"
f0_martin_cond[i] = 64/Re_w_cond[i]
f1_martin_cond[i]= (597/Re_w_cond[i])+3,85
ELSE
f0_martin_cond[i]= (1,8*log10(Re_w_cond[i])-1,5)^(-2)
f1_martin_cond[i]=39/(Re_w_cond[i]^0,289)

ENDIF

f_martin_cond[i]=(1/(cos(Beta_cond)/sqrt(0,18*tan(Beta_cond)+0
,36*sin(Beta_cond)+(f0_martin_cond[i]/cos(Beta_cond))) + ((1-
cos(Beta_cond))/(sqrt(3,8*f1_martin_cond[i])))) )^2 "friction
factor"
```

```
Nusselt_w_cond[i]=0,122*(Pr_w_cond[i]^(1/3))*((mu_l_water_cond
[i]/mu_wall_water_cond[i])^(1/6))*(f_martin_cond[i]*((Re_w_con
d[i]^2)*sin(2*Beta_cond)))^0,374 "Nusselt number. Should also
include the viscosity term"
k_w_cond[i] = conductivity(W_cond$;T=T_w_cond[i];x=0)  "water
conductivity"
h_water_cond[i] =(Nusselt_w_cond[i]*k_w_cond[i])/d_h_cond
"heat transfer coefficient water"

"Martin correlation refrigerant side"
G_ref_cond =m_dot_ref/(A_cross_cond*N_ch_cond)"mass flux
refrigerant"
mu_g_ref_cond[i] =viscosity(R$;T=T_ref_cond[i];x=1)
"viscosity of gas phase"
mu_wall_ref_cond[i]=viscosity(R$;T=((T_ref_cond[i]+T_w_cond[i]
)/2);x=1)"viscosity at wall"
Re_ref_cond[i]=(G_ref_cond*d_h_cond)/mu_g_ref_cond[i]"reynolds
number"
Pr_ref_cond[i]=Prandtl(R$;T=T_ref_cond[i];x=1)"prandtl number"
IF Re_ref_cond[i] < 2000 THEN "Parameter for friction factor
calculation"
f0_martin_ref_cond[i] = 64/Re_ref_cond[i]
f1_martin_ref_cond[i]= (597/Re_ref_cond[i] )+3,85
ELSE
f0_martin_ref_cond[i]=(1,8*log10(Re_ref_cond[i])-1,5)^(-2)
f1_martin_ref_cond[i]=39/(Re_ref_cond[i]^0,289)

ENDIF
f_martin_ref_cond[i]=(1/(cos(Beta_cond)/sqrt(0,18*tan(Beta_con
d)+0,36*sin(Beta_cond)+(f0_martin_ref_cond[i]/cos(Beta_cond)))
+ ((1-cos(Beta_cond))/(sqrt(3,8*f1_martin_ref_cond[i])))) )^2
"friction factor"
Nusselt_ref_cond[i]=0,122*(Pr_ref_cond[i]^(1/3))*((mu_g_ref_co
nd[i]/mu_wall_ref_cond[i])^(1/6))*(f_martin_ref_cond[i]*((Re_r
ef_cond[i]^2)*sin(2*Beta_cond)))^0,374 "Nusselt number. "
k_ref_cond[i] = conductivity(R$;T=T_ref_cond[i];x=1)
  "Refrigerant conductivity"
h_ref_cond[i]=(Nusselt_ref_cond[i]*k_ref_cond[i])/d_h_cond
"heat transfer coefficient water"
"Pressure drop"
{DELTAP_cond[i]=(2*f_martin_ref_cond[i]*(G_ref_cond^2)*DELTAy_
cond)/(d_h_cond*rho_m_cond)
DELTAP_cond_tot[i] = DELTAP_cond_tot[i-1] + DELTAP_cond[i]}

"State equation for T_water"
dtWdy_cond[i] = (2*N_ch_cond*(T_ref_cond-T_w_cond[i]) )
/(m_dot_water_cond*c_water_cond[i] *
(1/(h_ref_cond[i]*W_cond)+th_m_cond/(k_m_cond[i]*W_cond)+1/(h_
water_cond[i]*W_cond)))

i = i + 1
```

```
ELSE "CONDENSING SECTION"

T_ref_cond[i]=temperature(R$;P=P_ref_cond_local[i];h=i_ref_con
d[i]) "refrigerant temperature"
T_ref_cond_out =T_ref_cond[i-1]"outlet temperature of
rerigerant"
i_ref_out_cond = i_ref_cond[i-1]"refrigerant enthalpy at
condenser outlet"
x_ref_out_cond = x_ref_cond[i-1]"refrigerant quality at
condenser outlet"

c_water_cond[i] = cP(W_cond$; P=P_water_cond;T=T_w_cond[i])
"Specific heat capacity water"
k_m_cond[i] =
k_('Stainless_AISI316';(T_ref_cond[i]+T_w_cond[i])/2) "Metal
conductivity at local average temperature"
"----------HEAT TRANSFER COEFFICIENTS---------"
"Martin correlation one phase flow"
G_w_cond = m_dot_water_cond/(A_cross_cond*N_ch_cond) "mass
flux water"
mu_l_water_cond[i] =viscosity(W_cond$;T=T_w_cond[i];x=0)
"viscosity of liquid phase"
mu_wall_water_cond[i]=viscosity(W_cond$;T=((T_w_cond[i]+T_ref_
cond[i])/2);x=0) "viscosity gas phase"
Re_w_cond[i] =  (G_w_cond*d_h_cond)/mu_l_water_cond[i]
"reynolds number"
Pr_w_cond[i]=Prandtl(W_cond$;T=T_w_cond[i];x=0)
  "prandtl number"

IF Re_w_cond[i] < 2000 THEN "Parameter for friction factor
calculation"
f0_martin_cond[i] = 64/Re_w_cond[i]
f1_martin_cond[i]= (597/Re_w_cond[i] )+3,85
ELSE
f0_martin_cond[i]= (1,8*log10(Re_w_cond[i])-1,5)^(-2)
f1_martin_cond[i]=39/(Re_w_cond[i]^0,289)

ENDIF

f_martin_cond[i]=(1/(cos(Beta_cond)/sqrt(0,18*tan(Beta_cond)+0
,36*sin(Beta_cond)+(f0_martin_cond[i]/cos(Beta_cond))) + ((1-
cos(Beta_cond))/(sqrt(3,8*f1_martin_cond[i])))))^2 "friction
factor"
Nusselt_w_cond[i]=0,122*(Pr_w_cond[i]^(1/3))*((mu_l_water_cond
[i]/mu_wall_water_cond[i])^(1/6))*(f_martin_cond[i]*((Re_w_con
d[i]^2)*sin(2*Beta_cond)))^0,374 "Nusselt number"
k_w_cond[i] = conductivity(W_cond$;T=T_w_cond[i];x=0) "water
conductivity"
h_water_cond[i] = (Nusselt_w_cond[i]*k_w_cond[i])/d_h_cond
"heat transfer coefficient water"
```

```
"Longo 2015 correlation for condensation of saturated gas"
G_ref_cond = m_dot_ref/(A_cross_cond*N_ch_cond)"mass flux"
rho_g_cond[i] = density(R$;T=T_ref_cond[i];x=1)"density of
vapour phase"
rho_l_cond[i] = density(R$;T=T_ref_cond[i];x=0)"density of
liquid phase"

IF (x_ref_cond[i] > -100) THEN "IF sentence to avoid problems
with quality below zero"
G_eq_cond[i]=G_ref_cond *((1-x_ref_cond[i])+ x_ref_cond[i]
*(rho_l_cond[i]/rho_g_cond[i])^0,5)"equivalent mass flux"
ELSE
G_eq_cond[i] = G_eq_cond[i-1]
ENDIF

mu_l_cond[i]=viscosity(R$;T=T_ref_cond[i];x=0)"viscosity of
liquid phase"
Re_eq_cond[i]=(G_eq_cond[i] *d_h_cond)/mu_l_cond[i]
"equivalent reynolds number"
Pr_l_cond[i]=Prandtl(R$;T=T_ref_cond[i];x=0) "prandtl number
liquid phase"
k_ref_cond[i]=conductivity(R$;T=T_ref_cond[i];x=0)
"conductivity refrigerant"

IF (x_ref_cond[i] = -100) THEN
h_ref_cond[i] = h_ref_cond[i-1]
ELSE
h_ref_cond[i]=1,875*phi*(k_ref_cond[i]/d_h_cond)*(Re_eq_cond[i
]^0,445)*(Pr_l_cond[i]^(1/3))"two phase heat trans coeff"
ENDIF

"State equation for T_water"
dtWdy_cond[i]=(2*N_ch_cond*(T_ref_cond[i]-T_w_cond[i]) )
/(m_dot_water_cond*c_water_cond[i] *
(1/(h_ref_cond[i]*W_cond)+th_m_cond/(k_m_cond[i]*W_cond)+1/(h_
water_cond[i]*W_cond)))

"Pressure drop"
"Misc pressure drops except the frictional pressure drop"
g = 9,81 [m/s^2]"gravitational constant"
DELTAPgravity_cond = rho_m_cond*g*L_out_cond "gravity driven
acceleration"

DELTAPacc_cond = (G_ref_cond^2)*1*((1/rho_g_cond[i])-
(1/rho_l_cond[i]))"acceleration pressure, quality change is 1"

DELTAPmanifold_cond=1,5*(rho_m_cond*((G_ref_cond/rho_m_cond)^2
)*0,5) "inlet/outlet pressure loss"
```

```
DELTAP_cond_fric = 1000*(1,9*G_ref_cond^2)/(2*rho_m_cond)
"kinetic model from Longo 2010"

DELTAP_cond_all = DELTAP_cond_fric+  DELTAPmanifold_cond -
DELTAPacc_cond +  -DELTAPgravity_cond
P_cond_out =P_ref_cond - DELTAP_cond_all "Pressure at
condenser outlet"

i = i+1

ENDIF

UNTIL  (x_ref_cond[i-1] = -100) "End condition"

"-------WHILE LOOP FOR SUBCOOLING OF RERIGERANT-------------"
REPEAT
y_cond[i] = y_cond[i-1]+DELTAy_cond "Location in heat
exchanger"
L_out_cond = y_cond[i] "plate length"

"Water side"
T_w_cond[i] = T_w_cond[i-1]+dtWdy_cond[i-1]*DELTAy_cond "Water
temperature"
i_w_cond[i]=enthalpy(W_cond$;T=T_w_cond[i];P=P_water_cond)"Wat
er specific enthalpy"
q_dot_cond[i] = m_dot_water_cond*(i_w_cond[i-1]- i_w_cond[i])/
N_ch_cond "Heat transfered"
{T_w_real_out = T_w_cond[i-1]      "Water temperature at
outlet"
i_w_out_cond = i_w_cond[i-1] "water enthalpy at outlet"}
T_w_real_out = T_w_cond[i] "Water temperature at
outlet"
i_w_out_cond = i_w_cond[i] "water enthalpy at outlet"

"Refrigerant side"
P_ref_cond_local[i] = P_ref_cond  "local pressure"

i_ref_cond[i]=i_ref_cond[i-1]+
q_dot_cond[i]/(m_dot_ref/N_ch_cond) "Refrigerant specific
enthalpy"
T_ref_cond[i]=temperature(R$;P=P_ref_cond_local[i];h=i_ref_con
d[i])
{T_ref_cond_out =T_ref_cond[i-1]   "Temperature of
refrigerant"}
T_ref_cond_out =T_ref_cond[i] "Temperature of refrigerant"
{i_ref_out_cond = i_ref_cond[i-1]  "refrigerant enthalpy at
condenser outlet"}
i_ref_out_cond = i_ref_cond[i] "refrigerant enthalpy at
condenser outlet"
x_ref_out_cond = -100 "refrigerant quality at condenser
outlet"
```

```
c_water_cond[i]=cP(W_cond$;T=T_ref_cond[i];P=P_ref_cond_local[
i]) "Specific heat capacity water"
c_water_cond1[i]= cP(W_cond$; T=T_ref_cond[i];x=0) "Specific
heat liquid water"
k_m_cond[i]=k_('Stainless_AISI316';(T_ref_cond+T_w_cond[i])/2)
"Metal conductivity at local average temperature"

"----------HEAT TRANSFER COEFFICIENTS---------"
"Martin correlation water side"
G_w_cond = m_dot_water_cond/(A_cross_cond*N_ch_cond) "mass
flux water"
mu_l_water_cond[i] =viscosity(W_cond$;T=T_w_cond[i];x=0)
"viscosity of liquid phase"
mu_wall_water_cond[i]=viscosity(W_cond$;T=(T_w_cond[i]+T_ref_c
ond[i])/2;x=0) "viscosity at wall"
Re_w_cond[i] =(G_w_cond*d_h_cond)/mu_l_water_cond[i] "reynolds
number"
Pr_w_cond[i]=Prandtl(W_cond$;T=T_w_cond[i];x=0)
  "prandtl number"

IF Re_w_cond[i] < 2000 THEN "Parameter for friction factor
calculation"
f0_martin_cond[i] = 64/Re_w_cond[i]
f1_martin_cond[i]= (597/Re_w_cond[i] )+3,85
ELSE
f0_martin_cond[i]= (1,8*log10(Re_w_cond[i])-1,5)^(-2)
f1_martin_cond[i]= 39/(Re_w_cond[i]^0,289)
ENDIF

f_martin_cond[i]=(1/(cos(Beta_cond)/sqrt(0,18*tan(Beta_cond)+0
,36*sin(Beta_cond)+(f0_martin_cond[i]/cos(Beta_cond))) + ((1-
cos(Beta_cond))/(sqrt(3,8*f1_martin_cond[i])))) )^2 "friction
factor"
Nusselt_w_cond[i]=0,122*(Pr_w_cond[i]^(1/3))*((mu_l_water_cond
[i]/mu_wall_water_cond[i])^(1/6))*(f_martin_cond[i]*(
(Re_w_cond[i]^2)*sin(2*Beta_cond)))^0,374 "Nusselt number.
Should also include the viscosity term"
k_w_cond[i] = conductivity(W_cond$;T=T_w_cond[i];x=0) "water
conductivity"
h_water_cond[i]=(Nusselt_w_cond[i]*k_w_cond[i])/d_h_cond "heat
transfer coefficient water"

"Martin correlation refrigerant side"

G_ref_cond = m_dot_ref/(A_cross_cond*N_ch_cond)"mass flux
refrigerant"
mu_l_ref_cond[i]=viscosity(R$;T=T_ref_cond[i];x=0)"viscosity
of liquid phase"
mu_wall_ref_cond[i]=viscosity(R$;T=((T_ref_cond[i]+T_w_cond[i]
)/2);x=0) "viscosity at wall"
```

```
Re_ref_cond[i]=(G_ref_cond*d_h_cond)/mu_l_ref_cond[i]
"reynolds number"
Pr_ref_cond[i]=Prandtl(R$;T=T_ref_cond[i];x=0)"prandtl number"
IF Re_ref_cond[i] < 2000 THEN      "Parameter for friction
factor calculation"
f0_martin_ref_cond[i] = 64/Re_ref_cond[i]
f1_martin_ref_cond[i]= (597/Re_ref_cond[i] )+3,85
ELSE
f0_martin_ref_cond[i] = (1,8*log10(Re_ref_cond[i])-1,5)^(-2)
f1_martin_ref_cond[i] = 39/(Re_ref_cond[i]^0,289)
ENDIF

f_martin_ref_cond[i]=(1/(cos(Beta_cond)/sqrt(0,18*tan(Beta_con
d)+0,36*sin(Beta_cond)+(f0_martin_ref_cond[i]/cos(Beta_cond)))
+ ((1-cos(Beta_cond))/(sqrt(3,8*f1_martin_ref_cond[i])))))^2
"friction factor"
Nusselt_ref_cond[i]=0,122*(Pr_ref_cond[i]^(1/3))*((mu_l_ref_co
nd[i]/mu_wall_ref_cond[i])^(1/6))*(f_martin_ref_cond[i]*((Re_r
ef_cond[i]^2)*sin(2*Beta_cond)))^0,374 "Nusselt number. "
k_ref_cond[i] = conductivity(R$;T=T_ref_cond[i];x=0)
  "water conductivity"
h_ref_cond[i]=(Nusselt_ref_cond[i]*k_ref_cond[i])/d_h_cond
"heat transfer coefficient water"
{"Pressure drop"
DELTAP_cond[i]=(2*f_martin_ref_cond[i]*(G_ref_cond^2)*DELTAy_c
ond)/(d_h_cond*rho_m_cond)
DELTAP_cond_tot[i] = DELTAP_cond_tot[i-1] + DELTAP_cond[i]}

"State equation for T_water"
dtWdy_cond[i] = (2*N_ch_cond*(T_ref_cond-T_w_cond[i]) )
/(m_dot_water_cond*c_water_cond[i] *
(1/(h_ref_cond[i]*W_cond)+th_m_cond/(k_m_cond[i]*W_cond)+1/(h_
water_cond[i]*W_cond)))

i = i + 1

UNTIL(T_ref_cond[i-1]<(T_ref_cond - T_subcool))"end condition"

END
"----------END OF CONDENSER PROCEDURE-----------------------"
stepsize=3 [m] "Step size for control volume length"
{Working Fluid Variables}
R$ = 'R600' "Working fluid:R600, R1234ze(Z), ..."
W_cond$ = 'Water' "Working fluid to reject heat to, water"
W_evap$ = 'Water' "Working fluid to extract heat from, water"
m_dot_ref =  0,67 [kg/s] "Mass flow rate of refrigerant,
adjustable"
m_dot_water_cond = 10,0 [kg/s] "Mass flow rate for water in
condenser, set from boundary conditions"
m_dot_water_evap =7 [kg/s] "Mass flow rate for water in
evaporator"
```

```
"GEOMETRY OF EVAPORATOR"
N_ch_evap = 35 [-] "number of channel/plate pairs"
Beta_evap = 45[degrees] "chevron angle"
p_evap = 8[mm]*convert(mm;m)       "Corrugation pitch"
b_evap = 2[mm]*convert(mm;m)       "Height of corrugation"
A_cross_evap = W_evap*b_evap       "cross sectional area plate"
th_m_evap = 0,5 [mm]*convert(mm;m) "thickness of plate"
W_evap = 24,3[cm]*convert(cm;m)    "width of heat exhanger"
area_evap = L_out_evap*W_evap*N_ch_evap*2"area of heat
exchanger"
L_plate_evap = 0,450 [m]

"PRESSURES"
P_ref_evap =pressure(R$;T=T_ref_evap;x=1)"hot-side pressure"
P_water_evap = 1,5 [bar]*convert(bar;Pa) "cold-side pressure"

"TEMPERATURES"
T_ref_evap=convertTemp(C;K;44 [C]) "refrigerant inlet
temperature"
T_evap_superheat = 5 [K] "superheat temperature"
T_water_in_evap =convertTemp(C;K;55[C])"feed inlet
temperature"
T_water_out_evap=convertTemp(C;K;50[C]) "feed outlet
temperature"
T_avg_evap =(T_water_in_evap + T_water_out_evap)/2
V_water_evap=(m_dot_water_evap/density(W_evap$;T=T_avg_evap;P=
P_water_evap))*3600[s/h]
i_w_in_evap=enthalpy(W_evap$;T=T_water_in_evap;P=P_water_evap)
"intlet enthalpy of water at evaporator"
i_w_out_wanted_evap=enthalpy(W_evap$;T=T_water_out_evap;P=P_wa
ter_evap) "enthalpy needed at evaporator outlet"

q_dot_ref_evap = m_dot_ref*(i_ref_out_evap - i_ref_evap[1])
"heat transfered to refrigerant"
q_dot_w_evap = m_dot_water_evap*(i_w_in_evap - i_w_out_evap)
"heat transfered to water"
{q_dot_needed_evap = m_dot_water_evap*(i_w_in_evap -
i_w_out_wanted_evap) "heat needed to water stream"}
q_dot_needed_evap = Q_dot_ref_cond - W
"Unbalance"
UB_evap=(abs(q_dot_w_evap+q_dot_ref_evap))/(q_dot_w_evap+0,000
0000001[W]) "discrepancy between heat streams. This number
should be as close to 2 as possible"

"GEOMETRY OF CONDENSER"
N_ch_cond= 38 [-]"number plate pairs"
beta_cond = 45 [degrees]           "chevron angel"
p_cond = 8[mm]*convert(mm;m)       "Corrugation pitch"
b_cond = 2[mm]*convert(mm;m)       "Height of corrugation"
A_cross_cond = W_cond*b_cond       "cross sectional area plate"
```

```
W_cond = 24,3[cm]*convert(cm;m)    "width of heat exhanger"
th_m_cond = 0,5[mm]*convert(mm;m)  "thickness of plate"
area_cond = L_out_cond*W_cond*N_ch_cond*2 "area of heat
exchanger"
L_plate_cond = 0,450"Length of plates in condenser"

"Condenser variables"
P_ref_cond =pressure(R$;T=T_ref_cond;x=1) "hot-side pressure"
P_water_cond = 1,5 [bar]*convert(bar;Pa)  "cold-side pressure"
T_ref_cond=convertTemp(C;K; 100 [C]) "Wanted refrigerant
condensing temperature"
T_water_in_cond =convertTemp(C;K;85[C])"feed inlet
temperature"
T_water_out_cond = convertTemp(C;K;90[C]) "feed outlet
temperature"
T_subcool = 1 [K]
T_avg = (T_water_in_cond + T_water_out_cond)/2
V_water_cond=(m_dot_water_cond/density(W_cond$;T=T_avg;P=P_wat
er_cond))*3600[s/h]

i_water_in_cond=enthalpy(W_cond$;T=T_water_in_cond;P=P_water_c
ond)"inlet enthalpy of water into condenser"
q_dot_w_real_cond =m_dot_water_cond*(i_w_out_cond-
i_water_in_cond) "actual heat transfered to water in the
condenser"
q_dot_ref_cond=m_dot_ref*(h_condenser_inlet - i_ref_out_cond)
"heat transfered to refrigerant"

h_condenser_inlet = h[6]
T_condenser_inlet = T[6]

"Compressor variables"
HL=0,1 "Heatloss"
eta_is = -0,00000461*PR^6 + 0,00027131*PR^5-
0,00628605*PR^4+0,07370258*PR^3-0,46054399*PR^2+1,40653347*PR-
0,87811477
Lambda_is = 0,0011*PR^2-0,0487*PR+0,9979
PR = P[5]/P[4]
DELTAT_SGHX = 10 [K]
{"Pipe Variables}
k_pipe = 0,00015 [m]  "Absolute roughness"

"!Pipes"
L_1to2 = 1,5 [m]
L_3to4 = 1,5 [m]
L_5to6 = 0,75 [m]
L_8to9 = 1,5 [m]
L_10to11 = 1,5 [m]

D_pipe_12 = 0,10 [m]
D_pipe_34 = 0,11 [m]
```

```
D_pipe_56 = 0,06 [m]
D_pipe_89 = 0,03 [m]
D_pipe_1011 = 0,03 [m]

RR_12= k_pipe/D_pipe_12 "Realtive roughness"
RR_34= k_pipe/D_pipe_34
RR_56= k_pipe/D_pipe_56
RR_89= k_pipe/D_pipe_89
RR_1011= k_pipe/D_pipe_1011

{Pipe 1-2}
"! Working fluid properties"
T[1] = T_ref_out_evap
P[1]= P_evap_out
h[1]= i_ref_out_evap
s[1]=entropy(R$;T=T[1];P=P[1])     "Entropy"
x[1]=quality(R$;T=T[1];P=P[1])     "Quality"

call PipeFlow(R$; T[1]+0,0001[K]; P[1]; m_dot_ref; D_pipe_12;
L_1to2;RR_12: {h_T_12}; {h_H_12}; DELTAP_12; {Nusselt_T_12};
{f_12}; Re_12)
u_1= Re_12 * KinematicViscosity(R$;T=T[1];P=P[1])/ D_pipe_12

P[2]=P[1]-DELTAP_12                "Pressure"
h[2]=h[1]                          "No entalphy difference"
T[2]=Temperature(R$;P=P[2];h=h[2]) "Temperature"
s[2]=entropy(R$;P=P[2];h=h[2])     "Entropy"
x[2]=quality(R$;P=P[2];h=h[2])

{SGHX 2-3}
P[3] = P[2]- 51800 [Pa]
T[3] = T[2] + DELTAT_SGHX          "Temperature"
h[3] = enthalpy(R$;P=P[3];T=T[3])  "Enthalpy"
x[3] = quality(R$;P=P[3];T=T[3])   "Quality"
s[3]=entropy(R$;P=P[3];T=T[3])     "Entropy"
DELTAh_SGHE = h[3]-h[2]

{Pipe 3-4}
call PipeFlow(R$; T[3]+0,0001[C]; P[3]; m_dot_ref; D_pipe_34;
L_3to4;RR_34: {h_T_34}; {h_H_34}; DELTAP_34; {Nusselt_T_34};
{f_34}; Re_34)
P[4]=P[3]-DELTAP_34                "Pressure"
h[4]=h[3]                          "No entalphy difference"
T[4]=Temperature(R$;P=P[4];h=h[4]) "Temperature"
s[4]=entropy(R$;h=h[4];P=P[4])     "Entropy"
x[4]=quality(R$;h=h[4];P=P[4])
u_3= Re_34 * KinematicViscosity(R$;T=T[3];P=P[3])/ D_pipe_34

{Compressor 4-5}
{P[5]=Pressure(R$;T=T_estimate_cond;x=0)}
P[5] = P_out_comp
```

```
h_5_IS=ENTHALPY(R$;P=P[5];s=s[4]) "h5 ideal state as
isentropic"
w_IS=(h_5_IS-h[4]) "Entalphy diffrence of isentropic
compressor"
DELTAw=w_IS/eta_is "Real compressor entalphy difference"
W=m_dot_ref*DELTAw                "Compressor work"
h[5]=h[4]+DELTAw*(1-HL)           "Calculation of h5"
s[5]=entropy(R$;h=h[5];P=P[5])    "Properties for state 5"
T[5]=temperature(R$;h=h[5];P=P[5])
x[5]=quality(R$;h=h[5];P=P[5])
V_s=(m_dot_ref/(density(R$;T=T[4];P=P[4])*lambda_is))*3600[s/h
] "Suction volume"
nu_4=1/density(R$;T=T[4];P=P[4])"Specific volume at compressor
inlet"
T_discharge=T[5] "Discharge gas temperature"

{Pipe 5-6}
"! Working fluid properties"
call PipeFlow(R$; T[5]; P[5]; m_dot_ref; D_pipe_56;
L_5to6;RR_56: {h_T_56}; {h_H_56}; DELTAP_56; {Nusselt_T_56};
{f_56}; Re_56)
{DELTAP_56 = 0}
P[6]=P[5]-DELTAP_56               "Pressure"
h[6]=h[5]                         "No entalphy difference"
T[6]=Temperature(R$;P=P[6];h=h[6]) "Temperature"
s[6]=entropy(R$;P=P[6];h=h[6])    "Entropy"
x[6]=quality(R$;P=P[6];h=h[6])
u_5= Re_56 * KinematicViscosity(R$;T=T[5];P=P[5])/ D_pipe_56

{Condenser 6-7}
CALL
COND(T_water_in_cond;P_water_cond;P_ref_cond;T_ref_cond;T_wate
r_out_cond;W_cond$;R$;m_dot_water_cond;W_cond;m_dot_ref;th_m_c
ond; stepsize;h_condenser_inlet;
N_ch_cond;b_cond;A_cross_cond;beta_cond;p_cond;T_condenser_inl
et;T_subcool :
i_ref_out_cond;x_ref_out_cond;T_w_real_out;L_out_cond;i_w_out_
cond;P_cond_out;T_ref_cond_out;d_h_cond)

T[7]= T_ref_cond_out
P[7]= P_cond_out
h[7]= i_ref_out_cond
x[7] = x_ref_out_cond
s[7]=entropy(R$;P=P[7];T=T[7])

{Pressure tank 8}
x[8] = 0
T[8] = T_ref_cond - T_subcool
P[8] = Pressure(R$;T=T[8];x=x[8])
h[8] = enthalpy(R$; T=T[8];x=x[8])
s[8] =entropy(R$;T=T[8];x=x[8])
```

```
{Pipe 8-9}
"! Working fluid properties"
call PipeFlow(R$; T[8]-0,001[K]; P[8]; m_dot_ref; D_pipe_89;
L_8to9;RR_89: {h_T_89}; {h_H_89}; DELTAP_89; {Nusselt_T_89};
{f_89}; Re_89)
P[9]=P[8]-DELTAP_89                "Pressure"
h[9]=h[8]                          "No entalphy difference"
T[9]=Temperature(R$;P=P[9];h=h[9]) "Temperature"
s[9]=entropy(R$;P=P[9];h=h[9])     "Entropy"
x[9]=quality(R$;P=P[9];h=h[9])
u_8= Re_89 * KinematicViscosity(R$;T=T[8];P=P[8]-1)/ D_pipe_89

{SGHX 9-10}
h[10] = h[9] - DELTAh_SGHE "Propeties of state 9"
P[10]= P[9]
T[10]=temperature(R$;P=P[10];h=h[10])
s[10]=entropy(R$;T=T[10];P=P[10])
x[10]=quality(R$;T=T[10];P=P[10])
DELTAh_SGHE2 = h[9]-h[10] "Entalphy difference in SGHE"
DELTAT_SGHE_SC=T[9]-T[10]          "Degree of subcooling"
Q_SGHE = m_dot_ref*(h[9]-h[10])    "Heating capacity of SGHE"

{Pipe 10-11}
"! Working fluid properties"
call PipeFlow(R$; T[10]-0,0001[K]; P[10]; m_dot_ref;
D_pipe_1011; L_10to11;RR_1011: {h_T_1011}; {h_H_1011};
DELTAP_1011; {Nusselt_T_1011};  {f_1011}; Re_1011)
P[11]=P[10]-DELTAP_1011 "Pressure"
h[11]=h[10] "No entalphy difference"
T[11]=Temperature(R$;P=P[11];h=h[11]) "Temperature"
s[11]=entropy(R$;P=P[11];h=h[11]) "Entropy"
x[11]=quality(R$;P=P[11];h=h[11])
u_10= Re_1011 * KinematicViscosity(R$;T=T[10];P=P[11])/
D_pipe_1011

{Valve 11-12}
h[12]=h[11] "Constant enthalphy"
P[12]=P_ref_evap "No pressure drop in condenser"
T[12]=T_ref_evap
s[12]=entropy(R$;T=T[12];h=h[12])
x[12]=quality(R$;h=h[12];P=P[12])

{Evap entrance 12-13}
i_ref_LT = h[12]
h[13] = h[1]
P[13] = P[1]

"Calling the evaporator procedure"
CALL
EVAP(T_water_in_evap;T_water_out_evap;P_water_evap;P_ref_evap;
```

```
T_ref_evap;W_evap$;R$;m_dot_water_evap;N_ch_evap;W_evap;m_dot_
ref;th_m_evap;stepsize;b_evap;p_evap;A_cross_evap;Beta_evap;i_
ref_LT;T_evap_superheat : L_out_evap;
i_ref_out_evap;i_ref_evap[1];i_w_out_evap;P_evap_out;T_ref_out
_evap;DELTAP_evap_all;d_h_evap;T_w_evap_real_out)

{U-value for heat exchangers}
"!Evap"
DELTAT_1_evap = T_water_in_evap - T_ref_evap
DELTAT_2_evap = T_water_out_evap -T_ref_out_evap
DELTALMTD_evap = (DELTAT_1_evap - DELTAT_2_evap) /
ln(DELTAT_1_evap/DELTAT_2_evap)
U_evap = q_dot_ref_evap/(area_evap*DELTALMTD_evap)

"!Cond"
DELTAT_1_cond =T_condenser_inlet - T_water_in_cond
DELTAT_2_cond = T_ref_cond_out - T_water_out_cond
DELTALMTD_cond = (DELTAT_1_cond - DELTAT_2_cond) /
ln(DELTAT_1_cond/DELTAT_2_cond)
U_cond = q_dot_ref_cond/(area_cond*DELTALMTD_cond)


{!Optimization}
DELTAP_guess_comp = 287,5 [Pa]"guessing the pressure loss in
the pipe from compressor to condenser "
P_out_comp = P_ref_cond+DELTAP_guess_comp "outlet pressure
from HP compressor"
err_comp = abs(DELTAP_guess_comp- DELTAP_56)
err_temp_cond = abs(T_w_real_out - T_water_out_cond) "Error
function for mass flow of water, to fix the temperature
discrepancy between temperature out of the condenser and the
wanted tempererature out"
err_temp_evap = abs(T_water_out_evap-T_w_evap_real_out)
err_length_cond = abs(L_plate_cond - L_out_cond) "Err function
for plate length"
err_length_evap = abs(L_plate_evap - L_out_evap)"Err function
for plate length"
err_heat_evap = abs(q_dot_needed_evap - q_dot_w_evap) "error
function to find correct refrigerant mass flow"

COP = q_dot_ref_cond / W
```

Appendix C Scientific Paper

Cost Efficient Industrial Heat Recovery through Heat Pumps

Morten Aarnes
(*) Norwegian University of Science and Technology (NTNU), Kolbjørn Hejes v 1B
Institutt for energi- og prosessteknikk, Trondheim, 7491, Norway
morteaaa@stud.ntnu.no

ABSTRACT

Simulation models for R1234ze(Z), R600 and R600a were developed to investigate the possibilities of recovering heat from the flue gas from a natural gas boiler and use it to produce hot water for washing purposes. Economic evaluations were conducted to assess if an investment in a heat pump system is more profitable than an investment in a natural gas boiler. The heat pump systems were evaluated at different evaporation temperatures and a constant condensation temperature. R1234ze(Z) achieved the highest COP with 3,8 and an annual cost of 325 000 NOK/year resulting in a pay-off time of 3,3 years. R600 achieved higher performance than R600a. The operational costs were the biggest contributor to the annual costs, optimizing the operational conditions for the compressor are therefore of significant importance. A reduction in electricity prices had a large positive effect on the profitability. A reduction in the natural gas price had the opposite effect.

1. INTRODUCTION

Large amounts of low grade waste heat are not utilized in the industry due to not having a suitable temperature range. However, these temperatures ranges are often ideal heat source temperatures for high temperature heat pumps. Heat pump technology has matured over the past two decades and heat pumps are found increasingly in households and buildings, showing their capability and high performance. Their use is not so widespread in the industry, due to the higher investment cost and that they are seen as difficult and not very reliable (IEA-HPC, 2014).

High temperature heat pumps are capable of replacing combustion systems and electric heaters in several applications, reducing fuel and energy consumption and in turn reducing emissions of greenhouse gasses (Fukuda et al., 2014). With increasing energy prices and carbon taxes, conservation and efficient use of energy will become increasingly important in industrial operations (Chua et al., 2010). The refrigerants used for high temperature vapor compression heat pumps, have had a large negative impact on the environment. The increased focus on environmental effects of the refrigerants together with stricter regulation is forcing a shift towards a generation of refrigerants defined by a focus on global warming (Calm, 2008). Hydrocarbons and HFOs are some of the refrigerants that have shown potential for use in industrial high temperature heat pumps.

Ommen et al. (2015) compared the technical and economic working domains for single stage vapor compression heat pumps using different natural refrigerants. Performance were calculated with constant efficiencies and the heat pumps did not have any cycle improvements. The refrigerants that was compared are R717, R600a, R290, R744 and R134a for comparison. Best available technology was found by comparing net present value and payback period for the different solutions. Based on economic criteria the R600a heat pump was the most suitable system at high sink temperatures (>85 ºC), but the economic feasibility was reduced with increasing temperature lifts.

Kondou and Koyama (2015) did a thermodynamic assessment of several different heat pump cycles suitable for industrial heat recovery with the refrigerants R717, R365mfc, R1234ze(E), and R1234ze(Z). Calculations were based on a waste heat source of 80 ˚C producing pressurized water at 160 ˚C. The heat recovery systems were optimized with several stages of heat extraction to reduce the throttling losses and exergy losses in the condensers, which are connected in series. The systems show promising result, even at reduced heat source temperatures. However, the effects of pressure drop are not taken into account when doing the calculations and several cycles operates above their critical temperature.

2. CASE

The Lamborghini automobile manufacturing plant in Sant' Agata Bolognese is vertical integrated, including the production of carbon fiber used in the car manufacturing. The carbon fiber autoclaves are heated by natural gas fired oil boilers. The flue gas that is produced, has a temperature of 200ºC, where 30% of the energy corresponds to sensible heat that can be recovered by an economizer. The remaining energy is latent heat contained in the water vapor generated by the natural gas burning which is released at condensation at approximately 60 ºC. The factory has a need for 90 ºC hot water for washing purposes. A heat pump solution should be able to recover heat from the carbon fiber production process and use it to cover the hot water demand. Suitable heat pump components were found and their characteristics and price was used as the basis of the model. Simulation models of the heat pump solutions was developed and used to investigate the profitability of choosing a heat pump over a natural gas boiler.

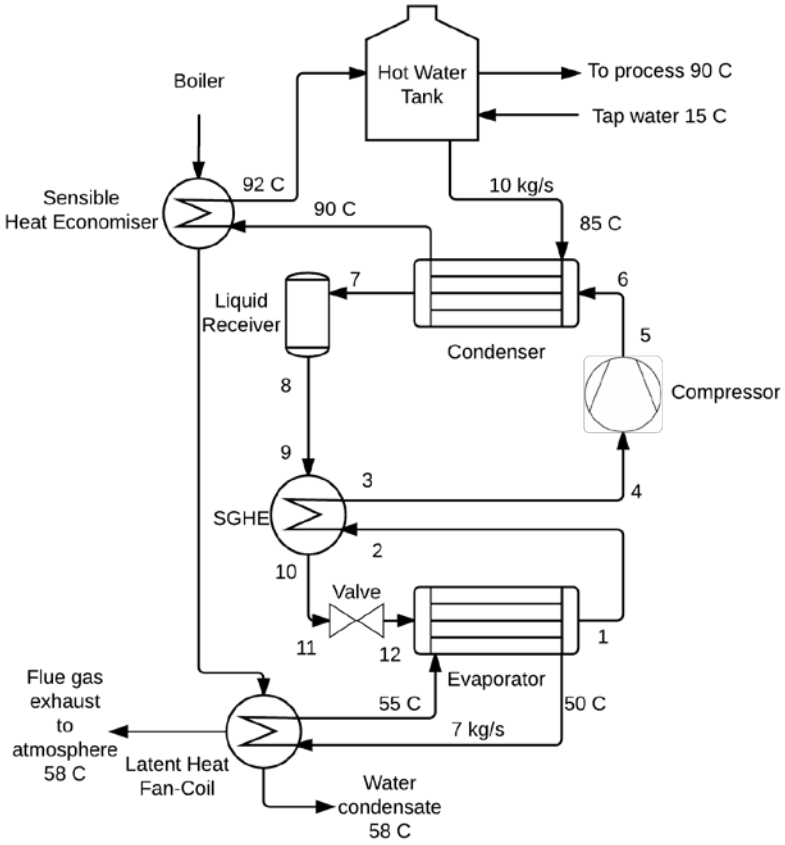

Figure 1 Schematic of plant with integrated heat pump system

The operating time of the heat pump is assumed to be 4400 hours a year. The amount of water needed to be heated in the condenser is set to 10 kg/s and the mass flow rate in the evaporator is set to be 7 kg/s. The required heat duty is approximately 210 kW, which equals to a yearly energy consumption of 924 000 kWh.
The evaporation temperature is varied between 40 ºC and 44 ºC while the condensation temperature is kept constant at 100 ºC.

3. HEAT PUMP MODEL

The model is developed in Engineering Equation Solver (EES) (Klein, 2015).

The heat exchangers are modeled with a numerical procedure to find the heat exchanger area and heat transfer needed to meet the required heat duties. The heat exchanger is divided into small control volumes and an energy balance is conducted. The step size for the calculations is chosen to be 3 m and there are 300 integration step equaling to a control volume length of 0,01 m. The state equations are derived from Nellis and Klein (2009) for a parallel flow plate heat exchanger. The state equation used to calculate the change in water temperature per length in the evaporator can be seen in (1) and the condenser in (2):

$$\frac{dT_H}{dx} = -\frac{2\,N_{ch}(T_H - T_C)}{\dot{m}_h c_H\left(\frac{1}{h_H W}+\frac{th_m}{k_m W}+\frac{1}{h_C W}\right)} \quad (1)$$

$$\frac{dT_C}{dx} = \frac{2\,N_{ch}(T_H - T_C)}{\dot{m}_C c_C\left(\frac{1}{h_H w}+\frac{th_m}{k_m w}+\frac{1}{h_C w}\right)} \quad (2)$$

The change in temperature is used to calculate the enthalpy change, which in turn gives the heat transferred to or from the refrigerant. The next control volume is calculated on the basis of values of the previous control volume, this procedure will go on until the desired outlet conditions are met. The temperature change in the refrigerant is given by the saturation pressure. The saturation pressure is affected by a pressure drop in the heat exchanger leading to a temperature fall.
The heat transfer coefficient is calculated using the Nusselt number:

$$h = \frac{Nu\,k}{d_h} \quad (3)$$

The hydraulic diameter for both the evaporator and condenser is calculated using (Martin, 1996):

$$d_h = \frac{2b}{\Phi} \quad (4)$$

$$\Phi(X) \approx \frac{1}{6}\left(\left(1+\sqrt{(1+X^2)}+4\sqrt{1+\frac{X^2}{2}}\right)\right) \quad (5)$$

$$X = \frac{b\pi}{\mathrm{p}} \quad (6)$$

3.1. Evaporator

The two-phase heat transfer coefficient is modeled with Amalfi et al. (2016b) correlation for flow boiling in plate heat exchangers in the region of 0<x<0,9:

$$Nu_{tp} = \begin{cases} 982\,\beta^{*1,101}\,We_m^{0,315}Bo^{0,320}\rho^{*-0,224} & ,Bd < 4 \\ 18{,}495\,\beta^{*0,248}Re_v^{0,135}Re_{lo}^{0,351}Bd^{0,235}Bo^{0,198}\rho^{*-0,223} & ,Bd \geq 4 \end{cases} \quad (7)$$

When the vapor quality is between 0,90<x<1 the heat transfer coefficient is modeled to decrease linearly down to 600 W/(m^{2}K). When x=1 the heat transfer coefficient for the refrigerant is found using the Martin correlation for single-phase flow in a plate heat exchanger (García-Cascales et al., 2007):

$$Nu = 0{,}122Pr^{\frac{1}{3}}\left(\frac{\mu}{\mu_{wall}}\right)^{\frac{1}{6}}(fRe^2\sin(2\beta))^{0,374} \quad (8)$$

The water side heat transfer coefficient is calculated using the Martin correlation for single-phase flow.

3.2. Condenser

The heat transfer coefficient for the superheated and subcooled region are calculated using the Martin correlation for single-phase flow. The two-phase heat transfer coefficient is modeled with Longo et al. (2015) correlation for condensation in plate heat exchangers:

$$h_{sat} = 1{,}875\,\Phi\left(\frac{k_l}{d_h}\right)Re_{eq}^{0,445}Pr_l^{1/3} \quad (9)$$

Table 1 Inputs to Heat Exchangers

Inputs	**Value**
L [m]	0,450
W [m]	0,243
N_{ch} [-]	Variable

p [m]	0,008
b [m]	0,002
β [deg]	45
Th_m [m]	0,0005
T_{sh} [K]	5
T_{sc} [K]	1

3.3. Compressor

The compressor work is calculated using isentropic efficiency and a heat loss. The heat loss is constant and equal to 10% of the compressor work. The isentropic and volumetric efficiency is calculated using the pressure ratio (Eikevik et al., 2016):

$$\eta_{is} = -0{,}00000461\,PR^6 + 0{,}00027131\,PR^5 - 0{,}00628605\,PR^4 + 0{,}07370258\,PR^3 - 0{,}46054399\,PR^2 + 1{,}40653347\,PR - 0{,}87811477 \quad (10)$$

$$\lambda = 0{,}0011\,PR^2 - 0{,}0487\,PR + 0{,}9979 \quad (11)$$

3.4. Suction Gas Heat Exchanger

The R600 and R600a models have an additional superheat of 10 K and a constant pressure drop around 50 kPa. R1234ze(Z) is modelled without a suction gas heat exchanger and therefore no additional pressure drop.

3.5. Pressure Loss in the System

The total pressure loss in the heat exchangers is calculated using (Amalfi et al., 2016a) and (Longo, 2010):

$$\Delta P_{tot,evap} = \Delta P_G + \Delta P_{acc} + \Delta P_{fric} + \Delta P_p \quad (12)$$

$$\Delta P_{tot,cond} = -\Delta P_G - \Delta P_{acc} + \Delta P_{fric} + \Delta P_p \quad (13)$$

$$\Delta P_G = \rho_m\, g\, L_{plate} \quad (14)$$

$$\Delta P_{acc} = G^2 \Delta x \left(\frac{1}{\rho_g} - \frac{1}{\rho_l}\right) \quad (15)$$

$$\Delta P_p = 0{,}75 \left[\left(\frac{G_p^2}{2\rho}\right)_{in} + \left(\frac{G_p^2}{2\rho}\right)_{out}\right] \quad (16)$$

The frictional pressure drop in the evaporator caused by the refrigerant is predicted using two-phase friction factor coefficient from (Amalfi et al., 2016b) and the friction factor coefficient from Martin correlation for single phase flow (García-Cascales et al., 2007):

$$\Delta P_{fric} = \frac{2\,f\,G^2 \Delta y}{d_h * \rho_m} \quad (17)$$

The frictional pressure drop in the condenser is predicted using a linear equation based on the kinetic energy per unit volume from (Longo, 2010) given in kPa:

$$\Delta P_{fric} = 1{,}90\,\frac{KE}{V} \quad (18)$$

$$\frac{KE}{V} = \frac{G^2}{2\,\rho_m} \quad (19)$$

The pressure loss in the pipes are calculated using the function PipeFlow (Klein, 2015). The pipe diameter is chosen on the basis of having flow velocities of around 9-10 m/s in the suction line, 6-7 m/s in the pressure pipeline and 2-3,5 m/s in the return lines to have an efficient oil return and moderate pressure/temperature loss.

3.6. Iterative Optimization

A set of error functions are used to find the correct input values that corresponds with the different operating conditions. EES' inbuilt MIN/MAX function was used to find the correct mass flow of the refrigerant at the base operating conditions by minimizing:

$$\mathrm{err_{temp;cond}} = \mathrm{abs}(\mathrm{T_{w;real;out}} - \mathrm{T_{water;out;cond}}) \quad (20)$$

The correct compressor outlet pressure was found minimizing the error function:

$$err_{comp} = abs(P_{guess;comp} - \Delta P_{56}) \quad (21)$$

The number channels in the evaporator and condenser was found by minimizing:

$$err_{length;cond} = abs(L_{plate;cond} - L_{out;cond}) \quad (22)$$

$$err_{length;evap} = abs(L_{plate;evap} - L_{out;evap}) \quad (23)$$

3.7. Economic Model

An economic model has been created to compare the operational and investment costs of the different heat pump solutions in addition to comparing them with a traditional heating solution. In this case a natural gas boiler is used for comparison. The annual cost for the different solutions is calculated by summing the annual capital cost, the annual operational cost and the annual maintenance cost. The maintenance cost is calculated as a percentage of the investment cost:

$$AC = \sum(I_0\ a)_n + \sum(W_e\ e) + \sum MC \quad (24)$$

To assess if it is profitable to invest in the different heat pump solutions over a natural gas boiler a profitability analysis is conducted. This is done using the Present Value Method and Pay-Off Time (Stene, 2016). The Present Value Method shows the absolute profitability of an investment. If a heat pump project has a PV>0 then its regarded as a profitable investment. PV is calculated by:

$$PV = \frac{B}{a} - I_0 \quad (25)$$

Pay-Off Time will result in the number of years it takes before the sum of net annual savings equals to the additional investment cost, while taking account of the real interest rate. Pay-Off Time is calculated by:

$$PO = \frac{ln\left[\left(1-\left(\frac{I_0}{B}\right)r\right)^{-1}\right]}{ln(1+r)} \quad (26)$$

Table 2 Inputs in economic model

Inputs	**Value**
r [%]	5
n [years]	25
τ [hours]	4400
Q [kW]	210
E_{tot} [kWh]	924 000
MC_{HP} [%]	6
MC_{gas} [%]	3
η_{gas} [-]	0,95
e_{gas} [NOK/kWh]	0,37
e_{el} [NOK/kWh]	1,10

4. RESULTS

4.1. Heat Pump Model

Table 3 shows the results of some of the most important variables for the 3 different refrigerants at changing evaporating temperatures.

Table 3 Simulation results for the different refrigerants at different evaporation temperatures

R600											
T_{evap}	W	V_s	COP	$N_{ch;evap}$	$N_{ch;cond}$	U_{cond}	U_{evap}	ΔP_{evap}	ΔP_{cond}	PR	$\dot{m}_{ref}$
40 °C	75487	508,2	2,826	15	47	1108	4637	52684	2297	5,563	0,67
41 °C	69037	456,9	3,029	18	44	1232	4544	39398	2742	5,116	0,67
42 °C	64226	419,2	3,196	22	41	1330	4476	29025	3298	4,775	0,67
43 °C	60564	390,6	3,35	27	39	1434	4381	21558	3738	4,512	0,67
44 °C	57553	366,7	3,484	35	38	1466	4598	15028	3981	4,285	0,67
R600a											
T_{evap}	W	V_s	COP	$N_{ch;evap}$	$N_{ch;cond}$	U_{cond}	U_{evap}	ΔP_{evap}	ΔP_{cond}	PR	$\dot{m}_{ref}$
40 °C	73760	376,8	2,835	14	45	1218	4724	63781	4358	4,789	0,8
41 °C	69122	348,7	2,966	16	42	1308	4629	51757	5128	4,505	0,8
42 °C	64878	322,4	3,123	20	40	1386	4510	37039	5741	4,226	0,8
43 °C	61733	302,8	3,27	25	40	1429	4423	26936	5728	4,015	0,8
44 °C	59398	287,4	3,399	33	40	1426	5711	18782	5729	3,836	0,8
R1234ze(Z)											
T_{evap}	W	V_s	COP	$N_{ch;evap}$	$N_{ch;cond}$	U_{cond}	U_{evap}	ΔP_{evap}	ΔP_{cond}	PR	$\dot{m}_{ref}$
40 °C	71580	543	2,961	17	60	772,8	3756	65761	1064	6,026	1,18
41 °C	64057	475,5	3,216	20	54	900,8	3730	50659	1728	5,439	1,18
42 °C	58515	427,5	3,424	24	51	953,7	3633	38448	2136	5,006	1,18
43 °C	54608	393,9	3,629	29	49	1042	3583	29960	2453	4,688	1,18
44 °C	51300	365,2	3,824	37	47	1121	3715	21212	2822	4,41	1,18

4.2. Economic Model

Figure 2 shows the annual cost for the 3 heat pumps and Figure 3 and Figure 4 shows the corresponding present value and pay-off time. In Figure 5 to Figure 7 is the results of a sensitivity analysis for the R1234ze(Z) heat pump at varying electricity prices. In Figure 8 to Figure 10 is the results of a sensitivity analysis for R1234ze(Z) heat pump at varying natural gas prices. R1234ze(Z) was used, because it was the most cost efficient cycle of the three.

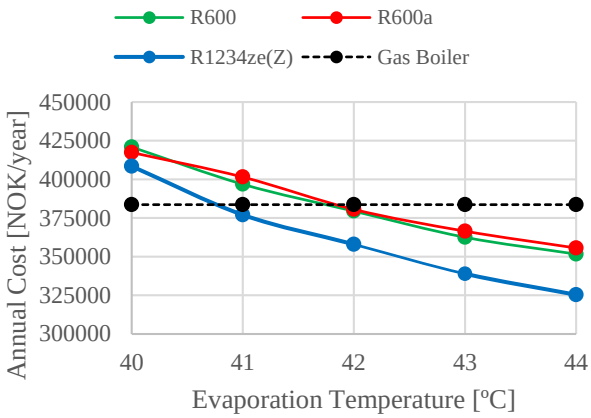

Figure 2 Annual Cost for different evaporation temperatures

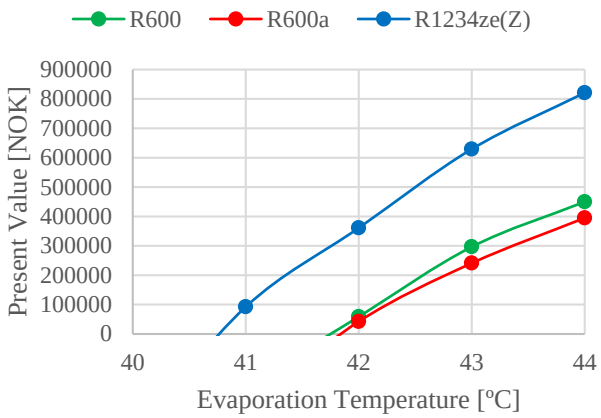

Figure 3 Present value for different evaporation temperatures

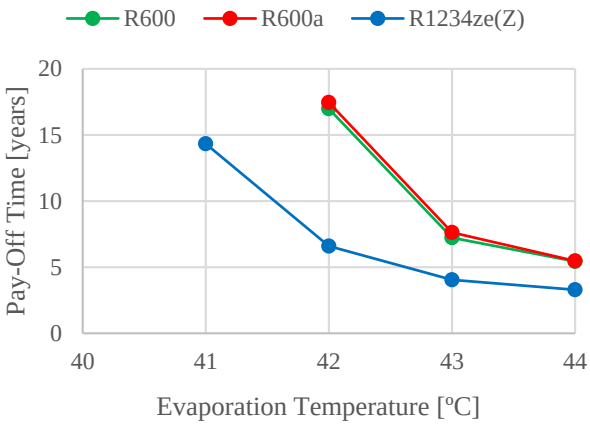

Figure 4 Pay-Off Time for different evaporation temperatures

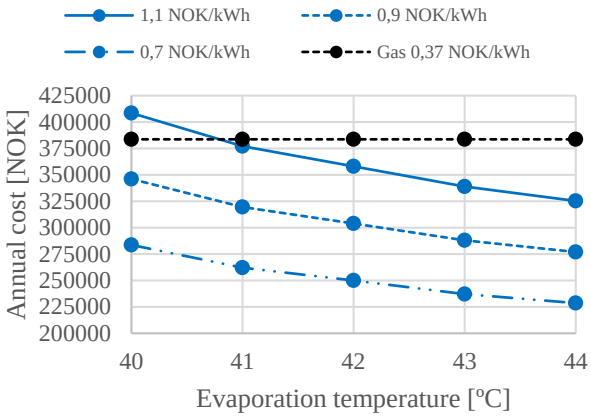

Figure 5 Annual cost for R1234ze(Z) at varying el prices

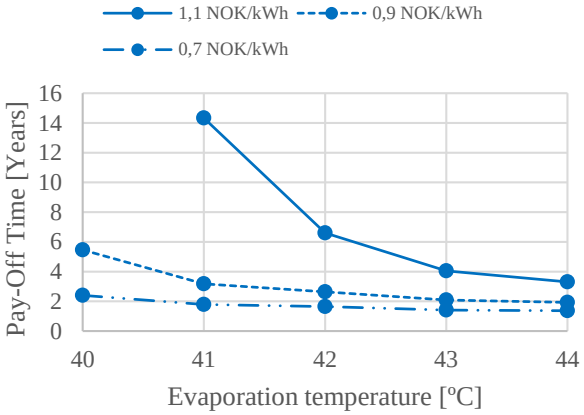

Figure 6 Pay-Off Time for R1234ze(Z) at varying el prices

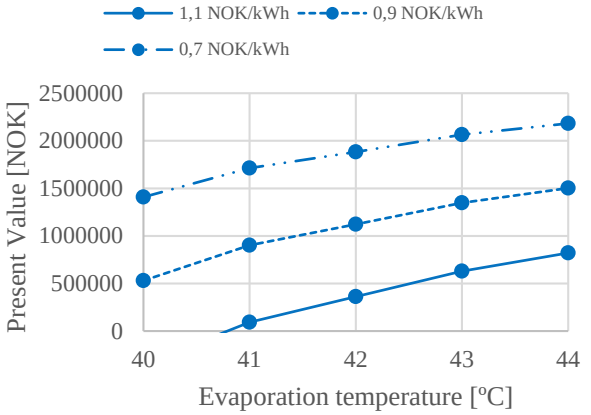

Figure 7 Present value for R1234ze(Z) at varying el prices

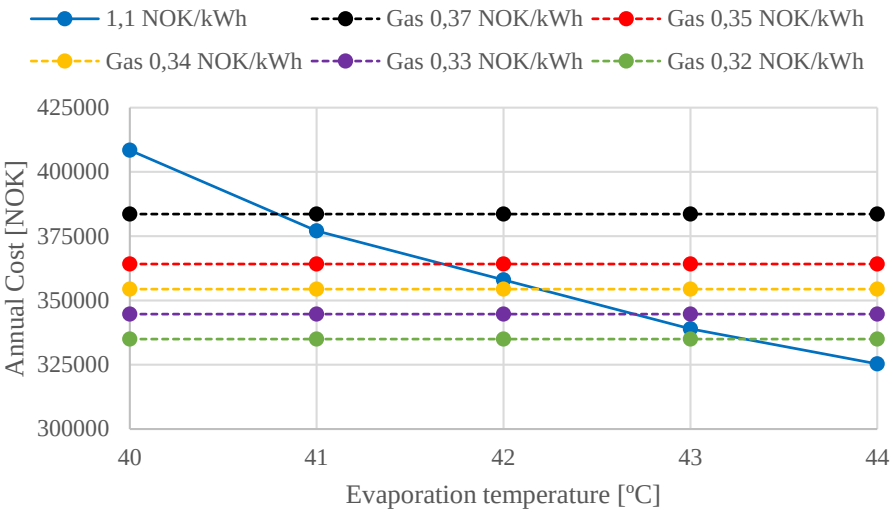

Figure 8 Annual cost for R1234ze(Z) and natural gas boiler at different natural gas prices

The pay-off time in Figure 10 for 0,34 NOK/kWh at 42 ºC is equal to 47 years and for 0,32 kWh at 43ºC is equal to 63 years. Far above the economic life time of 25 years.

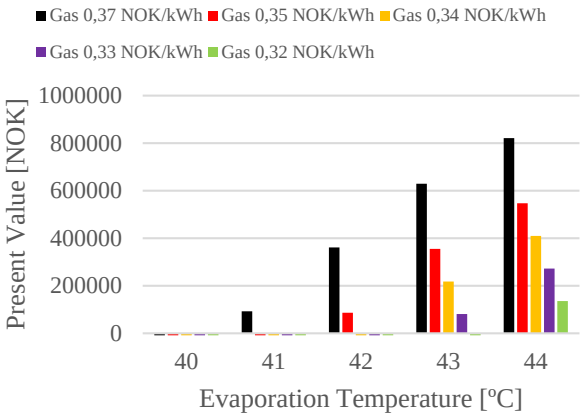

Figure 9 Present value R1234ze(Z) at varying natural gas price

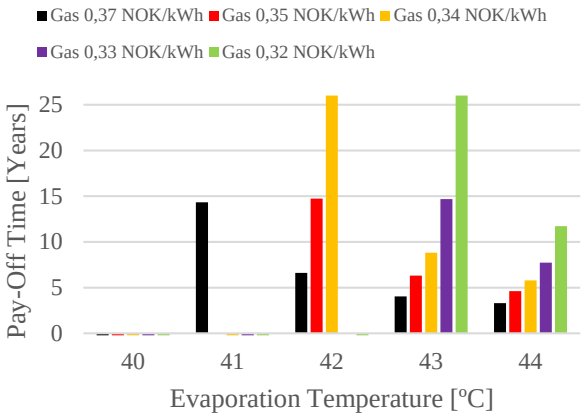

Figure 10 Pay-Off Time R1234ze(Z) at varying natural gas price

5. DISCUSSION

When evaluating the results, it is important to take into account that basis of the model. The correlations used for heat transfer and friction factor calculations in both the evaporator and condenser is based on experimental data that is measured in the temperature range of 10-20 ºC for the evaporator and 20-40 ºC for the condenser. The measurements are done for several different refrigerants, including HFCs, HFOs(R1234ze(E) and yf) and natural refrigerants (R600a, R290, etc.), but not for R600 and R1234ze(Z). The heat exchangers are modelled as parallel-flow heat exchangers, resulting in a large temperature difference at the inlet of the condenser. Using a counter-flow configuration could increase the heat exchanger efficiency further. Another thing to be noted is that the investment costs calculated only contains the components costs and not additional costs that could increase the total cost of the systems; installation costs, safety measures due to flammability, refrigerant cost, valves, control system etc. Reducing the profitability of investing in a heat pump system compared to a natural gas boiler, however a natural gas boiler system would also have higher investment costs than calculated here due to the same concerns.

The results show that it is possible to save large amounts of energy, by using a heat pump solution over competing heating solutions. At the base operating conditions, the COP for the cycle is close to 3 for R1234ze(Z) and 2,8 for R600 and R600a, which equals an energy saving of close to 67% and 62% respectively. By further optimizing the operating conditions, the energy saving will be close to 74% for R1234ze(Z), 71,5 % for R600 and 70,6 % for R600a. By increasing the evaporation temperature, the required heat transfer area is increased, reducing the pressure drop over the evaporator. The best result was achieved with an evaporation temperature of 44 ºC which gives a pinch point temperature of 1 K at the outlet of the evaporator, due to the 5 K superheat.

The reduction in pressure drop results in a reduction in the required compressor work of close to 30% from 40 ºC to 44 ºC. This is because of a reduced temperature lift and an increase is isentropic efficiency, due to a reduction in pressure ratio. An efficient compressor reduces discharge temperature, reducing the required area for desuperheating in the condenser, resulting in a reduction in the condenser size. Another positive effect of a reduction in pressure ratio is an increase in volumetric efficiency and an increase in vapor density, reducing the required compressor volume, reducing the size of the compressor. The compressor work and size has a large contributing factor on the annual cost of the system. Optimizing the compressor work is essential, when wanting an efficient system.

In regards to the economic evaluations, it can be seen that the annual costs are heavily affected by the annual operating costs. None of the cycle improvements added more to the investment costs than it saved in operating costs. This could be different if the COP was a lot higher, since the reduction in energy saving per COP will be smaller at increasing COP. When the difference in electricity and natural gas prices are as large as they are, it is important to optimize the heat pump solution to have achieve a profitable investment.

From the sensitivity analysis it can be seen that for low electricity prices has a large effect on the annual costs, and countries with cheap electricity, like Norway, have a higher chance of making heat pumps a profitable investment than countries with high electricity prices. A lower electricity price also opens up for a larger investment, making it possible to increase the efficiency even further. The gas prices could not decrease much before the R1234ze(Z) heat pump would become unprofitable. With increased awareness on global warming, it is not unreasonable to assume an increase in the price for fossil fuels or increased taxation on CO_2, which will further favor a heat pump solution using environmental friendly refrigerants.

The results from this paper shows that both R600 and R1234ze(Z) has a better operating efficiency than R600a. Ommen et al. (2015) results indicate that R600a is the most suitable of refrigerants they investigate for high sink temperatures. This would imply that both R600 and R1234ze(Z) are an even better choice for high sink temperatures.

6. CONCLUSION

Heat pumps have the potential to reduce the energy consumption in industrial heating processes and at the same time being a profitable investment, even in markets where the electricity prices are a lot higher than fossil alternatives. However, the importance of optimizing the cycle is increasingly important when the electricity prices are high. A heat pump might cost less to operate yearly than a natural gas boiler, however if the savings are minimal, the additional investment cost might make the investment unprofitable. It is therefore important to do economic evaluations when considering in investing in a heat pump solution.

In the simulations, R1234ze(Z) achieves the highest COP of the three systems and the lowest annual costs making it the most profitable system. R600 achieves higher performance than R600a, making R600a the least favorable of the three refrigerants. The operational cost is the biggest contribution to the annual cost for all systems. All tested cycle improvements saved more money from operational cost than it added to the capital costs.

NOMENCLATURE

Latin Letters

a	Annuity Factor	[-]
b	Height of Corrugation	[m]
B	Annual Earnings/Savings	[NOK]
Bd	Bond Number	[-]
Bo	Boiling Number	[-]
c	Heat Capacity	[J/kgK]
COP	Coefficient of Performance	[-]
d_h	Hydraulic Diameter	[m]
e	Energy Price	[NOK/kWh]
E_{tot}	Energy Demand	[kWh]
f	Friction Factor Coefficient	[-]
G	Mass Flux	[kg/m^{2}s]
h	Heat Transfer Coefficient	[W/m^{2}K]
I_0	Additional Investment	[NOK]
k	Thermal Conductivity	[W/mK]
KE	Kinetic Energy	[J]
L	Length	[m]
$\dot{m}$	Mass Flow Rate	[kg/s]
n	Number of Years	[years]
MC	Maintenance Cost	[NOK/year]
N_{ch}	Number of Channels	[-]
Nu	Nusselt Number	[-]
p	Corrugation Pitch	[m]
P	Pressure	[Pa]

Greek Letters

β	Chevron Angle	[deg]
η	Efficiency	[-]
μ	Viscosity	[kg/ms]
ρ	Density	[kg/m^3]
λ	Volumetric Efficiency	[-]
Φ	Enlargement Factor	[-]
τ	Running Time	[hours]

Subscripts

acc	Acceleration
C	Cold
comp	Compressor
cond	Condenser
eq	Equivalent
evap	Evaporator
fric	Frictional
g	Vapor
G	Gravitational
Gas	Gas Boiler
H	Hot
HP	Heat Pump
is	Isentropic
l	Liquid
lo	Liquid Only

Q	Heat Duty	[W]	m	Mean/Homogenous
Pr	Prandtl Number	[-]	p	Port
PR	Pressure Ratio	[-]	plate	Heat Exchanger Plate
r	Real Interest Rate	[%]	sc	Subcool
Re	Reynolds Number	[-]	sh	Superheat
T	Temperature	[K]	tot	Total
th_m	Thickness of Plate	[m]	tp	Two-Phase
U	Overall Heat Transfer Coefficient	[W/m^{2}K]	wall	Plate wall
V	Volume	[m^3]		
V_s	Required Compressor Volume	[m^3/h]		
W	Work	[W]		
w	Width	[m]		
We	Weber Number	[-]		
y	Length	[m]		

REFERENCES

AMALFI, R. L., VAKILI-FARAHANI, F. & THOME, J. R. 2016a. Flow boiling and frictional pressure gradients in plate heat exchangers. Part 1: Review and experimental database. *International Journal of Refrigeration,* 61**,** 166-184.

AMALFI, R. L., VAKILI-FARAHANI, F. & THOME, J. R. 2016b. Flow boiling and frictional pressure gradients in plate heat exchangers. Part 2: Comparison of literature methods to database and new prediction methods. *International Journal of Refrigeration,* 61**,** 185-203.

CALM, J. M. 2008. The next generation of refrigerants – Historical review, considerations, and outlook. *International Journal of Refrigeration,* 31**,** 1123-1133.

CHUA, K. J., CHOU, S. K. & YANG, W. M. 2010. Advances in heat pump systems: A review. *Applied Energy,* 87**,** 3611-3624.

EIKEVIK, T. M., TOLSTOREBROV, I., BREDESEN, A. M., REKSTAD, H., PETTERSEN, J., AFLEKT, K. & ELGSÆTHER, M. 2016. *TEP 4255 - Heat pumping processes and systems,* NTNU, NTNU EPT.

FUKUDA, S., KONDOU, C., TAKATA, N. & KOYAMA, S. 2014. Low GWP refrigerants R1234ze(E) and R1234ze(Z) for high temperature heat pumps. *International Journal of Refrigeration,* 40**,** 161-173.

GARCÍA-CASCALES, J. R., VERA-GARCÍA, F., CORBERÁN-SALVADOR, J. M. & GONZÁLVEZ-MACIÁ, J. 2007. Assessment of boiling and condensation heat transfer correlations in the modelling of plate heat exchangers. *International Journal of Refrigeration,* 30**,** 1029-1041.

IEA-HPC 2014. Application of Industrial Heat Pumps, Part 2. *IEA HPP ANNEX 35.* International Energy Agency Heat Pump Centre.

KLEIN, S. 2015. Engineering Equation Solver Professional 9.935-3D. Madison, WI: F-Chart Software.

KONDOU, C. & KOYAMA, S. 2015. Thermodynamic assessment of high-temperature heat pumps using Low-GWP HFO refrigerants for heat recovery. *International Journal of Refrigeration,* 53**,** 126-141.

LONGO, G. A. 2010. Heat transfer and pressure drop during hydrocarbon refrigerant condensation inside a brazed plate heat exchanger. *International Journal of Refrigeration,* 33**,** 944-953.

LONGO, G. A., RIGHETTI, G. & ZILIO, C. 2015. A new computational procedure for refrigerant condensation inside herringbone-type Brazed Plate Heat Exchangers. *International Journal of Heat and Mass Transfer,* 82**,** 530-536.

MARTIN, H. 1996. A theoretical approach to predict the performance of chevron-type plate heat exchangers. *Chemical Engineering and Processing: Process Intensification,* 35**,** 301-310.

NELLIS, G. & KLEIN, S. 2009. *Heat transfer,* Cambridge, Cambridge University Press.

OMMEN, T., JENSEN, J. K., MARKUSSEN, W. B., REINHOLDT, L. & ELMEGAARD, B. 2015. Technical and economic working domains of industrial heat pumps: Part 1 – Single stage vapour compression heat pumps. *International Journal of Refrigeration,* 55**,** 168-182.